MANTLE XENOLITHS FROM THE ATTAWAPISKAT KIMBERLITE FIELD, JAMES BAY LOWLANDS, ONTARIO

Kimberley R. Scully

A thesis submitted in conformity with the requirements
for the degree of Master of Science
Graduate Department of Geology
University of Toronto

0-612-50404-2

Mantle Xenoliths from the Attawapiskat Kimberlite Field, James Bay Lowlands, Ontario

Master of Science
January 2000

Kimberley R. Scully
Department of Geology, University of Toronto

ABSTRACT

A chemical investigation of coarse textured, garnet-bearing peridotite xenoliths and xenocrysts from the Attawapiskat kimberlite field was undertaken. The kimberlites occur in the James Bay Lowlands, in the Sachigo subprovince of the Superior Craton.

Fragments of coarse textured lherzolite, harzburgite and eclogite occur as microxenoliths (≤ 1.5 cm diameter). Most of the xenoliths occur as one or two phase assemblages (olivine ± orthopyroxene, clinopyroxene, garnet, spinel). Garnet-bearing assemblages were investigated for the purposes of geothermobarometry.

Calculated pressures and temperatures of equilibration indicate that garnet harzburgites equilibrated at depths within the diamond stability field, and garnet lherzolites at depths within the graphite stability field. All the xenoliths equilibrated near a $40 mWm^{-2}$ subcratonic steady-state geothermal gradient.

Extensive modal metasomatism occurred in the mantle prior to xenoliths being incorporated into the kimberlite magma. This metasomatism extended to great depths below the Superior Craton in the Attawapiskat region.

ACKNOWLEDGEMENTS

I would like to thank Professor Daniel J. Schulze for his guidance and, most importantly, the patience to supervise my studies for two years.

Special thanks also to professor's James Brenan and Mike Gorton, my illustrious committee members; Claudio Cermignani and George Kretschmann for hours of help on the microprobe; George Taylor and Sean McConville for their ultra-quick thin section preparation; Don Boucher, Herman Gruter, and Julie Kong at Monopros Ltd. for discussion; Bruce Jago and Dante Canil for important data; Professors E.T.C. Spooner and Jim Mungall at UofT; The administrative staff at the Department of Geology, University of Toronto and the Earth Sciences Department at Erindale College; and Lori-ann Pizzolato for important (and sometimes even geological!) discussions.

Samples of the Attawapiskat kimberlites were provided to Professor Schulze by Monopros Ltd.. Research was performed grants from Lithoprobe and NSERC. Thank you all.

Last, but certainly not least, I thank my family and friends – who probably didn't understand most of it, but graciously pretended they did.

TABLE OF CONTENTS

LIST OF TABLES

LIST OF PLATES

CHAPTER 2: PETROGRAPHY

LIST OF FIGURES

LIST OF APPENDICIES

CHAPTER 1: INTRODUCTION

1.1 Introduction

The Earth's mantle constitutes approximately two thirds of the planet, and yet it remains largely inaccessible to detailed study. Geophysical investigations reveal complex heterogeneities in the mantle. Geophysical data cannot, however, reveal the chemical processes that take place there to create the observed heterogeneities. Direct chemical analysis of the mantle is possible through analysis of xenoliths of mantle material (spinel and garnet-bearing peridotites, eclogite, and rare dunite), brought to the surface by kimberlite and certain other alkaline volcanic rocks. Kimberlites are ultrapotassic, volatile-rich magmas which originate at depths greater than 200 km below the surface of the Earth, below thick, cool Archean craton roots (Mitchell, 1986). As they rise towards the surface, kimberlites entrain fragments of the mantle through which they pass. These fragments provide petrologists with small pieces of the mantle rocks, and as such act as "windows" to the mantle below.

The cool peridotitic roots of Archean cratons have been identified as the source region for diamonds recovered from kimberlites and lamproites (Mitchell, 1986). Academic and economic interest in understanding the way diamonds form in their source region has stimulated studies of mantle xenoliths recovered from kimberlite pipes. Many mantle xenoliths are recovered from active diamond mines. Diamond exploration and mining companies study xenolith chemistry to help design exploration programs specific to the mantle rock-types sampled by kimberlites in an effort to target the most lucrative prospects.

Discoveries of kimberlite pipes and diamonds in Canada during the last two decades have provided opportunities to examine several new suites of mantle xenoliths, allowing research into the mantle below the Canadian Shield, the worlds largest Archean craton (Card and Ciesielski, 1986). The Attawapiskat kimberlite field, in the Superior Province of the Canadian Shield, in northern Ontario, was discovered by Monopros Ltd. in 1984. This study is an investigation of the chemistry of minerals from xenoliths recovered from exploration drill core from the Attawapiskat kimberlites. The data have been used to constrain the composition of the mantle below the western Superior craton, determine the subcratonic geothermal gradient at Attawapiskat, and to qualify modal metasomatism in the source region.

1.2 Regional Setting

The Attawapiskat kimberlite field is located approximately 120 km west of James Bay on the Attawapiskat River in Northern Ontario (Figures 1-1 to 1-3). There are 18 kimberlite pipes in the Attawapiskat cluster. Sixteen of the pipes are owned by Monopros Ltd.. The remaining two pipes, MacFadyen 01 and 02, are owned by KWG-Spider Resources. The pipes lie within the James Bay Lowlands physiographic region, an area of dense muskeg swamp and stunted spruce forests on the southern limit of permafrost (Johnson et al., 1991; Figure 1-2). The kimberlites intrude Archean basement rocks of the Superior Province, Palaeozoic and Mesozoic sedimentary rocks of the Moose River Basin, and Quaternary and Holocene glacial and lake deposits on the north and south shores of the Attawapiskat River (Figure 1-3).

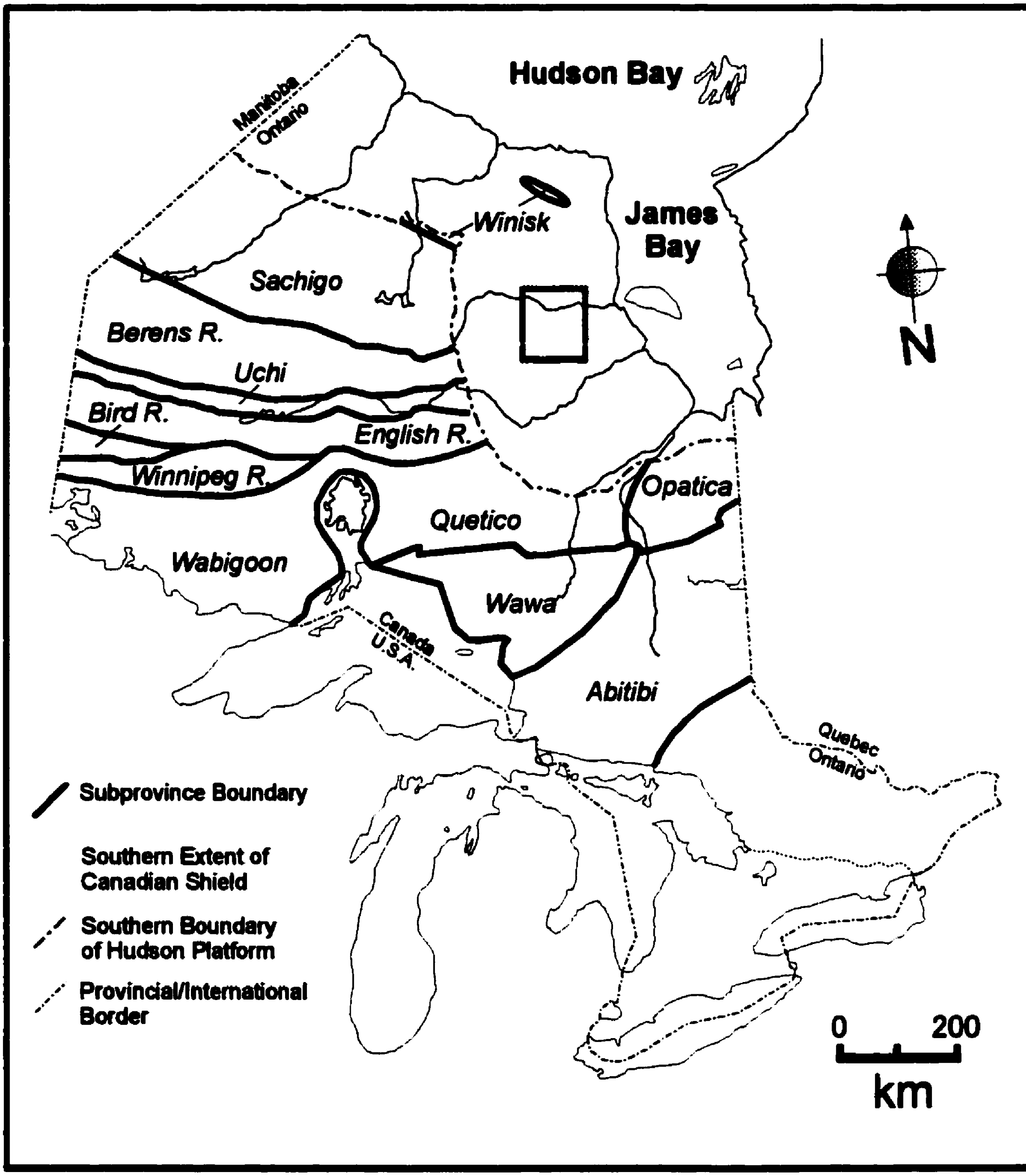

Figure 1-1: Subprovince divisions of the Superior Province within Ontario. Boxed area is detailed in Figure 1-3. Modified after Thompson et al., (1991); Subprovince boundaries from Card and Ciesielski (1989).

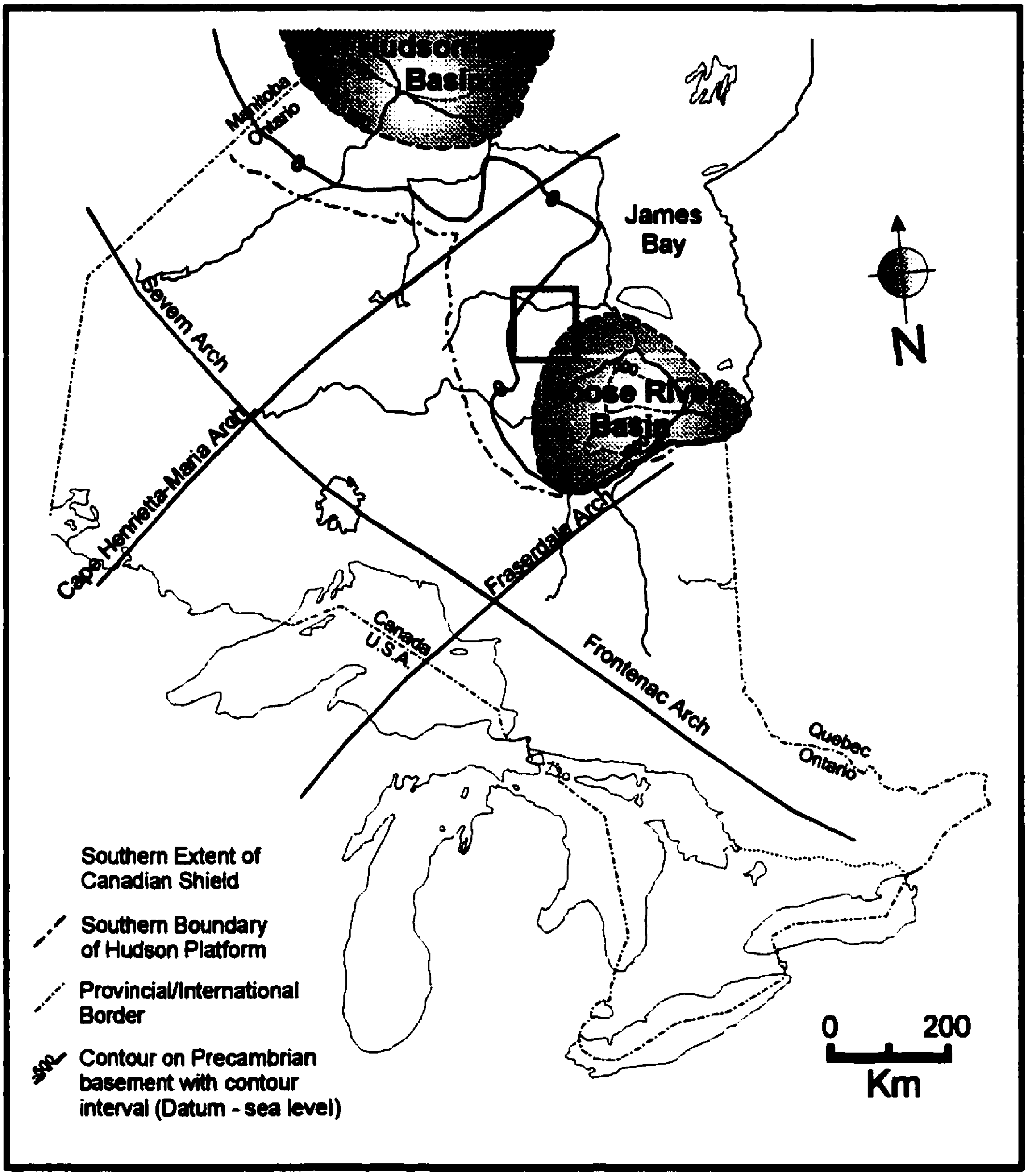

Figure 1-2: Hudson Bay and Moose River Sedimentary Basins, with associated continental arches. Boxed area is detailed in Figure 1-3. The Attawapiskat kimberlite pipes lie at the zero (0) displacement line between the Moose River Basin and the Cape Henrietta-Maria Arch. Modified after Thompson et al., (1991).

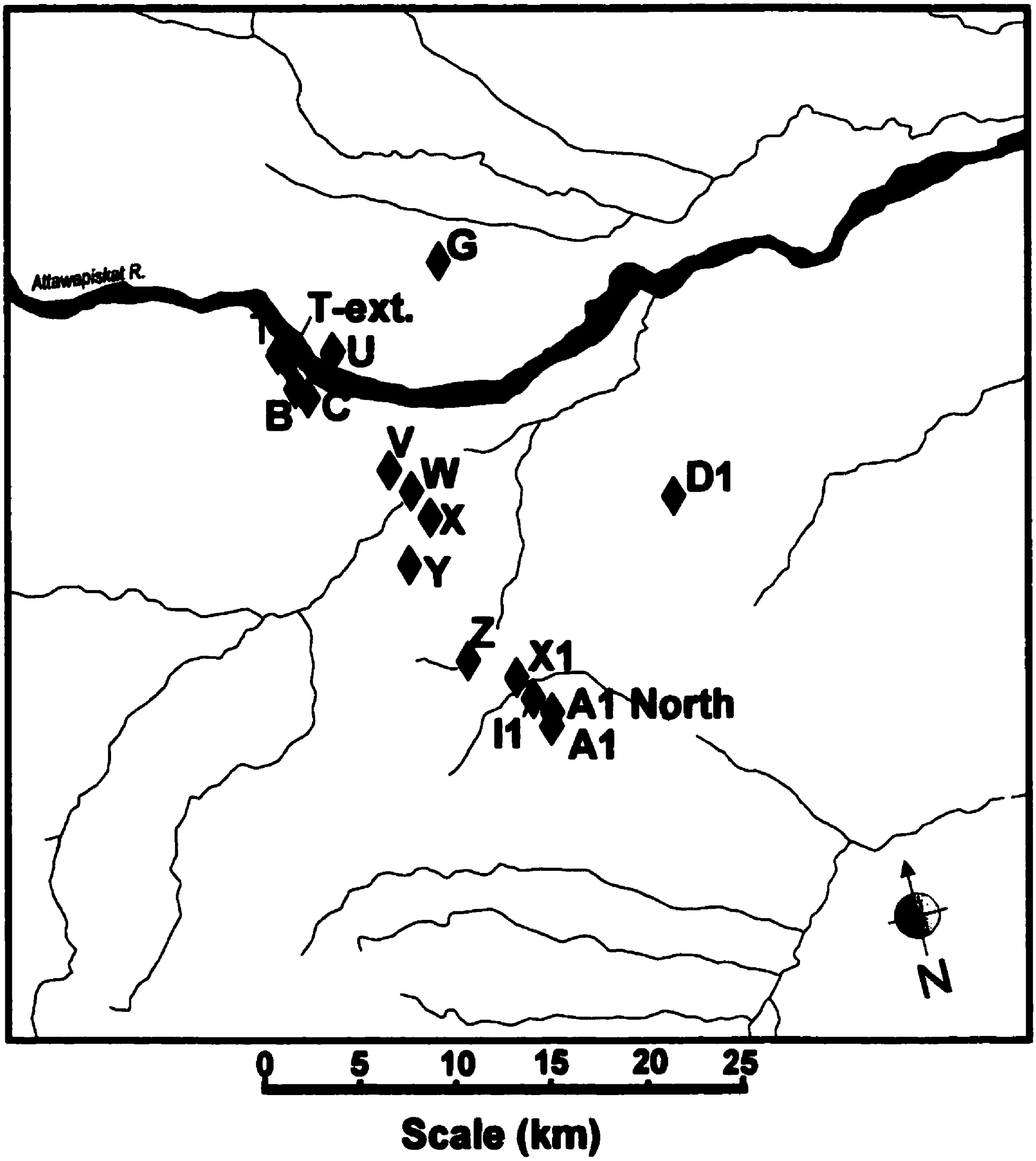

Figure 1-3: The Attawapiskat kimberlite field. Kimberlite pipes are represented by black diamonds, with names beside each pipe. Modified after Sage (1996).

Regional tectonics associated with craton accretion in the Superior Province created a province-wide basin and dome structure (Williams et al., 1991; Johnson et al., 1991). Intracratonic basins acted as depocentres for the influx of sediments associated with increased erosion rates during the Appalachain orogeny. The Hudson Bay Platform in northern Ontario, and St. Lawrence Platform in southern Ontario, were the two major depocenters active during the Palaeozoic and Mesozoic (Johnson et al., 1991). Deposition in northern Ontario was centred on two intracratonic basins, the large northern Hudson Bay Basin, underlying most of what is now Hudson Bay and James Bay, and the much smaller Moose River Basin, underlying the southwest tip of James Bay (Johnson et al., 1991 - Figure 1-2.). The two basins are divided by the north-east trending Cape Henrietta-Maria Arch (an extension of the transcontinental arch - Sanford and Norris, 1975). The Moose River Basin is bounded on the southeast by the Fraserdale Arch, the northeast by the Saguenay Arch, and by the Severn Arch – Fraserdale Arch to the southwest (Johnson et al., 1991; Williams et al., 1991). Sedimentary rocks of the Hudson Bay Platform cover approximately 320,000 km^2 of northern Ontario, underlying Hudson Bay and James Bay, and much of the current land surface surrounding the bays (Johnson et al., 1991). The Attawapiskat kimberlites lie on the northwest flank of the Moose River basin, near the inflection point from the basin to the Cape Henrietta-Maria Arch.

Sedimentation in the Moose River Basin began in the middle to upper Ordovician and continued intermittently to the mid to upper Cretaceous (Sanford and Norris, 1975). The sedimentary rocks of the Moose River Basin consist of limestones and dolostones, with intercalated shales and sandstones. The youngest sedimentary rocks preserved in the immediate vicinity of the kimberlite pipes are the 428-421 Ma reef and inter-reef deposits of the Attawapiskat Formation (Sanford and Norris, 1975). These resistant biohermal dolostones and limestones form outcrops along the banks of the Attawapiskat River. Locally, the Attawapiskat Formation conformably overlies the middle Silurian age limestones and dolostones of the Ekwan Formation. The Attawapiskat formation is conformably overlain by the upper Silurian age evaporitic deposits of the Lower Member of the Kenogami River Formation to the north of the kimberlite cluster (Johnson et al., 1991). Fragments of the Kenogami formation strata are preserved as xenoliths in the kimberlites, indicating that the pipes erupted before the current level of erosion of the Palaeozoic sediments was attained (Kong et al., 1999).

Archean rocks of the Superior and Hearn Provinces, and the Proterozoic Trans-Hudson Orogen, are completely covered by the sedimentary rocks of the Hudson Bay Platform along the Hudson Bay coast (Williams et al., 1991). Sedimentary rocks of the Moose River Basin lie completely within the boundaries of the Superior Province (Williams et al., 1991). The basement rock in the region of the Attawapiskat kimberlites is the northern part of the Sachigo subprovince, just south of the contact between the Sachigo and Winisk subprovinces (Card and Ciesielski, 1986; Thurston et al., 1991). The Sachigo subprovince consists of granite-greenstone belts, separated by granite pluton and metasedimentary units (Thurston et al., 1991; Henry et al., 1997). Ages of these basement rocks range from 2.65 – 3.17 Ga, making the Sachigo the oldest subprovince of the Superior Craton (Thurston et al., 1991; Henry et al., 1997).

A teleseismic study by Grand (1987) reported a good resolution, high-velocity root below the northwest Superior Province to a depth of ~ 400 km. Results from Grand

(1987) also indicate that the lithosphere-asthenosphere boundary is at least 200 km below the surface in the vicinity of the pipes.

Resistant cliffs of biohermal deposits of the Attawapiskat formation are discontinuous along the banks of the river near the location of the kimberlite pipes, with swamp-covered lows intermittent between the outcrops. Suchy and Stearn (1993) attribute the intermittent lows to several faults associated with a continent-wide fault system. The Attawapiskat kimberlites occur in the vicinity of several of these faults (Figure 1-4).

Quaternary deposits in the Attawapiskat region consist of two thin till sheets, overlain by marine Holocene deposits (Kong et al., 1999). Thickness of these glacial and modern marine sediments ranges from 5.5 – 54.0 m over the kimberlites (Kong et al., 1999).

1.2.1 Kimberlite Geology

1.2.1.1 Kimberlite

The Attawapiskat kimberlites were discovered in 1984 by Monopros Ltd., using a combination of sediment sampling for kimberlite indicator minerals and aeromagnetic surveys. Pipes were named based on geophysical grid coordinates (example, Alpha-1 at the intersections of lines "A" and "1"). For this study, the names of the pipes have been abbreviated to letter-number combinations ("A1"), or just letters ("V") where appropriate. The kimberlites lie along a northwest trend, primarily to the south of the Attawapiskat River (Figure 1-3). The trend is similar to that of the kimberlite pipe occurrences in the Northwest Territories (Kong et al., 1999), and along the northwest

a)

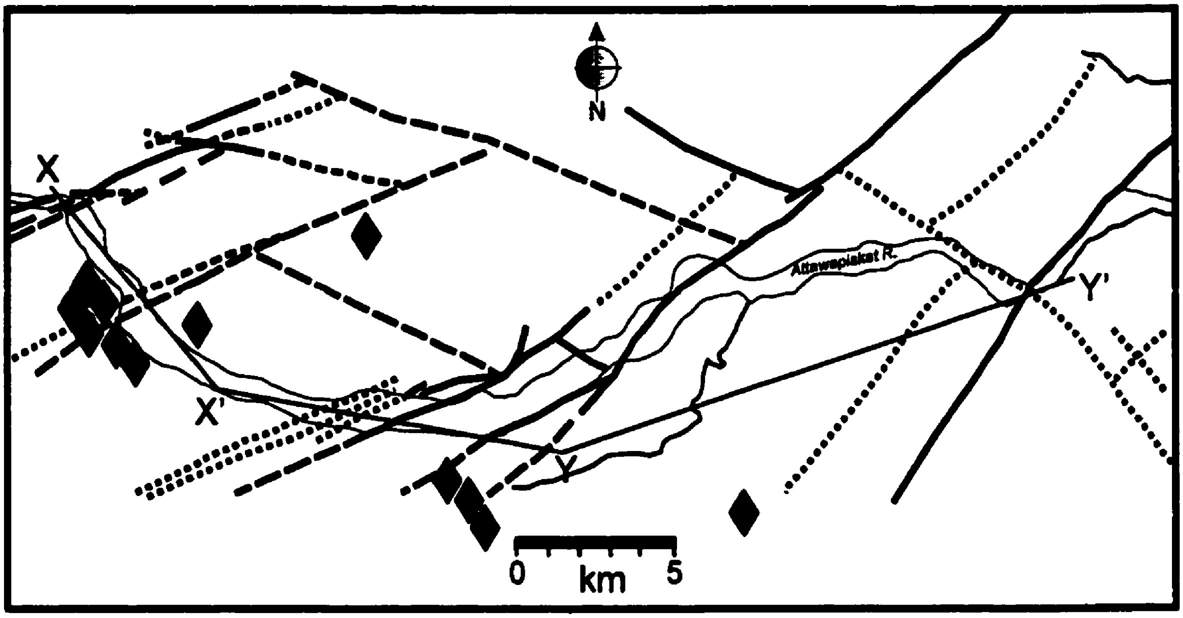

b)

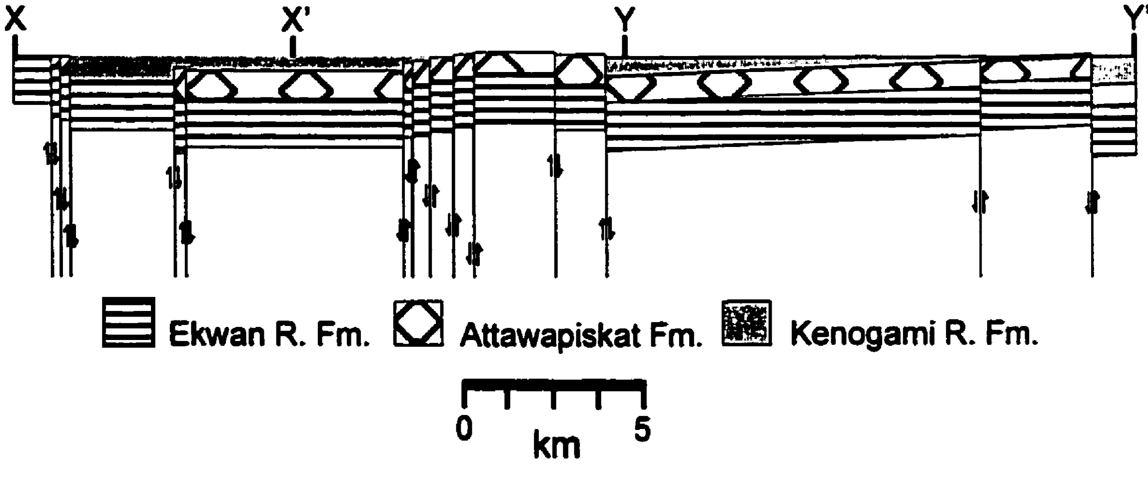

Figure 1-4: Faults in the vicinity of the Attawapiskat kimberlite field. *Solid lines* - faults, *dashed* to *dotted* - inferred faults, with increasing uncertainty. **a**) Plan view. Black diamonds - kimberlite pipes. Line X-X'-Y-Y' is cross section presented in b. **b**) Cross section X-X'-Y-Y'. Vertical scale is exaggerated. Modified from Suchy and Stearn (1993).

trend for kimberlites within the Canadian Shield defined by Sage (1996). Rocks of two of the pipes outcrop, one to the south of the river ("X"), and one that is incised by the Attawapiskat River and thus outcrops on the riverbank ("U"). Surface area of the pipes ranges from 0.4 – 15 ha (Kong et al., 1999). Fifteen of the 16 pipes are diamondiferous, and bulk sampling of several pipes is ongoing (Kong et al., 1999; Don Boucher, personal communication). Xenoliths from several of the 16 Monopros Ltd. pipes were investigated in this study.

Two mineralogical and textural types of kimberlite occur. Spinel-carbonate kimberlite and monticellite kimberlite both occur as macrocrystic uniform to segregationary textured hypabyssal kimberlite, and macrocrystic pyroclastic kimberlite (Kong et al., 1999). Many of the kimberlite bodies have textures gradational between segregationary hypabyssal kimberlite and pyroclastic kimberlite (Kong et al., 1999). Most of the diatremes appear to be the result of single intrusions. Pipes "A1 North", "D1", "T" and "V", however, have geophysical signatures which suggest multiple pulses of kimberlite magma emplacement (Kong et al., 1999).

Various ages have been determined for several of the Attawapiskat pipes. Rb/Sr on phlogopite from the Monopros Ltd. pipes yielded model ages of 155 – 170 Ma (Kong et al., 1999). U/Pb ages from perovskite grains recovered from the two MacFadyen pipes give ages of 177 – 179 Ma ∀ 2.2 Ma (Hetman, 1996; Kong et al., 1999). Whereas 15 of the pipes have normal magnetic polarization, pipe "U" has reverse magnetic polarization, indicating it erupted during a reversal of the Earth's magnetic field. It has been determined that pipe "U" is older than the other pipes (Hetman, 1996; Kong et al., 1999).

1.2.1.2 Xenoliths

The Attawapiskat kimberlite pipes contain numerous country-rock xenoliths. Fragments of Moose River Basin sedimentary rocks are abundant. Xenoliths of the Ekwan, Attawapiskat and Kenogami formations range in size from # 1 cm to 30 cm, and are angular to subrounded. Most of the sedimentary fragments display little or no evidence of thermal alteration induced by entrainment within the kimberlite magma. Many of the country rock fragments contain fossils with very delicate features (such as individual coral septae) that are perfectly preserved and unaffected by the kimberlite magma.

Fragments of Archean basement rocks are also common, and garnet + clinopyroxene ± plagioclase (granulite facies rock), tonalitic and amphibolitic gneiss ± garnet have been identified by Moser and Krogh (1995). Moser et al. (1997) reported an age range of 2920-3050 Ma for one rock-forming event, recorded in detrital zircons from amphibolite-facies paragneiss xenoliths. Moser et al. (1997) also presented U/Pb, Rb/Sr and Sm/Nd analyses of metamorphic zircons from granulite-facies xenoliths as evidence for high-temperature metamorphism of the deep crust at Attawapiskat which occurred sometime between the late Archean and late Proterozoic.

Ultramafic xenoliths are common in some pipes ("A1", "G1", "D1") and absent in pipe "Y". The vast majority of mantle fragments occur as microxenoliths (#1 cm diameter), consisting of one or more phases. Single crystals, especially olivines, are the dominant mantle fragments. Most of the composite mantle fragments are coarse-textured, metasomatized garnet lherzolites and harzburgites. Large (∃ 1 cm) single crystals of garnet, olivine, clinopyroxene and ilmenite (megacrysts) are present in the kimberlites. Fluidal-textured, disrupted garnet peridotites and eclogite fragments are rare, but have been recovered from several pipes.

1.3 Previous Work

The Attawapiskat kimberlites are owned by Monopros Ltd., a subsidiary of De Beers Consolidated Mines Ltd.. Kong et al. (1997) presented an account of the exploration and discovery of the Attawapiskat kimberlite pipes. Kong et al. (1999) outlined exploration, discovery, geology of the kimberlites and xenoliths. Results of chemical analysis of a small group of mantle xenoliths from the Attawapiskat kimberlites are detailed in Schulze and Hetman (1997). Hetman (1996) gave a detailed chemical and petrographic analysis of ilmenite-silicate intergrowths recovered from diamond drill core. Alkaline intrusions of kimberlite, carbonatite and alnoite affinity from Hearst, Ontario (~250 km south of Attawapiskat), discovered by aeromagnetic survey by BP Resources, Canada, are described by Janse et al. (1989).

Kimberlite pipes from Kirkland Lake, Ontario, approximately 400 km to the southeast of the study area, are the geographically closest other kimberlite field to Attawapiskat. Kirkland Lake kimberlite exploration, discovery, and chemical and petrographic analyses are surveyed by Sage (1996). Chemical analyses of kimberlites and xenocrysts from Kirkland Lake are presented in Brummer et al. (1992a, 1992b). Mantle xenoliths from Kirkland Lake pipes were described by Meyer et al. (1994), Sage (1996), and Vicker (1997).

1.4 Methodology

1.4.1 Sample Preparation

Kimberlite diamond drill core was made available to the University of Toronto by Monopros Ltd. and was examined for ultramafic xenoliths. Multi-phase assemblages were extracted for chemical and petrographic analysis. Mantle xenoliths are quite small (≤ 1.5 cm) in these rocks, and often consist of only one or two phases. To prevent loss of material during preparation, xenoliths were mounted in 2.5 cm diameter epoxy rings. Samples were ground until the minerals desired for analysis were exposed, and then polished at the University of Toronto thin section laboratory. Heavy mineral separates were created by Overburden Drilling Management Ltd., using chip samples from reverse-circulation drilling for bulk ore analysis (pipe "V"), and crushed drill core fragments (pipes "A" and "G"). Mineral mounts of garnet, chromite, and clinopyroxene were created using grains from the 0.5-1.0 mm size fraction. Thin sections of sheared lherzolite samples were made at the University of Toronto thin section laboratory.

1.4.2 Mineral Chemical Analysis

Major element chemical analysis of seven minerals (garnet, olivine, clinopyroxene, orthopyroxene, chromite, amphibole and phlogopite) was done using a Cameca SX-50 electron microprobe at the Duncan Ramsey Derry Laboratory at the Department of Geology, University of Toronto. Minerals were analyzed in wavelength dispersive mode, and data corrections were made on-line using standard SX-50 PAP procedures. An accelerating voltage of 15 kV was used for garnet, clinopyroxene, orthopyroxene, phlogopite and amphibole, and 20 kV for chromite and olivine. Beam currents used were 20 nA (chromite), 25 nA (orthopyroxene, clinopyroxene, amphibole) and 30 nA (orthopyroxene, clinopyroxene, olivine, garnet). Phlogopite grains were analyzed using a beam current of 8 nA to prevent volatilization of Cl and F. Count times for each element varied according to the mineral being analyzed, and are summarized along with other operational specifications in Appendix A.

CHAPTER 2: PETROGRAPHY

2.1 Introduction

Xenoliths in kimberlite indicate that the Earth's upper mantle consists predominantly of olivine, with large amounts of orthopyroxene and some clinopyroxene. Classification of mantle rock types is based on modal abundance of olivine, orthopyroxene and clinopyroxene, as depicted in the IUGS ultramafic rock triangle (Figure 2-1). Pyroxenites, rocks consisting of < 40 modal % olivine and > 60 modal % pyroxene (orthopyroxene and/or clinopyroxene), and which include olivine websterite and websterite, are rare as xenoliths in kimberlite. No pyroxenite xenoliths were recovered from the Attawapiskat core.

The term "peridotite" encompasses all of those ultramafic rock types with 40-100 modal % olivine. Subdivision of peridotites is based on the presence of orthopyroxene and/or clinopyroxene. Although the IUGS classification defines harzburgite as containing up to 5 modal % clinopyroxene and wehrlite with up to 5 modal % orthopyroxene, it is accepted practice in mantle xenolith studies to use the term lherzolite for any peridotite that contains both orthopyroxene and clinopyroxene. Further subdivision of peridotite rocks is based on accessory minerals. MgAl-spinel is the most common accessory phase in cratonic peridotites at pressures below ~ 20 kbar (> 60 km depth). Above 20 kbar, garnet is the stable Al-bearing accessory mineral. Cr-rich spinel may coexist with garnet at pressures >20 kbar, and occur as the Cr-bearing phase during the metasomatic breakdown of garnet.

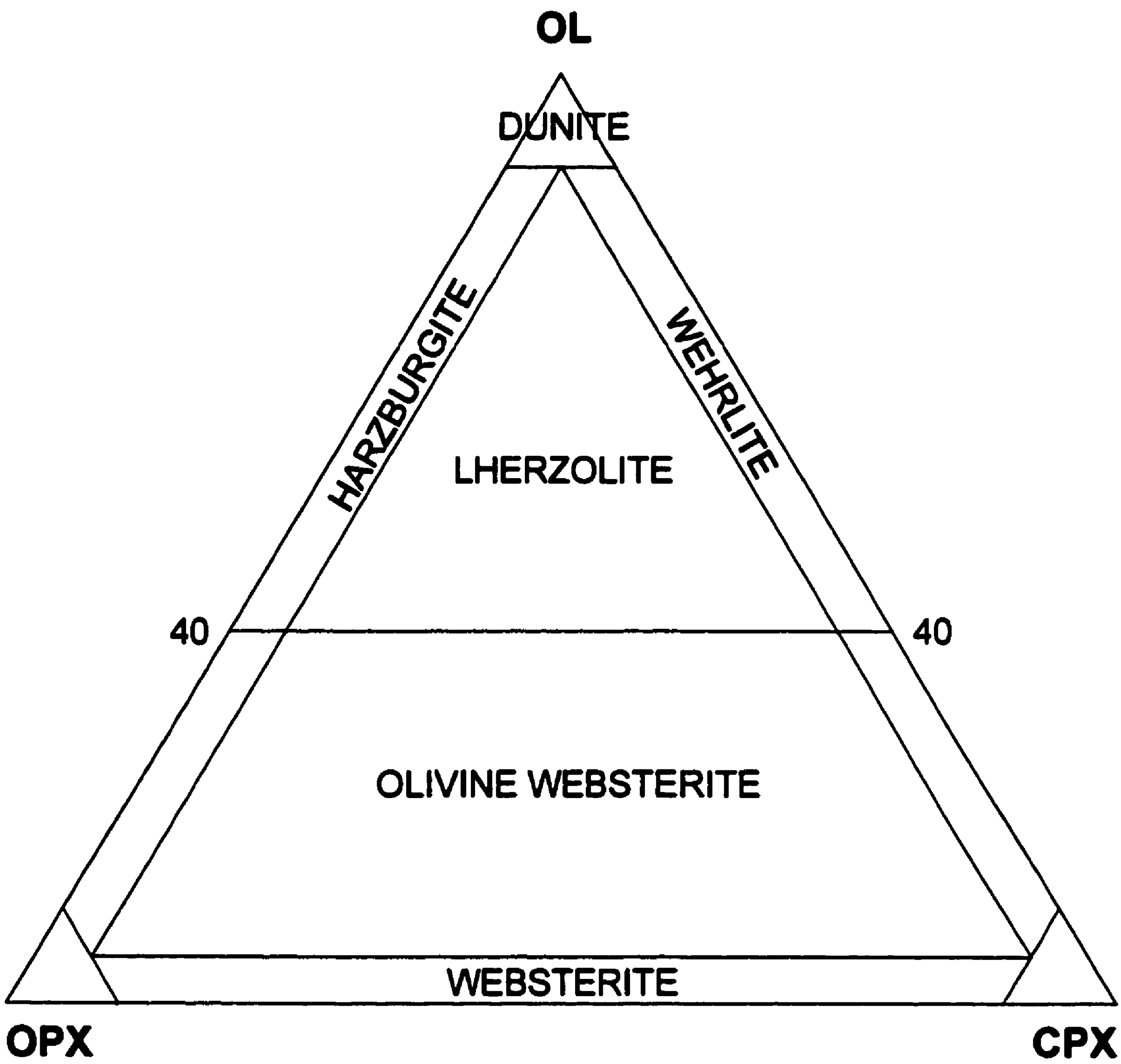

Figure 2-1: IUGS major ultramafic rock-types in terms of olivine (OL), clinopyroxene (CPX), and orthopyroxene (OPX). Lherzolite and harzburgite may have garnet at high-pressure (>15kbar, ~900°C) or spinel at lower pressures (10-15kbar, ~900°C) as accessory phases (Haggerty, 1995). Eclogite (not shown) is grossular-pyrope-almandine garnet + omphacitic diopside.

2.2 Attawapiskat Xenoliths

The small size and fragility of the Attawapiskat xenoliths prohibited thin sectioning, so petrographic observations were made using reflected light microscopy and back-scattered imagery in the electron microprobe. Mineral identification was facilitated by x-ray dispersive spectroscopy (EDS scanner) in the electron microprobe.

Mantle xenoliths from the Attawapiskat kimberlites occur as rounded to subrounded microxenoliths ($\leq$1.5 cm diameter) of one or more phases. The most common mantle xenoliths are garnet-olivine pairs, however several olivine + garnet + orthopyroxene (harzburgite) xenoliths were also recovered.

Olivine occurs as fresh, equant unstrained grains commonly < 2 mm in diameter (Plates 1, 3, 4 and 6). Xenoliths containing fresh equant olivine grains may be classified as "coarse" using the terminology of Harte (1977). Minor secondary serpentinization occurs along olivine grain margins and in cracks and veins. The extent to which individual grains of olivine have been serpentinized may vary between grains within a single xenolith.

Garnet grains may vary from 0.5 to 7 mm in diameter. Garnets are generally clear, red to purple coloured rounded grains. Garnets in eclogite xenoliths are orange-pink in colour. Many garnets have multiple fractures filled with fine-grained phlogopite, small euhedral spinels, and fine-grained alteration material.

Peridotite garnets are commonly partially replaced by phlogopite ± amphibole ± chromite. Garnets may also be replaced by clinopyroxene. The two replacement types have the following textures:

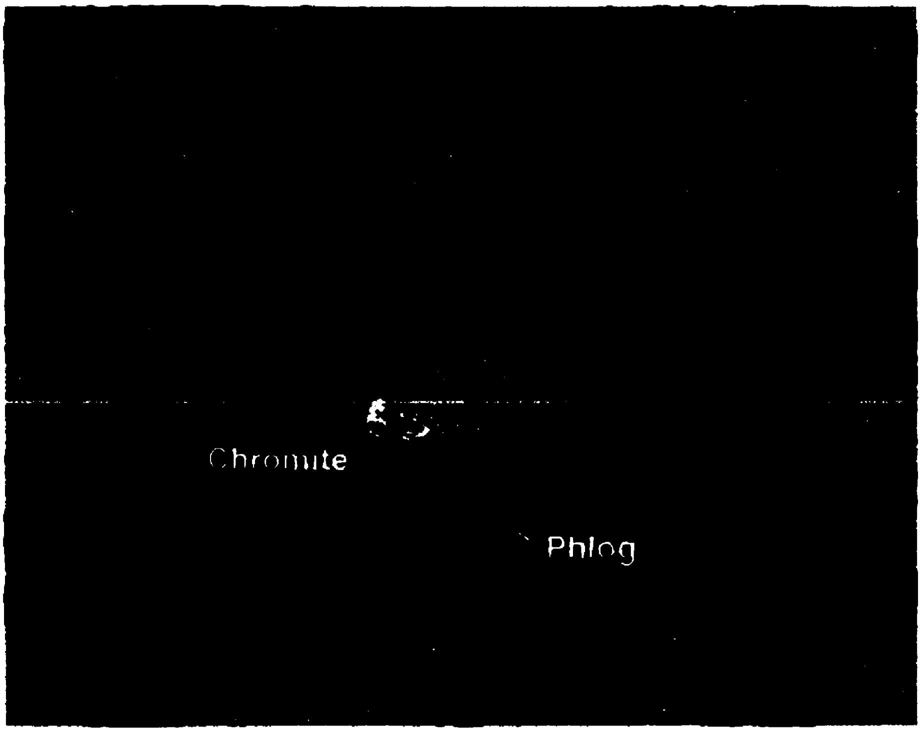

Plate 1: Garnet lherzolite 13-95-34. Garnet (Gnt) is partially replaced by amphibole (Amph), phlogopite (Phlog) and chromite. Other garnets in this sample have been completely replaced by amph + phlog + chromite. Field of view = 4 mm.

Plate 2: Sample 13-95-49. Garnet (Gnt) partially replaced by amphibole (Amph), phlogopite (Phlog) and chromite. Note that the chromite occurs as vermicular inclusions in the phlogopite and amphibole. Field of view = 4mm.

1) Partial replacement of garnet by very fine grained (<< 1 mm) flakes of phlogopite ± fine grained (≤1 mm) amphibole, where either phlogopite or both phlogopite and amphibole have vermicular inclusions of chromite. The garnet has embayed contacts with both phlogopite and amphibole. Garnets do not have kelyphite rims. (Plates 1 and 2).

2) Partial replacement by clinopyroxene, without any associated phlogopite. Garnet grain margins are embayed where in contact with the clinopyroxene (Plates 3, 4 and 6).

Two primary clinopyroxene grains were found, in samples 13-102-05 and 13-102-12 (pipe "X"). The primary clinopyroxene occurs as small (~ 2 mm diameter), subrounded, bright green grains without exsolution textures. No alteration of the clinopyroxene grains was evident. Clinopyroxenes in two eclogite samples are dark green, rounded, unaltered grains without any inclusions or exsolution lamellae.

Orthopyroxene is typically rare, and is extensively altered to serpentine where present. Orthopyroxene grains are generally small (~ 2 mm), coarse equant, and opaque blue-white where altered to serpentine. Four grains have clear, pale-yellow cores that have sharp contacts with serpentine replacing the grain rims (Plates 4 and 5).

2.2.1 Metasomatic Minerals

With the exception of just a few olivine – garnet pairs, mantle xenoliths at Attawapiskat have undergone some degree of metasomatism. Fine-grained alteration material with associated phlogopite and chromite filled cracks and infiltrated along grain margins. Most of the garnet-bearing xenoliths have garnets which have been partially

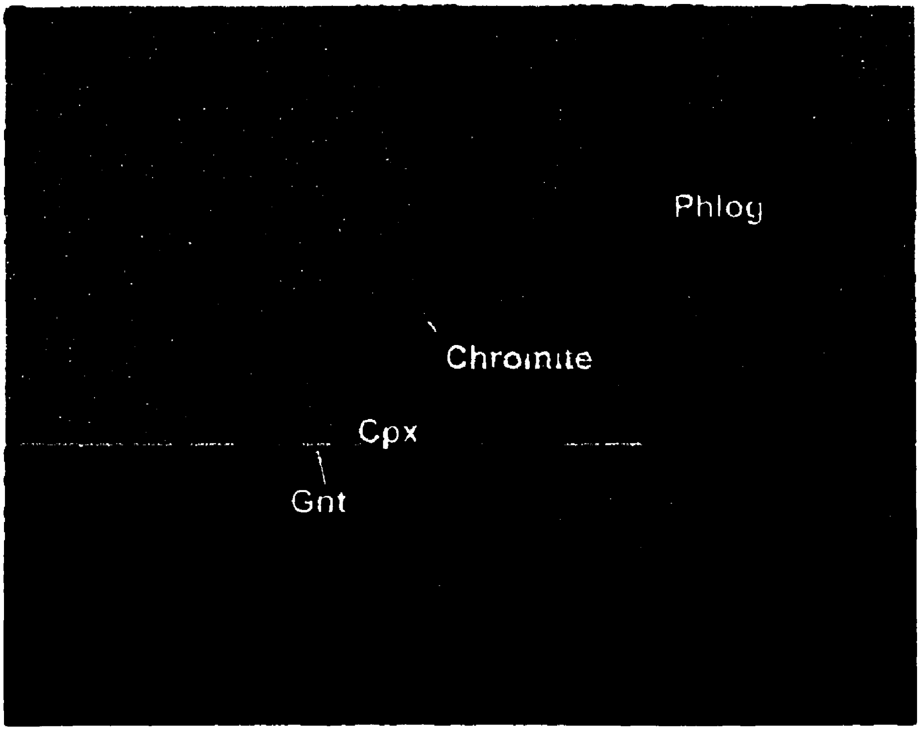

Plate 3: Garnet lherzolite 13-95-63. Garnet (Gnt) is partially replaced by clinopyroxene (Cpx). Phlogopite (Phlog) and Chromite are secondary minerals. The garnet has embayed margins where it is in contact with the clinopyroxene. Olivine - Oliv. Field of view = 4 mm.

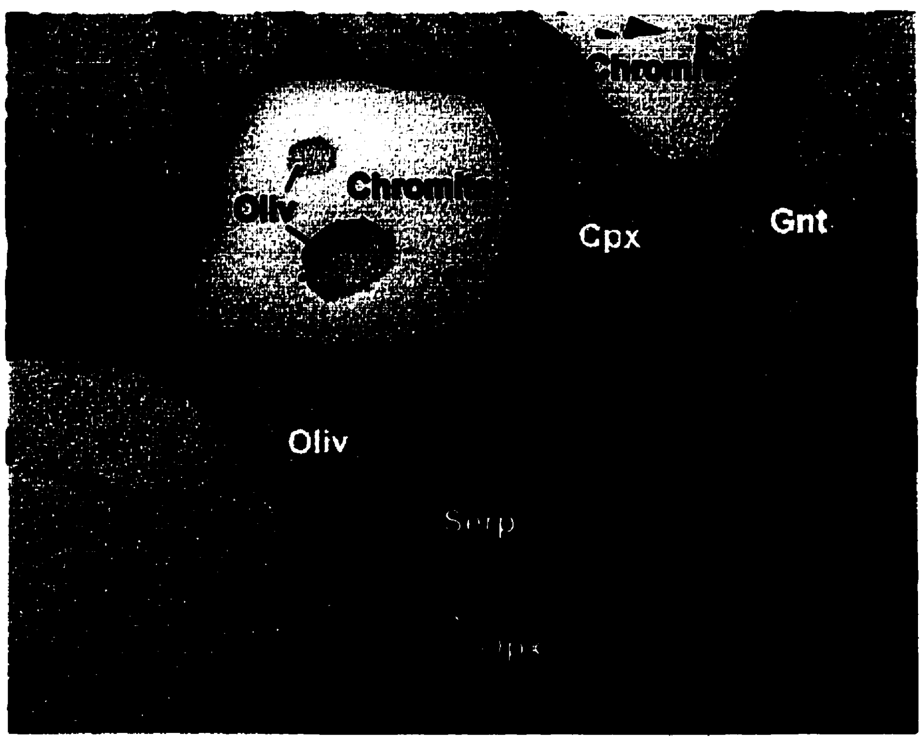

Plate 4: Garnet lherzolite 13-97-83. Clinopyroxene (Cpx) partially replaces garnet (Gnt). The orthopyroxene (Opx) is almost completely altered to serpentine (Serp) - only the very core of the grain is preserved. Olivine - Oliv. Field of view = 4 mm.

replaced with phlogopite ± amphibole ± chromite. Some garnets have been partially replaced by clinopyroxene.

Phlogopite occurs in three different textural associations:

1) As very fine-grained mantles on garnet and olivine, as mantles around the whole xenolith, and filling veins and cracks interstitial to and within major phases. The phlogopite grains are euhedral and are green-brown in colour. The phlogopites occur with fine-grained alteration material (phlogopite textural type "1" – Plate 3).

2) As a single, optically continuous precipitate filling veins in garnet and olivine, similar to igneous orthocumulate texture (phlogopite textural type "2").

3) As large flakes, occurring with amphibole to partially replace garnet. Phlogopites of this association may or may not have vermicular inclusions of chromite (phlogopite textural type "3" – Plates 1, 2 and 3).

Amphibole occurs with phlogopite and chromite to partially replace Cr-pyrope garnet. The amphibole occurs as very fine-grained (<< 1 mm) euhedral to anhedral grains, green-brown in colour, within small "clots" of metasomatic minerals. Many amphibole grains have vermicular inclusions of chromite oriented along cleavage planes (Plates 1 and 2).

Chromite occurs as three different textural types:

1) Primary chromite grains preserved either as inclusions in garnet and olivine, or as large grains such as those in sample 13-97-83 (Plate 4). The chromites are relatively large (1 – 3 mm), subrounded and completely encapsulated within the host silicate phase where occurring as inclusions in garnet and olivine (chromite textural type "1").

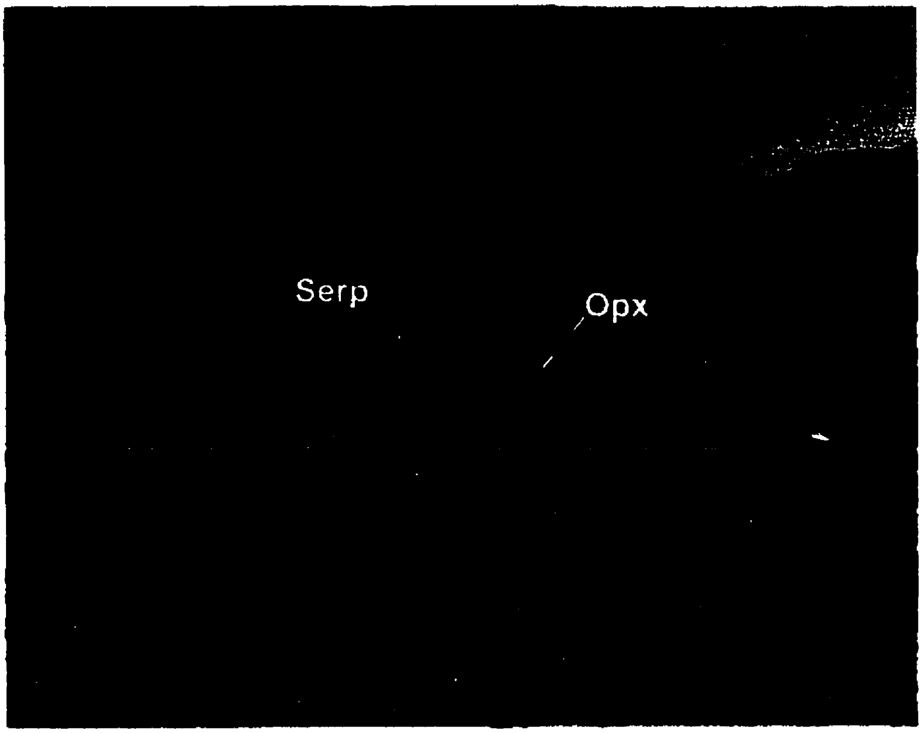

Plate 5: Garnet harzburgite 13-97-78. Orthopyroxene (Opx) is almost completely altered to serpentine. The core of the orthopyroxene grain is unaltered. Field of view = 4mm.

Plate 6: Garnet harzburgite 13-97-78. Garnet (Gnt) is partially replaced by clinopyroxene (Cpx) only. There are three small chromite inclusions in the clinopyroxene, and one in the garnet. Olivine - Oliv. Field of view = 4mm.

2) As secondary grains in veins and cracks in garnet and olivine. Secondary chromites are small (≤ 1 mm diameter) coarse euhedral octahedra set in the fine-grained alterations material filling cracks and veins in garnets (chromite textural type "2" – Plate 2).

3) As small vermicular inclusions in amphibole and phlogopite replacing garnet (Plate 1). The inclusions are very small (<< 1 mm diameter) and follow cleavage planes in the phlogopite and amphibole. Included in this textural group are four small rounded chromite inclusions in garnet and clinopyroxene in sample 13-97-78 (chromite textural type "3" – Plate 6).

Clinopyroxene partially replaces garnet in several garnet – olivine pairs and in garnet harzburgite sample 13-97-78 (Plate 6). The clinopyroxene is bright green in hand sample. It is optically continuous around the rim of the garnet, and has embayed contacts with the replaced garnet. The clinopyroxenes rarely have chromite inclusions, however sample 13-79-78 has clinopyroxene with three small chromite inclusions (Plates 3, 4 and 6).

Table 2-1: Petrographic Summary

		Primary Minerals					Metasomatic Minerals				Secondary Minerals			
Pipe	SAMPLE	oliv	opx	gnt	cpx	chromite	phlog	amph	cpx	chromite	phlog	chromite	serp	Rock Type Classification
G	13-95-28			x			x	x						crustal garnet
G	13-95-32			x					x		x	x		metasomatized garnet
G	13-95-33	x	x	x			x				x		x	gnt. harzburgite
G	13-95-34	x		x			x	x		x	x	x	x	gnt-oliv pair
G	13-95-35	x	x	x									x	gnt. harzburgite
G	13-95-42	x	x	x		x							x	gnt-chr harzburgite
G	13-95-47	x		x					x		x			gnt-oliv pair
G	13-95-48	x		x			x	x		x	x	x	x	gnt-oliv pair
G	13-95-49			x			x	x		x	x	x		metasomatized garnet
G	13-95-50	x		x										gnt-oliv pair
G	13-95-52	x		x					x		x	x		gnt-oliv pair
G	13-95-54			x	x									eclogite
G	13-95-56	x		x							x	x	x	gnt-oliv pair
G	13-95-59	x		x					x		x	x		gnt-oliv pair
G	13-95-66	x		x										gnt-oliv pair
G	13-95-67	x	x	x					x		x	x	x	gnt. harzburgite
G	13-95-70	x		x						x				gnt-oliv pair
A1	13-97-78	x	x	x									x	gnt. harzburgite
A1	13-97-81	x		x					x		x	x	x	gnt-oliv pair
A1	13-97-82	x		x							x	x		gnt-oliv pair
A1	13-97-83	x	x	x		x			x	x		x	x	gnt. lherzolite
A1	Att-A1-P1	x	x	x	x									disrupted gnt. lherzolite
A1	Att-A1-P2	x	x	x	x									gnt. lherzolite
V	13-99-18	x	x	x	x						x			gnt. lherzolite
X	13-102-04			x					x	x				metasomatized garnet
X	13-102-05	x		x	x						x	x		lherzolite
X	13-102-09	x		x							x	x		lherzolite
X	13-102-12	x		x	x				x		x	x	x	lherzolite
X	13-102-15			x					x		x	x		metasomatized garnet

CHAPTER 3: MINERAL CHEMISTRY

3.1 Introduction

Multiphase xenoliths of mantle material preserve the chemical state of the mantle prevalent at the time of kimberlite eruption. Chemical analyses of equilibrium assemblages in xenoliths may be used to determine the pressure and temperature of rock formation. Pressure-temperature pairs may be equated to depth, allowing for characterization of vertical chemical variations in the mantle.

In addition to ultramafic xenoliths, kimberlites contain abundant xenocrysts, which are single mineral grains from disaggregated mantle rocks. These dense mantle minerals are routinely removed from crushed kimberlite during bulk ore analysis using dense-media separation. Xenocrysts removed from kimberlite are referred to as "heavy mineral separates". Heavy mineral separate analyses may be used to compliment and augment xenolith data.

Mineral chemical results for xenoliths recovered from Attawapiskat core, and heavy mineral separates from pipes "A1", "G" and "V" are listed in Appendix B.

3.2 Detailed Mineral Chemistry

3.2.1 Heavy Mineral Separates

Small splits of heavy mineral separates of crushed kimberlite from pipes "A1", "G" and "V" were picked for all grains of garnet, and pipe "V" concentrate for chromite, and green clinopyroxene (chrome diopside). The number of grains analyzed from each split (n = number of grains) is indicated on the figures accompanying each section.

3.2.1.1 Garnet

Garnets were picked from the heavy mineral separates and pooled, then small splits poured out into a separate container before mounting, to avoid biased picking of one colour of garnet over another. This method of grain selection allows for a statistically sound representation of the various types present, and was done for pipes "A1", "G" and "V".

Figures 3-1, 3-2 and 3-3 shows variation in CaO with Cr_2O_3 for garnets from heavy mineral separates. Gurney (1984) showed that 85% of garnet diamond inclusions have compositions that fall above 2 wt% Cr_2O_3 in the CaO-poor portion of the CaO – Cr_2O_3 plot area. Although the 85% field does not delimit a particular garnet paragenesis, Fipke et al. (1995) observed that the line approximately divides garnets of harzburgite (low-Ca) and lherzolite (higher-Ca) parageneses. CaO and Cr_2O_3 contents of garnets may therefore be used to determine the identity of the parent rock, particularly in cases where no other primary minerals are preserved, or for single garnet xenocrysts. This method of discrimination has been used for many of the garnet – olivine pairs recovered from the Attawapiskat kimberlites.

Garnets which have >2 wt% Cr_2O_3 (peridotitic) have 3.6 – 10.6 wt% CaO. Cr_2O_3 contents range to 9.05 wt%, 10.0 wt% and 8.6 wt% for pipes "A1", "G" and "V", respectively. Mg# (mol % Mg/(Mg+Fe) x 100%) for the peridotite garnets ranges from

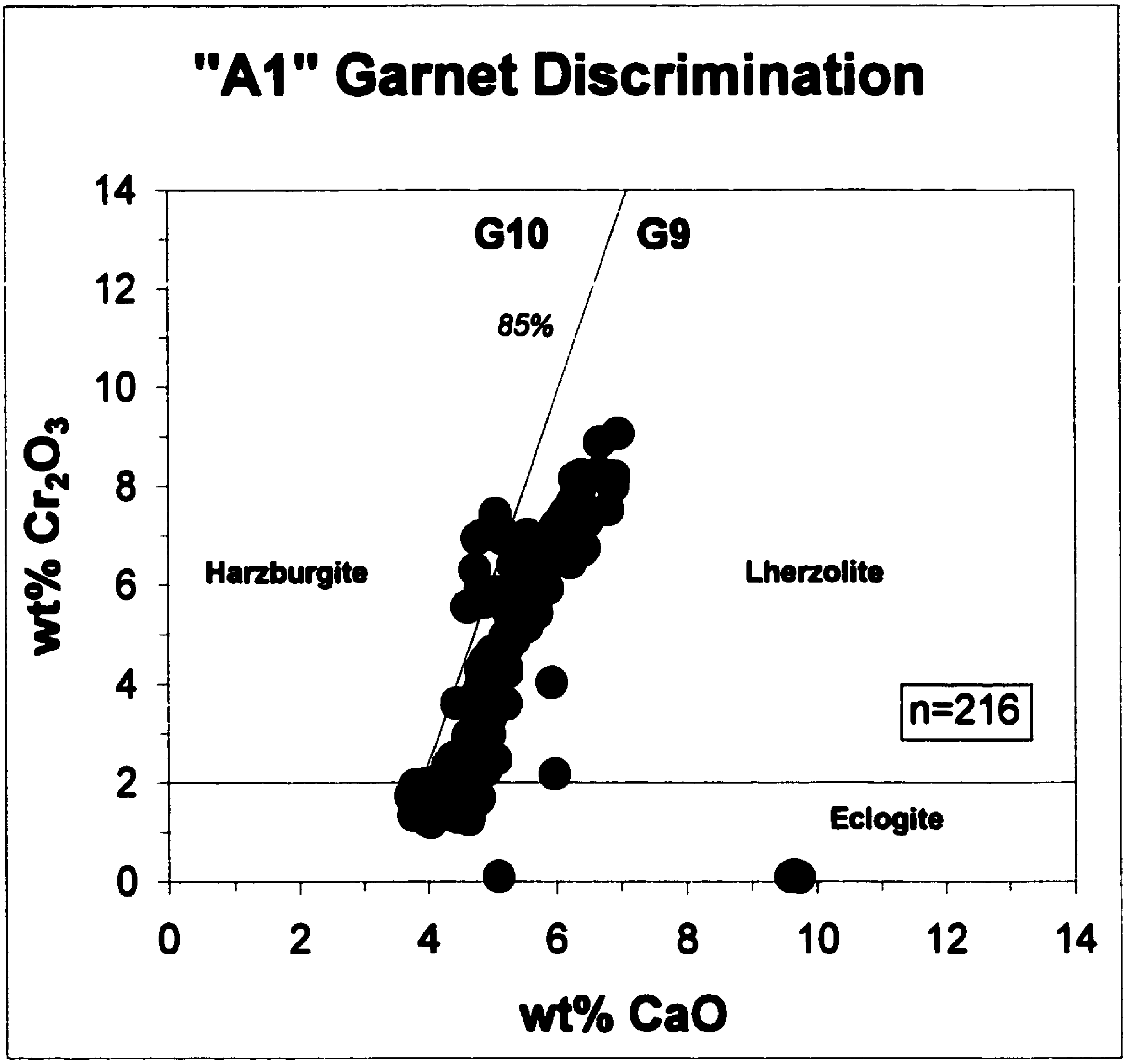

Figure 3-1: Garnet discrimination based on CaO and Cr_2O_3 content, for garnets from pipe "A1" concentrate. Fields based on Gurney (1984).

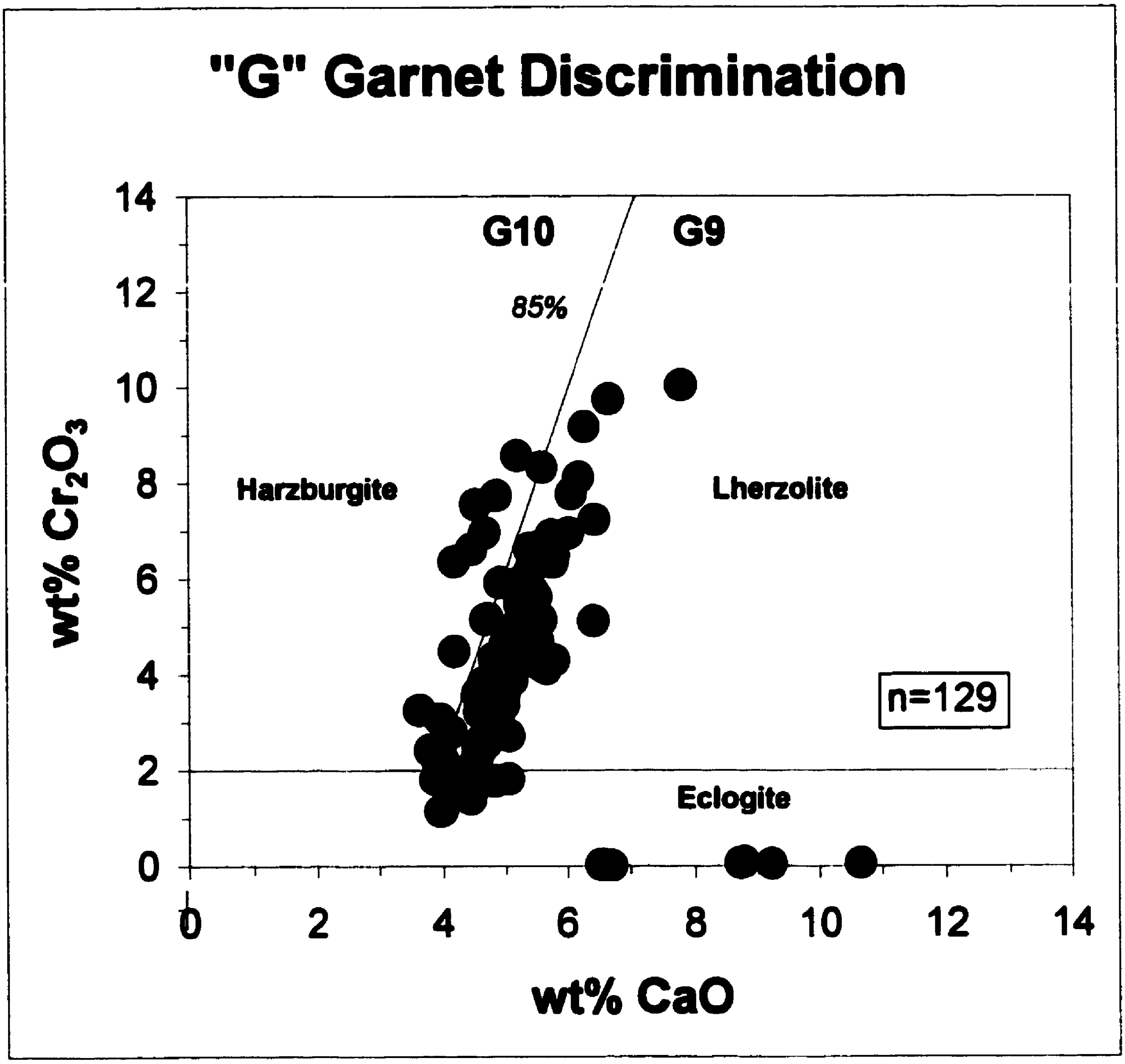

Figure 3-2: Garnet discrimination based on CaO and Cr_2O_3 content, for garnets from pipe "G" concentrate. Fields as in Figure 3-1.

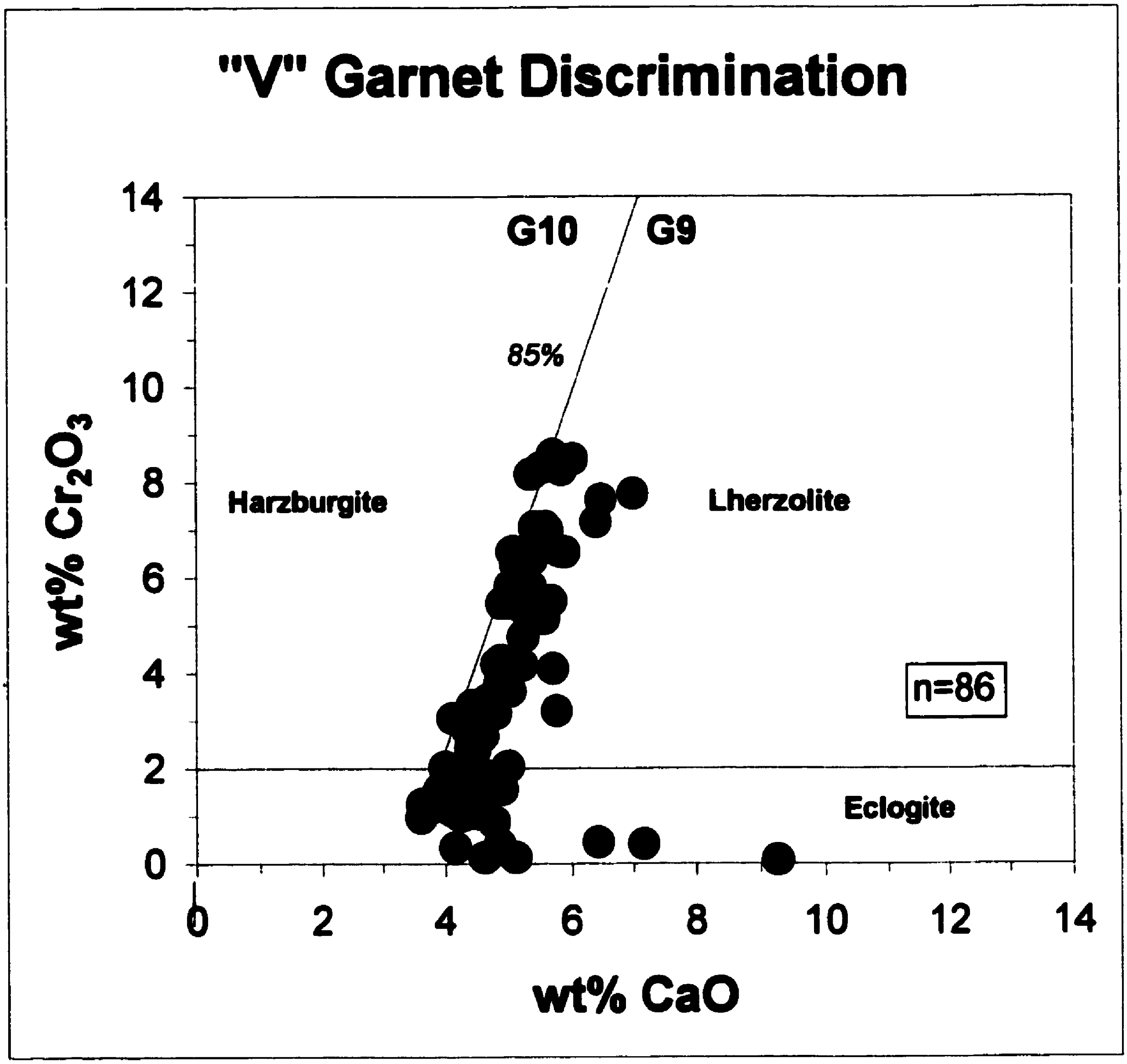

Figure 3-3: Garnet discrimination based on Ca and Cr_2O_3 content, for garnets from pipe "V" concentrate. Fields as in Figure 3-1.

75 – 83 for all three pipes. The majority of the peridotite garnets are lherzolitic (Figures 3-1, 3-2, and 3-3).

Eclogite garnets are differentiated from those of peridotitic paragenesis by MgO and Cr_2O_3 content. Worldwide, eclogite garnets usually contain ≤0.49 wt% Cr_2O_3, but in some cases may contain up to 7.2 wt% Cr_2O_3 (Dawson and Carswell, 1990). Low-Cr_2O_3 garnets with high MgO contents may be considered lherzolitic (Dawson and Carswell, 1990). A cutoff of maximum 2 wt% Cr_2O_3 is used to identify eclogite garnet xenocrysts from concentrate in Figures 3-1, 3-2 and 3-3. This arbitrary cutoff is favoured by Fipke et al. (1995) for prospecting samples (heavy minerals separates from glacial deposits used in drift prospecting for kimberlites), and is used here to distinguish garnets of lherzolite and harzburgite paragenesis from those of megacryst and eclogite paragenesis.
Many Cr-poor megacrysts have Cr_2O_3 contents which coincide with the eclogite and peridotite fields in Figures 3-1, 3-2 and 3-3. Megacryst garnets may be differentiated from peridotite garnets by TiO_2 content (Schulze, 1997 – Figures 3-4 and 3-5). Discrimination between megacryst and eclogitic garnets may be aided by TiO_2 contents, but the division is unclear. Eclogite garnets worldwide have < 0.3 wt% TiO_2 (Dawson and Carswell, 1990). The Cr-poor megacryst garnets at Attawapiskat have very low TiO_2 contents (Schulze, personal communication), so discrimination between the two suites was limited. Garnets from the Attawapiskat concentrates with < 2 wt% Cr_2O_3 and > 0.2 wt% TiO_2 were classified as a Cr-poor megacrysts. The remaining garnets (< 2 wt% Cr_2O_3 and 2 wt% TiO_2) may be eclogitic, crustal, or very low TiO_2 megacrysts.
Garnets from both eclogite and crustal rocks (garnet-bearing amphibolite country rocks) have low Cr_2O_3 contents that fall along the Cr-poor axis in Figures 3-1, 3-2 and 3-3.

a)

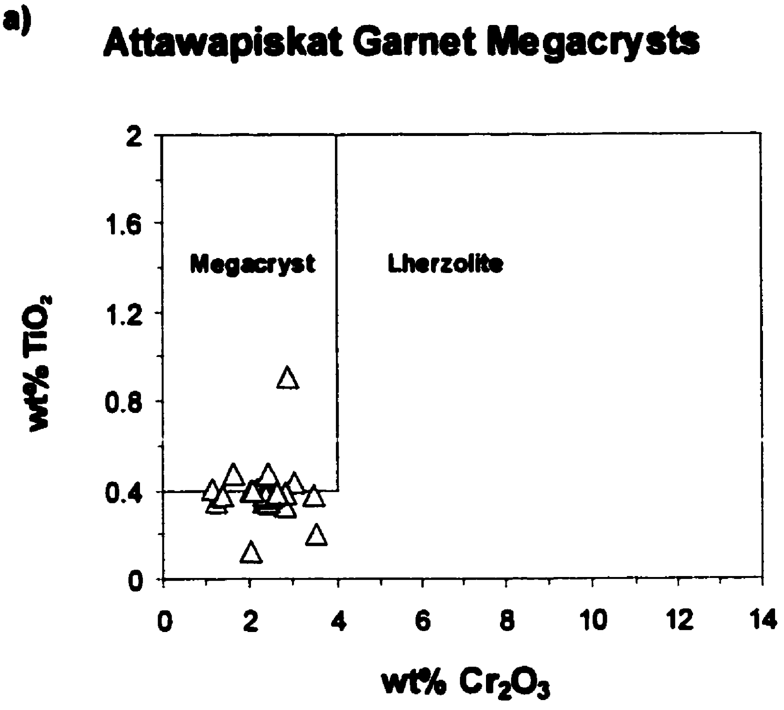

b)

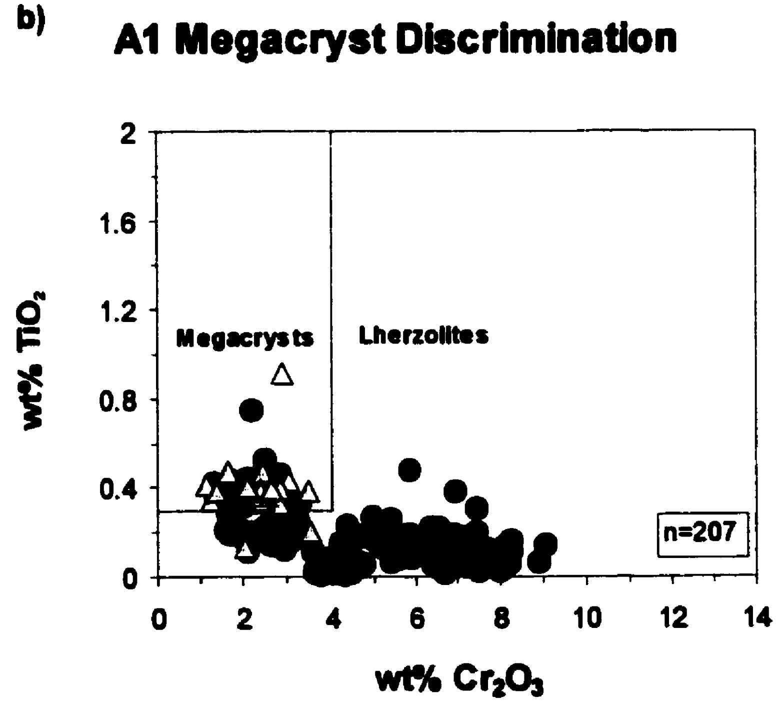

Figure 3-4: a) Attawapiskat pipe "A1" megacryst compositions plotted as Cr_2O_3 vs TiO_2. Attawapiskat megacrysts have lower TiO_2 values than the field for worldwide megacrysts from Schulze (1997). b) Garnets from "A1" concentrate (purple circles), with Attawapiskat megacrysts plotted for comparison (yellow triangles). The field for megacrysts has been lowered to 0.2 wt% TiO_2 to accommodate the low-TiO_2 megacrysts at Attawapiskat. Attawapiskat megacryst data - Schulze (personal communication).

a)

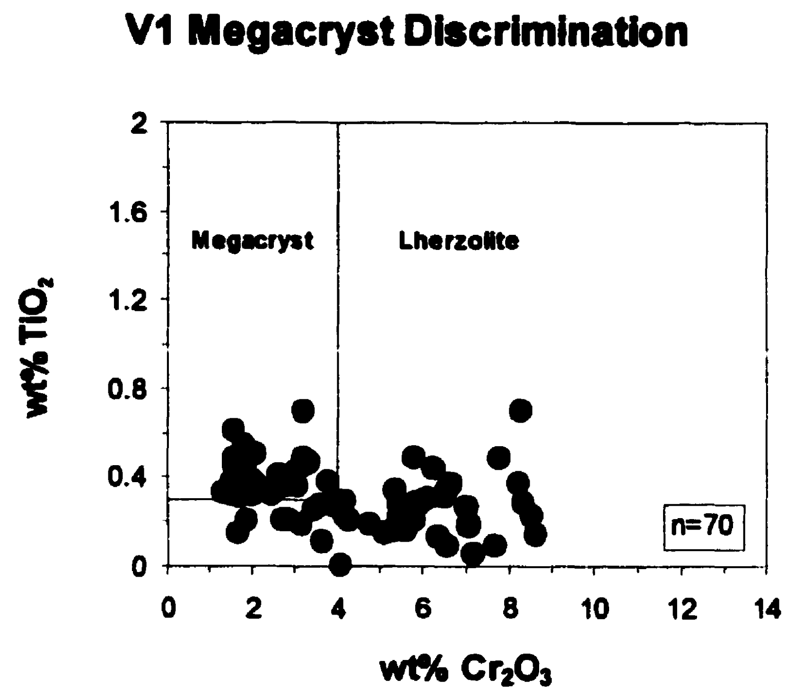

b)

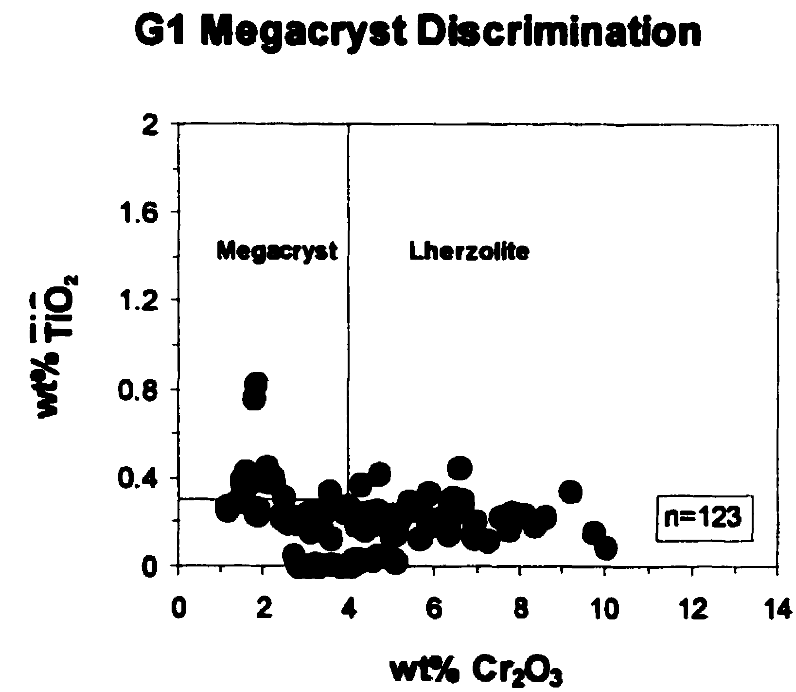

Figure 3-5: Cr_2O_3 vs TiO_2 for garnets from concentrate from **a)** pipe "G" and **b)** pipe "V". Fields for discrimination between lherzolite and megacryst garnets are from Schulze (1997). See text, and Figure 3-4, for discussion.

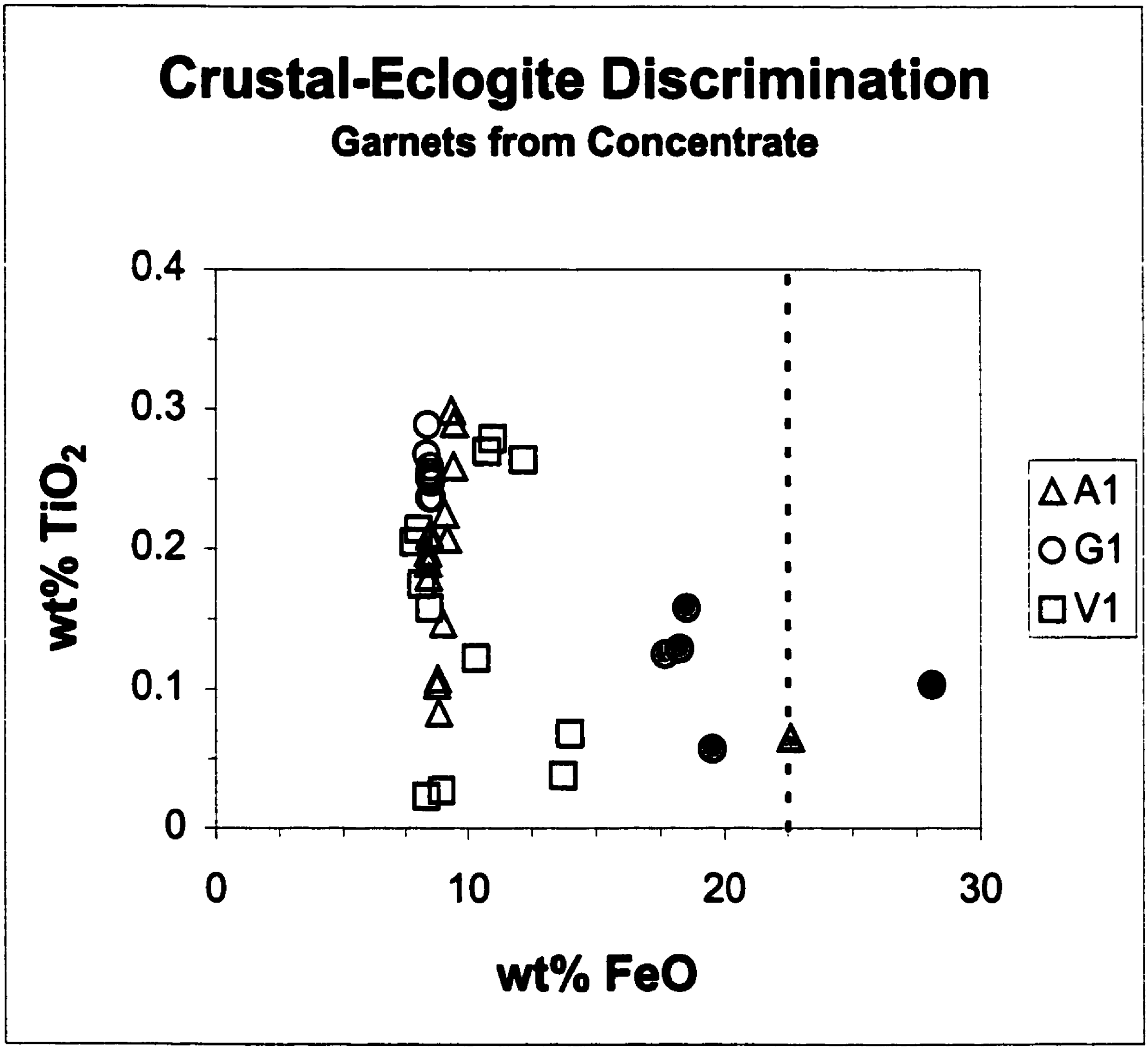

Figure 3-6: Variation in TiO_2 content with FeO (calculated as Fe^{2+}) for low-Cr_2O_3 garnets from pipes "A1", "G" and "V". Fields for eclogite and crustal garnets from Schulze (1997). A region of overlap between the crustal and eclogite fields extends from ~ 18.0-23.0 wt% FeO. *Open symbols* – eclogite; *Black symbols* – crustal; *Grey symbols* – paragenesis undetermined using this discrimination.

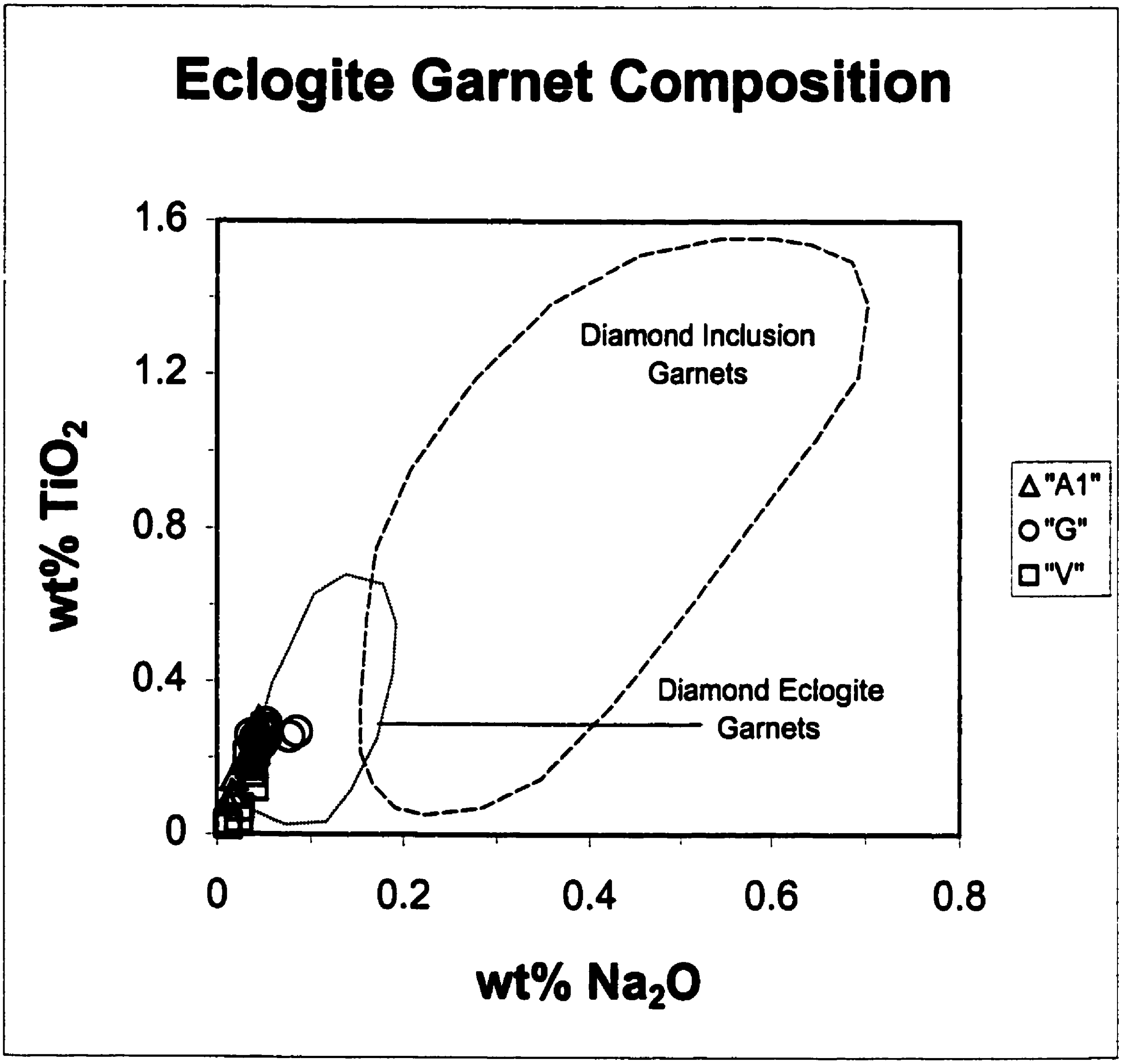

Figure 3-7: Eclogite garnet composition. Garnets occurring as inclusions in diamond have different compositions to garnets from diamond-bearing eclogites (dashed and dotted fields, respectively). Attawapiskat eclogite garnets fall just inside the field of garnets from diamond-bearing eclogites worldwide. Fields from Fipke et al. (1995).

Discrimination between eclogite and crustal garnets may be aided by variation in TiO_2 and FeO contents (Schulze, 1997 – Figure 3-6). The heavy mineral concentrates contained very few crustally-derived garnets. The narrow range of FeO content for the Attawapiskat analyses in the eclogite field is inconsistent with the range of values in eclogite garnets from Schulze (1997). The cluster of FeO values may imply that these garnets are not eclogitic. Eclogite garnet xenocrysts have compositions which correspond to those from diamond-bearing eclogites worldwide (Fipke et al., 1995 – Figure 3-7). Further classification of these garnets is not possible.

3.2.1.2 Clinopyroxene

Bright-green Cr-diopsides from "V" heavy mineral concentrate have 0.24 – 2.6 wt% Cr_2O_3. They are Mg- and Ca-rich (14.7 – 17.6 wt% MgO, 14.1 – 23.1 wt% CaO), and Fe-poor (1.5 – 4.7 wt% FeO, all Fe calculated as Fe^{2+}). Bright green Cr-diopsides are typical of lherzolite and garnet-lherzolite rocks, whereas diopsides from high-temperature sheared lherzolites and eclogites are typically pale green.

The enstatite-diopside solvus has been developed as a geothermometer by several authors (see Finnerty and Boyd, (1987) for review). Equilibrium temperatures calculated for garnet lherzolites from worldwide localities using various enstatite-diopside solvus thermometers often have two "groups", one at low temperature and one at high-temperature, with a "gap" in between (Harte, 1983). The gap in temperature is related to Ca-Mg-Fe contents of the clinopyroxenes. Harte (1983) notes that the gap between the corresponds to Ca/(Ca+Mg) values of ~ 0.43 (~ 1100 °C). A plot of Ca/(Ca+Mg) versus wt% FeO for the Attawapiskat "V" clinopyroxenes reveals there is no gap in the

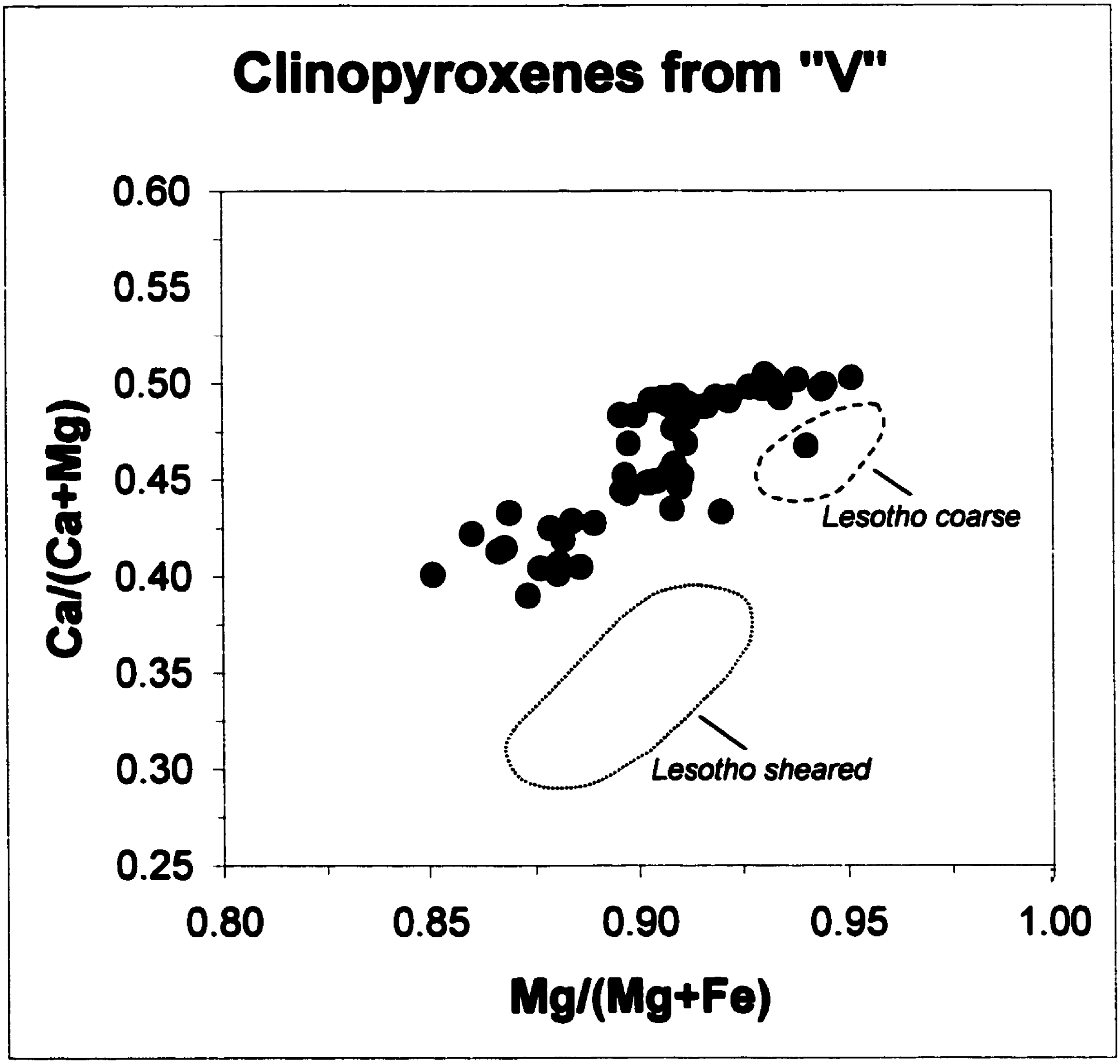

Figure 3-8: Clinopyroxenes from pipe "V" concentrate. Clinopyroxene xenocryst compositions are more ferroan than those clinopyroxenes from coarse and sheared lherzolites from Lesotho. Lesotho Data from Boyd (1973), Cox et al. (1973) and Nixon and Boyd (1973).

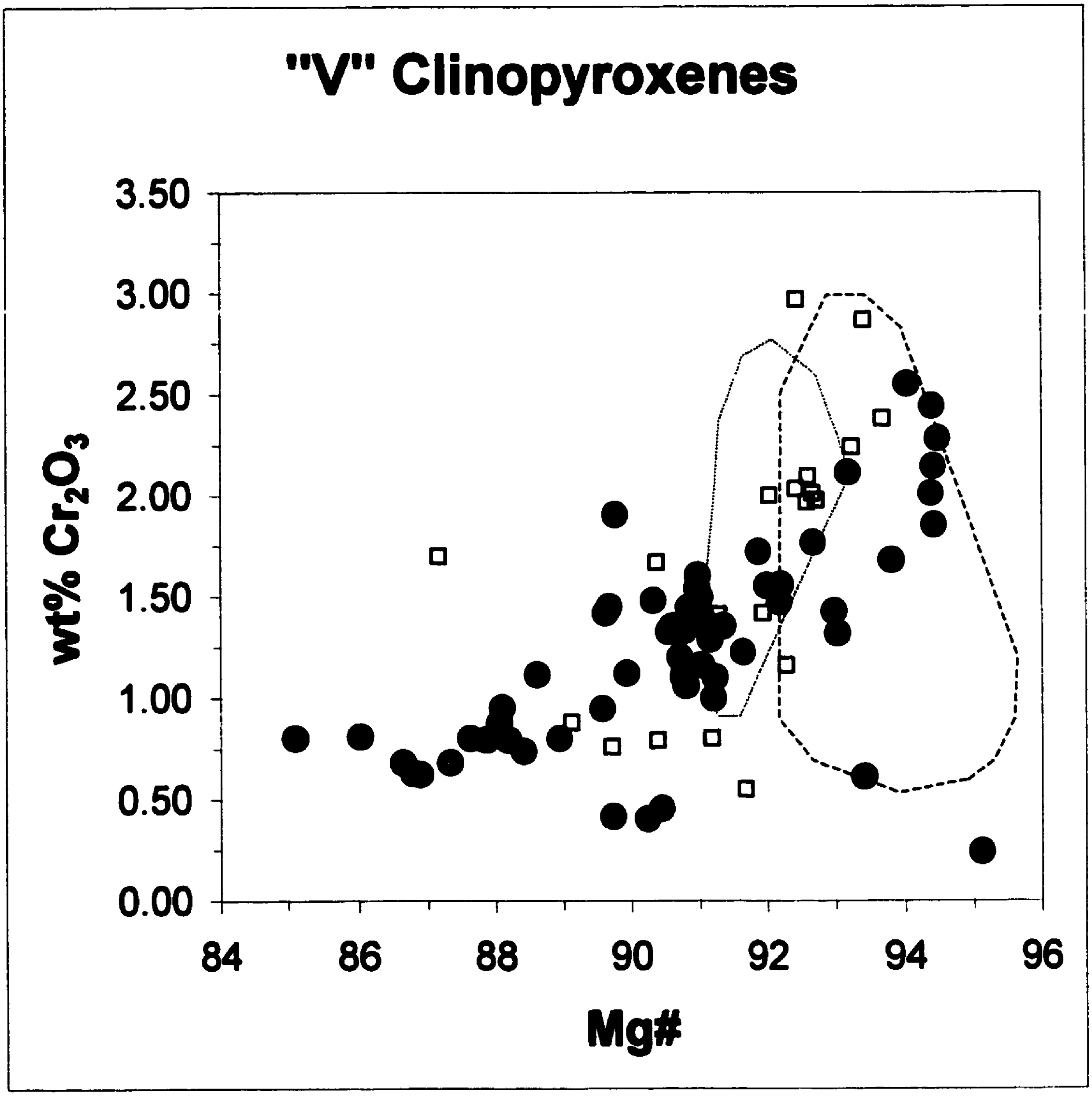

Figure 3-9: Variation in Cr_2O_3 content with Mg# (Mg/(Mg+Fe)), for clinopyroxenes from "V" concentrate. Fields from Kopylova et al., (1999) for clinopyroxenes in xenoliths from Jericho, Northwest Territories, Canada: *dashed* – spinel-garnet coarse-textured peridotite; *dotted* – garnet-bearing coarse-textured peridotite. □ - Kirkland Lake clinopyroxenes from coarse garnet lherzolites (data from Sage, 1996, and Vicker, 1997).

Ca/(Ca+Mg) values (Figure 3-8). The "V" clinopyroxenes are particularly FeO-rich compared to those clinopyroxenes from coarse or sheared Lesotho lherzolites (Boyd, 1973; Cox et al., 1973; Nixon and Boyd, 1973).

Variation in Cr_2O_3 with Mg# for clinopyroxenes is compared with fields for clinopyroxenes from coarse spinel-garnet lherzolite and coarse garnet lherzolite from Jericho, Northwest Territories (Kopylova et al., 1999), and for coarse garnet lherzolite from Kirkland Lake, Ontario (Vicker, 1997) in Figure 3-9.

3.2.1.3 Orthopyroxene

Ten green orthopyroxene grains were randomly picked as green Cr-diopside from the "V" concentrate. These enstatites ($En_{90.7-93.6}$) have Cr_2O_3 contents ranging from 0.20-0.41 wt% Cr_2O_3 and TiO_2 from 0.45 – 1.1 wt% TiO_2 (Figure 3-10a). Mg#'s fall in the restricted range 91.8 – 94.2. Compositions of the 10 Attawapiskat orthopyroxenes fall within the enstatite diamond inclusion field of Fipke et al. (1995 – Figure 3-10b), as do orthopyroxenes from many mantle peridotites. Compositions are similar to orthopyroxenes from worldwide sources (Nixon, 1987).

3.2.1.4 Chromite

The Cr_2O_3 contents of 77 spinels from pipe "V" concentrate range from 47.1 – 63.8 wt% Cr_2O_3, with 18.9 – 40.4 wt% FeO (calculated as total Fe), and 7.0 – 12.0 wt% MgO. Variation in Cr/(Cr+Al) with $Fe^{2+}/(Fe^{2+}+Mg)$ shows that chromite compositions fall in the field of lherzolite and harzburgite chromites defined by Haggerty (1995 - Figure 3-11). The extensive overlap in the lherzolite-harzburgite field and diamond

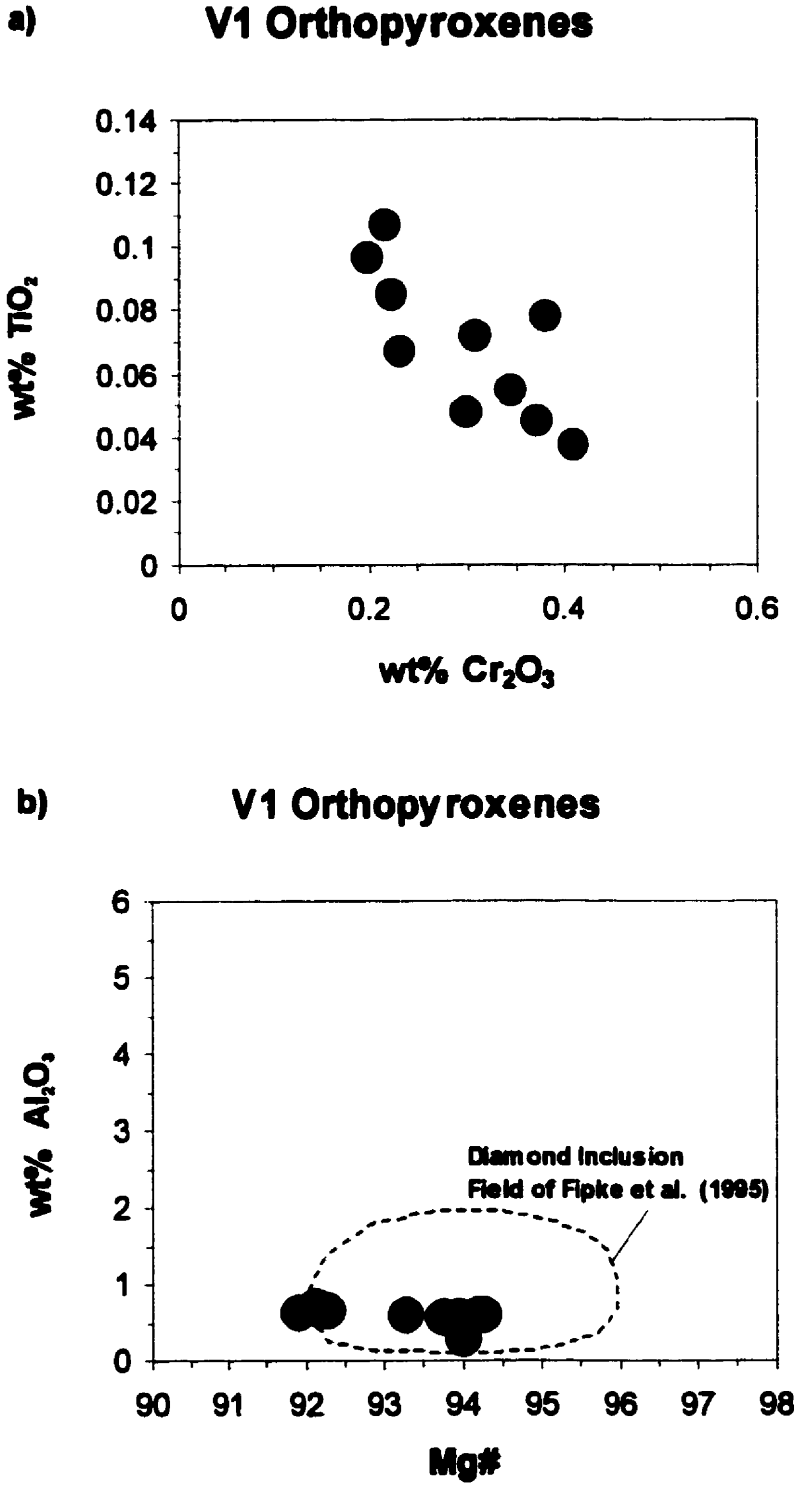

Figure 3-10: Orthopyroxenes in xenoliths. **a)** Variation in wt% TiO_2 with wt% Cr_2O_3. **b)** Mg# (mol% Mg/(Mg+Fe) x 100%) vs wt% Al_2O_3. Orthopyroxene compositions fall within the field of diamond inclusions of Fipke et al. (1995).

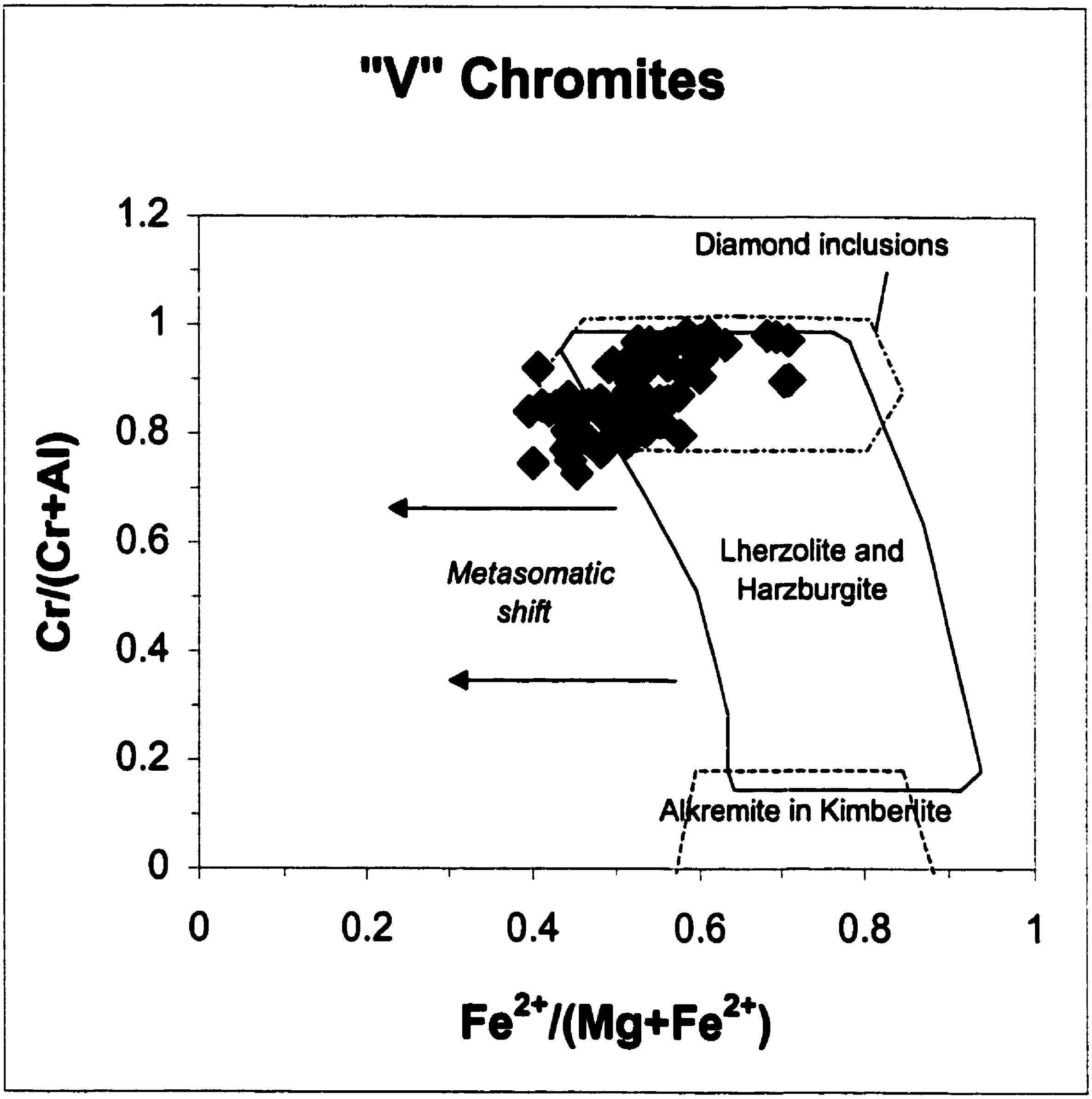

Figure 3-11: Compositions of chromites from "V" concentrate, with fields from Haggerty (1995) superimposed. The chromites from concentrate fall within the region of overlap between the lherzolite-harzburgite and diamond inclusion fields. The same chromite compositions plotted as wt% MgO vs wt% Cr_2O_3 in Figure 3-12 fall well outside of the diamond inclusions field of Fipke et al. (1995). The significance of the Haggerty (1995) diamond inclusion field is uncertain.

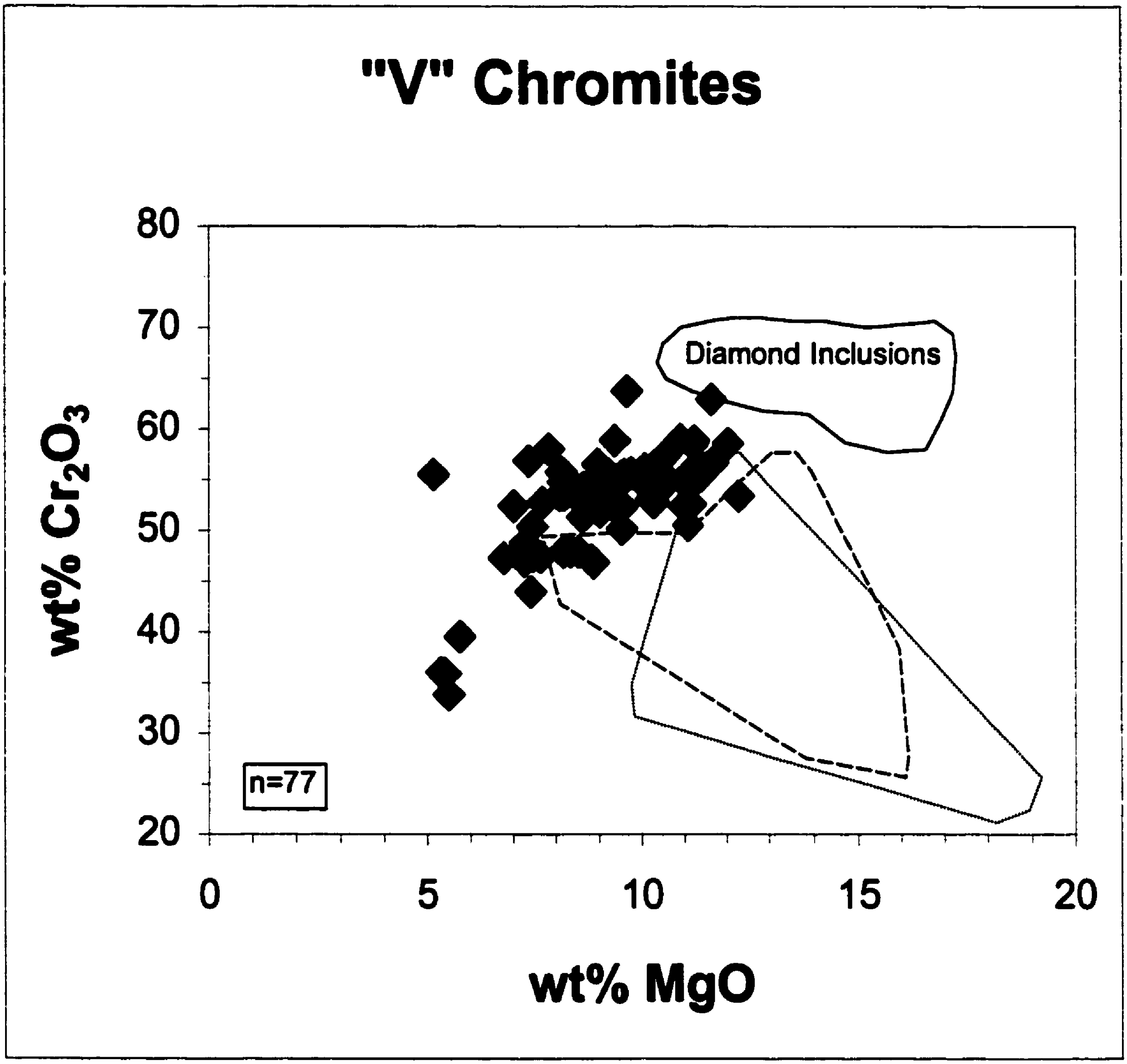

Figure 3-12: Pipe "V" chromite compositions compared to those from Kirkland Lake (*dotted*) and Ile Bizard (*dashed*) fields. The "V" chromites have a negative MgO-Cr_2O_3 trend compared to the two other Canadian localities. The "V" chromite compositions fall well outside the field of diamond inclusions defined by Fipke et al. (1995). Data for Kirkland Lake and Ile Bizard from Fipke et al. (1995).

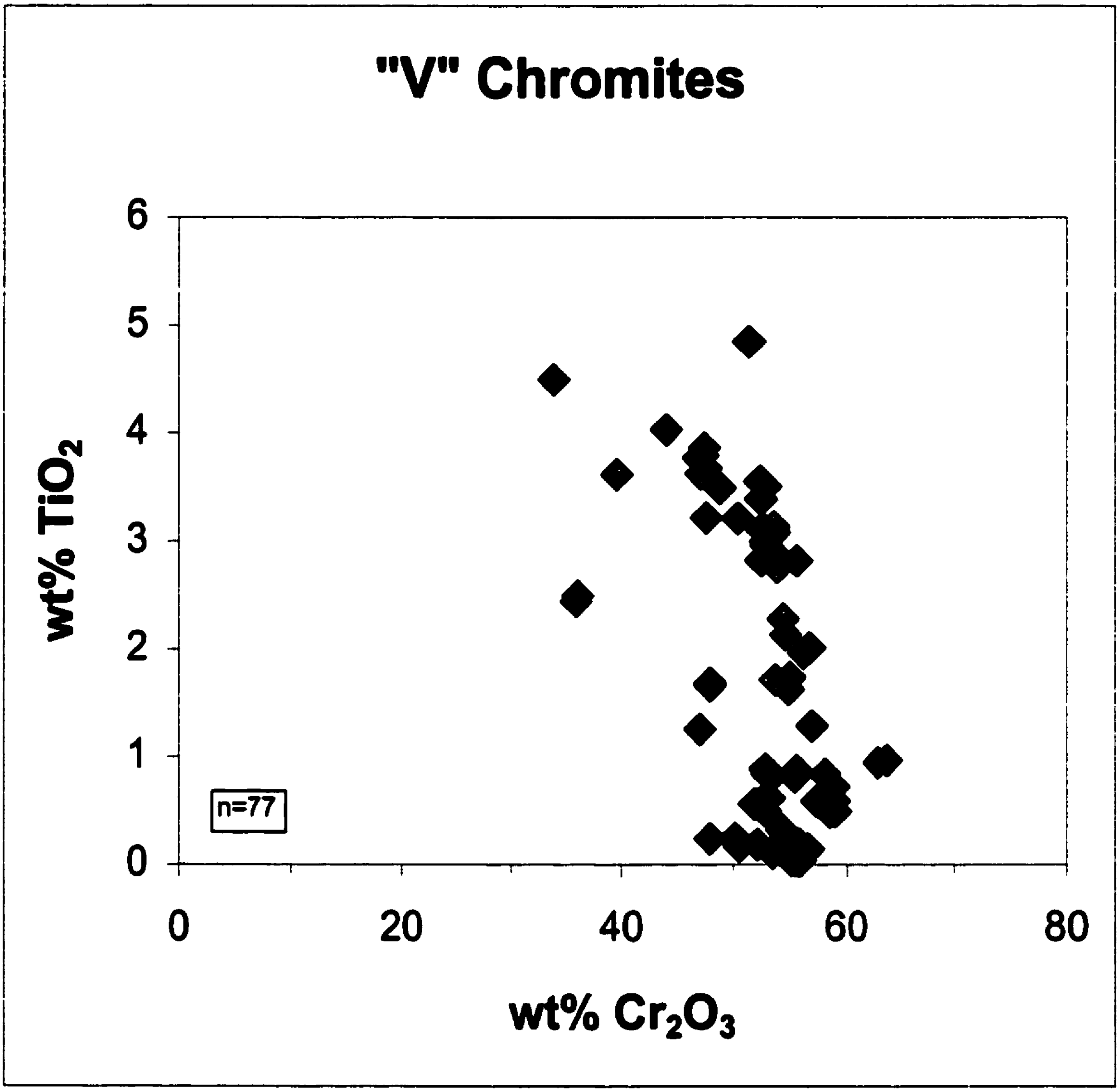

Figure 3-13: Variation in wt% TiO_2 with wt% Cr_2O_3 for "V" chromites. Compositions decrease in TiO_2 with increasing Cr_2O_3.

inclusion field of Haggerty (1995) is unexplained. Figure 3-12, a plot of MgO vs Cr_2O_3 contents for the same chromites, shows they fall well outside of the field for chromites as diamond inclusions defined by Fipke et al. (1995). The Fipke et al. (1995) discriminant is more rigorous than that of Haggerty (1995). Chromites from "V" concentrate have a positive Cr-Mg-enrichment trend compared to chromites from Kirkland Lake, Ontario, and Ile Bizard, Quebec (Fipke et al., 1995 – Figure 3-12).

The "V" chromites from concentrate show a weak negative trend on a plot of Cr_2O_3 versus TiO_2 (Figure 3-13). Chromites with < 2 wt% TiO_2 have similar compositions to chromites in the Attawapiskat xenoliths (see section *3.3.2.3*)

3.2.2 Xenoliths: Primary and Metasomatic/Secondary Assemblages

In addition to the four primary silicate phases in peridotites (lherzolite – olivine + clinopyroxene + orthopyroxene ± garnet, harzburgite – olivine + orthopyroxene ± garnet), the majority of the xenoliths have metasomatic assemblages of phlogopite + amphibole ± chromite and fine-grained alteration material, or clinopyroxene only, as well as secondary minerals such as serpentine. Where present, orthopyroxene is heavily altered to secondary serpentine. Only clear, unaltered orthopyroxene cores were analyzed.

3.2.2.1 Primary Minerals: Olivine

Olivines from lherzolites and harzburgites are Mg-rich, with Mg#'s ranging from 90.1 – 92.7 ($Fo_{90.3\text{-}92.9}$). These values are slightly lower than those for olivines from southern Africa xenoliths (Kimberley lherzolites (coarse and sheared) and harzburgites,

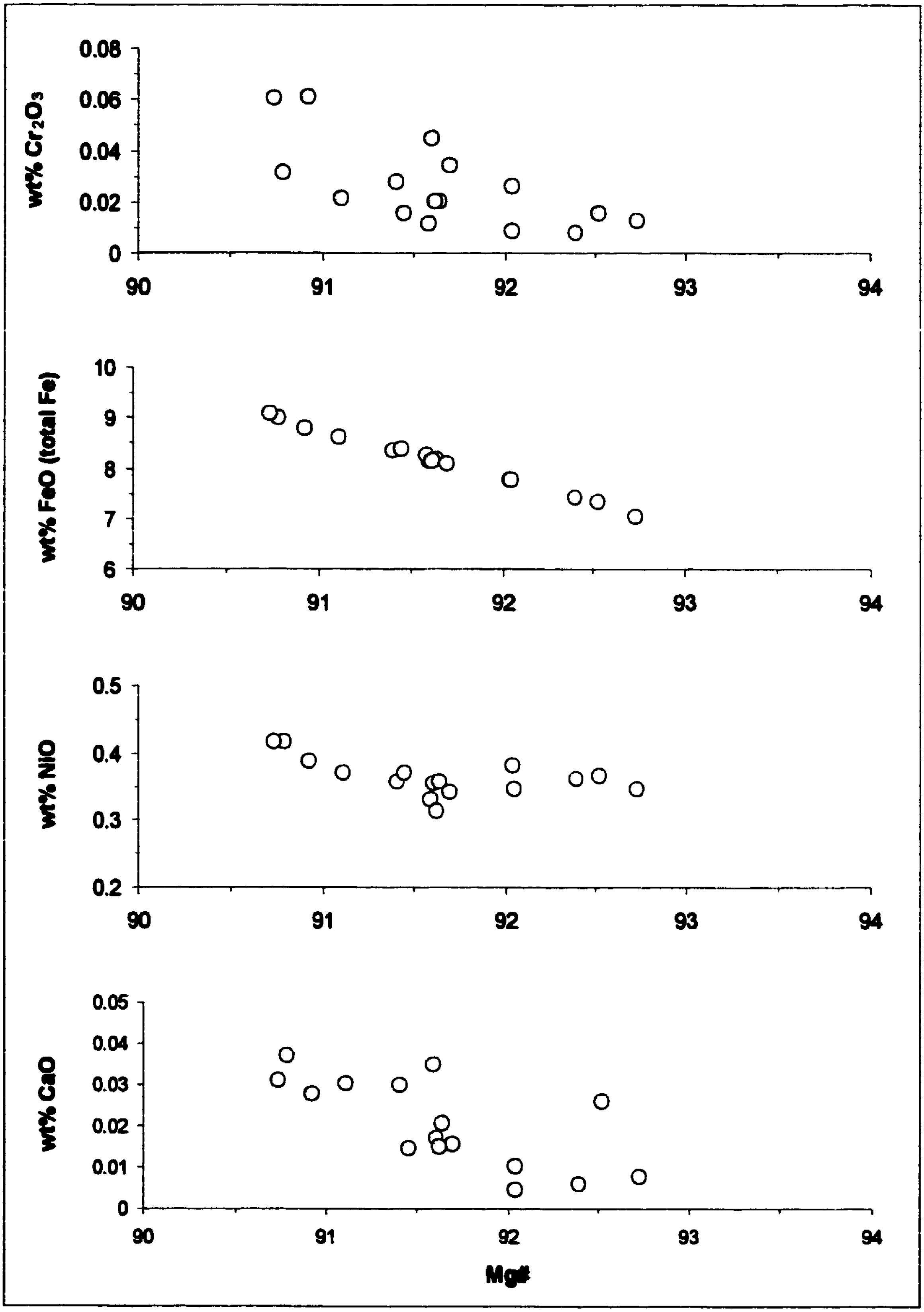

Figure 3-14: Chemical trends in olivines from xenoliths. All of the olivines are MgO-rich, and depleted in CaO, FeO, Na_2O, and Cr_2O_3.

Mg#'s 91 – 94 (Boyd and Nixon, 1978); Kimberley harzburgites, Mg#'s 93 – 95 (Schulze 1995); Finsch, average Mg# 92.9, (Shee et al., 1992); Northern Lesotho, Mg#'s 91 – 94 (Nixon and Boyd, 1973)). Attawapiskat olivine Mg#'s are similar to those from other Canadian localities (Jericho, Slave Province, Northwest Territories, Mg#'s 88.0 – 93.0 (Kopylova et al., 1999); Grizzly and Torrie, Slave Province, Northwest Territories, Mg#'s 90.6 – 93.8 (MacKenzie and Canil, 1999); Kirkland Lake, Ontario, Mg#'s 85.0 – 93.3 (most > 90), (Vicker, 1997)). Olivine in contact with amphibole in garnet harzburgite 13-97-78 has grain rims slightly depleted in MgO, CaO and Cr_2O_3, and enriched in FeO, compared to its core composition.

3.2.2.2 Garnet

Garnets in xenoliths are markedly depleted in CaO compared to garnet xenocrysts from concentrate (garnets from heavy mineral separates from pipes "A1", "G" and "V" are dominantly lherzolitic – see section 3.1). Six xenoliths may be classified as harzburgite based on CaO and Cr_2O_3 content of garnet (Dawson, 1980 – Figure 3-15). Sample 13-95-59 plots to the low-CaO side of the 85% line in Figure 3-15, at ~ 2 wt% Cr_2O_3. Although this garnet analysis falls within the eclogite field in Figure 3-15, the xenolith contains olivine, so it is in fact a Cr-poor harzburgite fragment. All xenoliths containing garnet with > 2 wt% Cr_2O_3 are classified as either lherzolitic or harzburgitic. Mg#'s for the lherzolite and harzburgite garnets range from 80.2 – 86.5.

Three xenoliths containing orange garnet were analyzed and their compositions fall in the eclogite field in Figure 3-15. Paragenesis (either crustal or eclogitic) was determined using TiO_2 and FeO contents of the garnets. Two of the xenoliths (13-95-42

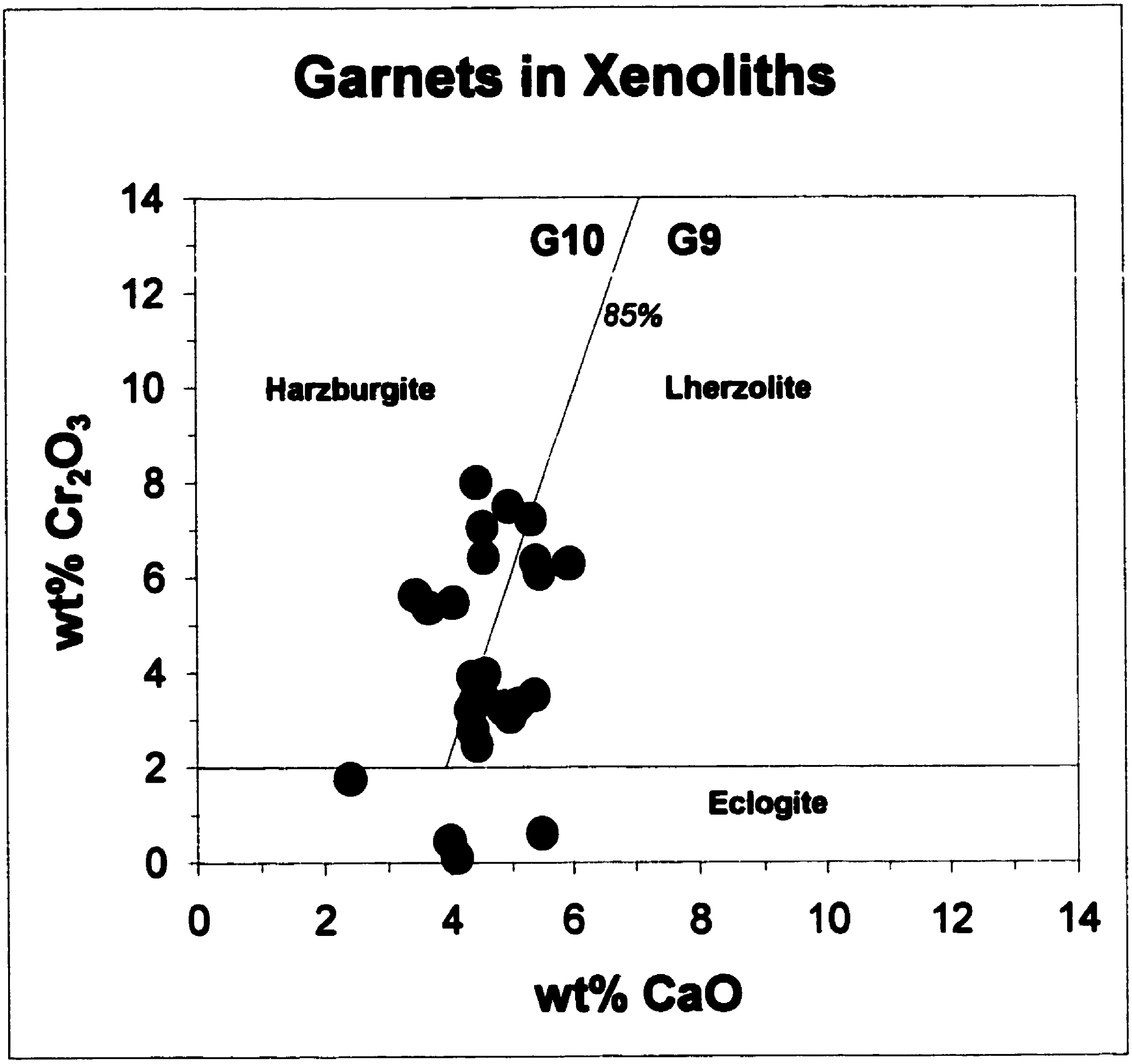

Figure 3-15: Garnet discrimination based on CaO and Cr_2O_3 contents of garnets in xenoliths. Fields as in Figure 3-1.

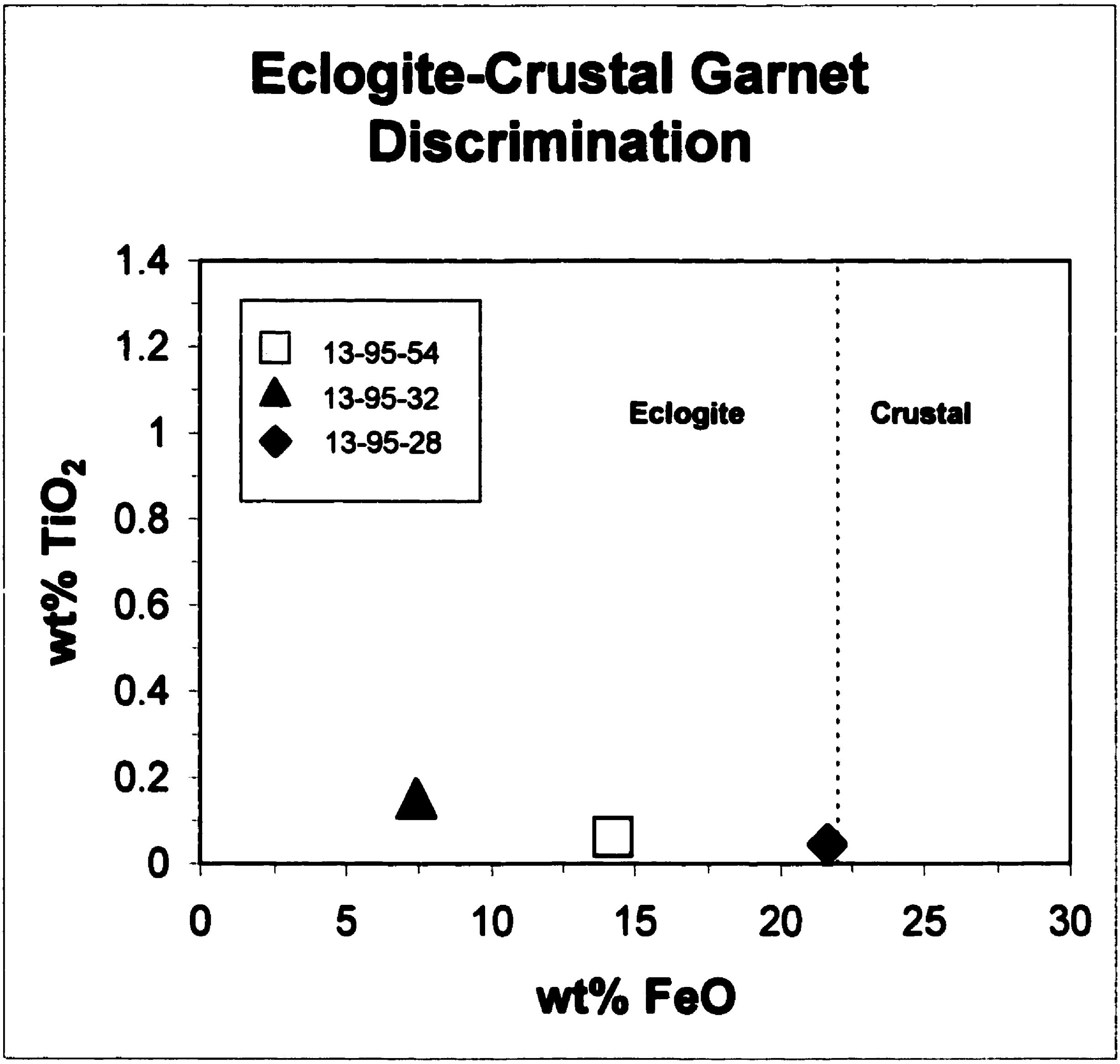

Figure 3-16: Eclogite/crustal garnet discrimination for garnets that plot in the eclogite field in Figure 3-15. Samples 13-95-54 and 13-95-32 are eclogites; sample 13-95-28 falls in the region of overlap between the two fields. This sample contains amphibole and phlogopite, and is probably crustally derived – see text for discussion. Eclogite and crustal fields after Schulze (1997).

and 13-95-54, both pipe "G") contain bright green diopside. Garnet compositions for these two samples fall within the field of eclogite garnets defined by Schulze (1997) based on their TiO_2 and FeO contents (Figure 3-16). The third xenolith (13-95-28, pipe "G"), contains bright green amphibole and large flakes of green-brown phlogopite. The composition of the garnet in xenolith 13-95-28 falls in a region of overlap between the eclogite and crustal fields in Figure 3-16. The high FeO content of the garnet and the presence of amphibole and phlogopite suggest this sample is of crustal origin, so it will not be discussed further. Mg#'s for the eclogite garnets are 84.0 (13-95-32) and 67.7 (13-95-54).

Three garnets are compositionally zoned. Samples 13-97-83 (pipe "A1"), 13-102-05 and 13-102-12 (both pipe "X"), have decreasing Cr_2O_3 and CaO from core to rim. Samples 13-97-83 and 13-102-12 contain other garnet grains that do not have chemical zoning.

3.2.2.3 Clinopyroxene

Two xenoliths (13-102-05 and 13-102-12, both pipe "X") contain one clinopyroxene grain each. Both grains are Cr-diopsides, and have compositions corresponding to clinopyroxenes from coarse garnet lherzolites worldwide (Harte, 1983; Meyer, 1987; Nixon, 1987; Haggerty, 1995). No compositional zoning was noted. The two xenoliths do not contain orthopyroxene, so thermobarometric calculations were not possible.

3.2.2.4 Orthopyroxene

Orthopyroxene grains are Mg-rich ($En_{91.3-93.1}$), but have higher FeO contents than the 10 green orthopyroxene grains recovered from pipe "V" concentrate (Figure 3-17). The orthopyroxene compositions form two small "clusters", one with Mg# ~92, the other with Mg# ~93.0 – 93.5 (Figure 3-17). The two orthopyroxenes with Mg# ~92 are from garnet harzburgite fragments 13-95-35 (pipe "G") and 13-97-78 (pipe "A1"). The three orthopyroxenes with Mg#'s between 93.0 and 93.5 are from garnet lherzolites 13-95-33 (pipe "G") and 13-97-83 (pipe "A1"), and garnet harzburgite 13-95-67 (pipe "G"). Orthopyroxenes from both lherzolite and harzburgite samples fall within the field of orthopyroxene diamond inclusions defined by Fipke et al. (1995).

Some of the orthopyroxene grain cores appear to have very slight enrichment in Cr_2O_3 and TiO_2 where they are in direct contact with secondary serpentine replacing the grain rim. No change in Al_2O_3 content at the contact between the fresh orthopyroxene core and serpentinized rim that could affect geobarometric calculations was observed.

3.2.3 Metasomatic Minerals

Metasomatic amphibole and phlogopite, with or without associated chromite, partially or wholly replace garnet in the majority of the xenoliths recovered from Attawapiskat kimberlite. Metasomatic clinopyroxene partially replaces garnet in some garnet – olivine pairs.

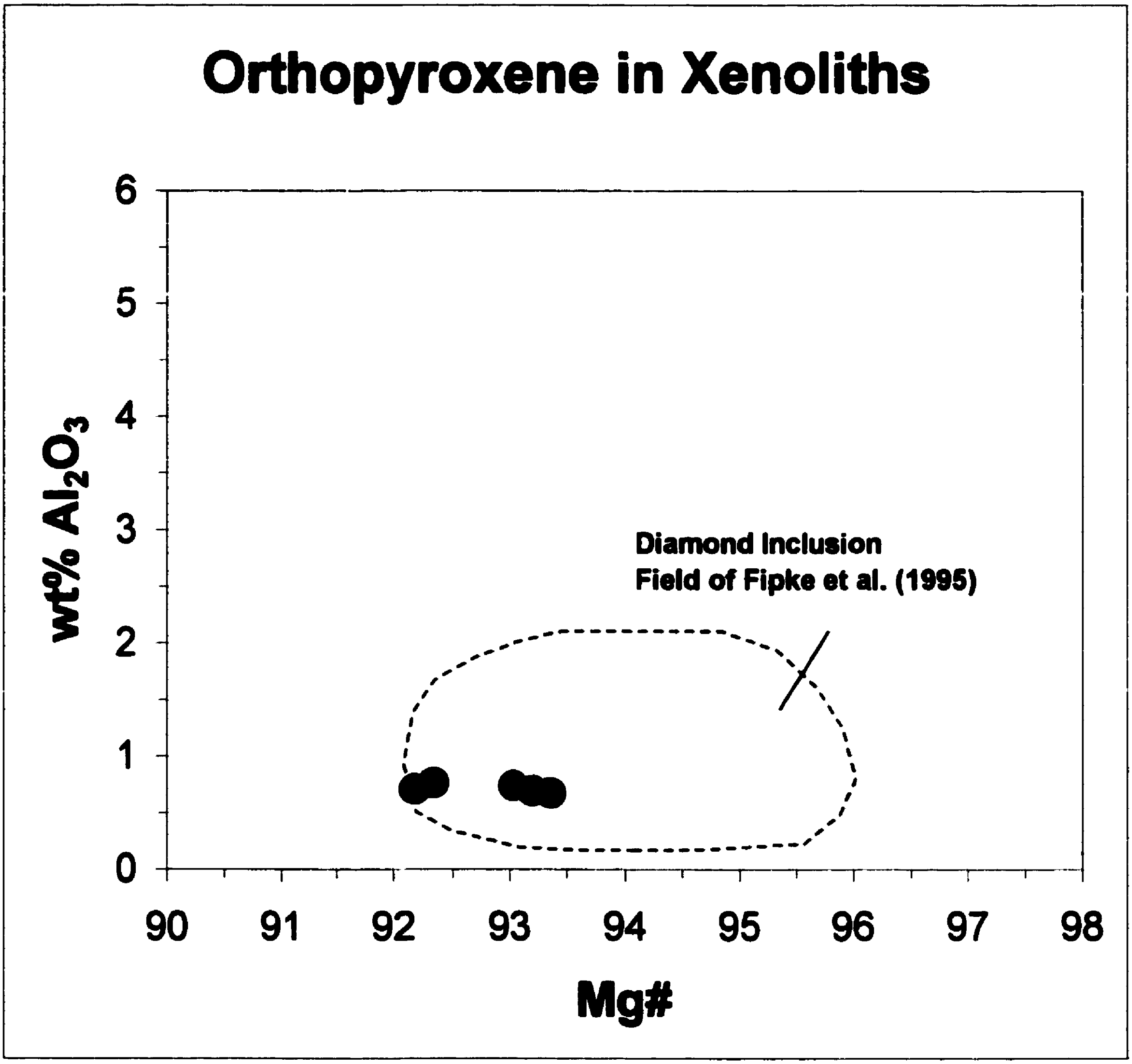

Figure 3-17: Orthopyroxene compositions from coarse peridotite xenoliths. Two "groups" of orthopyroxene occur, one with Mg# ~92 (garnet harzburgites 13-95-35 and 13-97-78), the other with Mg# 93.0-93.5 (garnet lherzolites 13-95-33 and 13-97-83, and garnet harzburgite 13-95-67). Orthopyroxene compositions fall within the field of diamond inclusions of Fipke et al. (1995).

3.2.3.1 Amphibole

Amphibole replacing garnet in sample 13-95-49 has high Al_2O_3 and CaO contents (13.2 wt% Al_2O_3 and 10.0 wt% CaO), and moderate to high MgO and FeO contents (18.4 wt% MgO and 3.4 wt% FeO). The amphibole may be classified as a pargasite (Leake et al., 1997). The pargasite has high chrome content (2.2 wt% Cr_2O_3).

3.2.3.2 Phlogopite

Phlogopites have 0.4-2.1 wt% Cr_2O_3 and up to 1.1 wt% TiO_2. Totals for microprobe analysis are somewhat lower than expected for phlogopites containing ~4 – 5 wt% H_2O. The phlogopite grains in xenoliths from Attawapiskat are heavily altered, and so yield low oxide totals during electron microprobe analysis (Appendix B). The phlogopite grains are poor in the volatile elements Cl and F (up to 0.15 wt% Cl and 0.4 wt% F). Phlogopite grains occurring with amphibole ± chromite to replace garnet have slightly elevated MgO and Na_2O contents, and lower Cr_2O_3 contents, compared to the fine-grained phlogopites filling veins and fractures.

Figure 3-18 depicts phlogopite compositions in terms of TiO_2 and Cr_2O_3. The fields in Figure 3-18 are from Erlank et al. (1987) and Field et al. (1989), who correlate texture and accompanying metasomatic assemblage to phlogopite composition. "Stage A" and "Stage B" phlogopites are of metasomatic origin; "Stage A" phlogopites occur with amphibole, "Stage B" with clinopyroxene (Erlank et al., 1987; Field et al., 1989). Secondary phlogopites are the result of host-rock reaction with a volatile-rich fluid during kimberlite eruption (Erlank et al., 1987; Field et al., 1989).

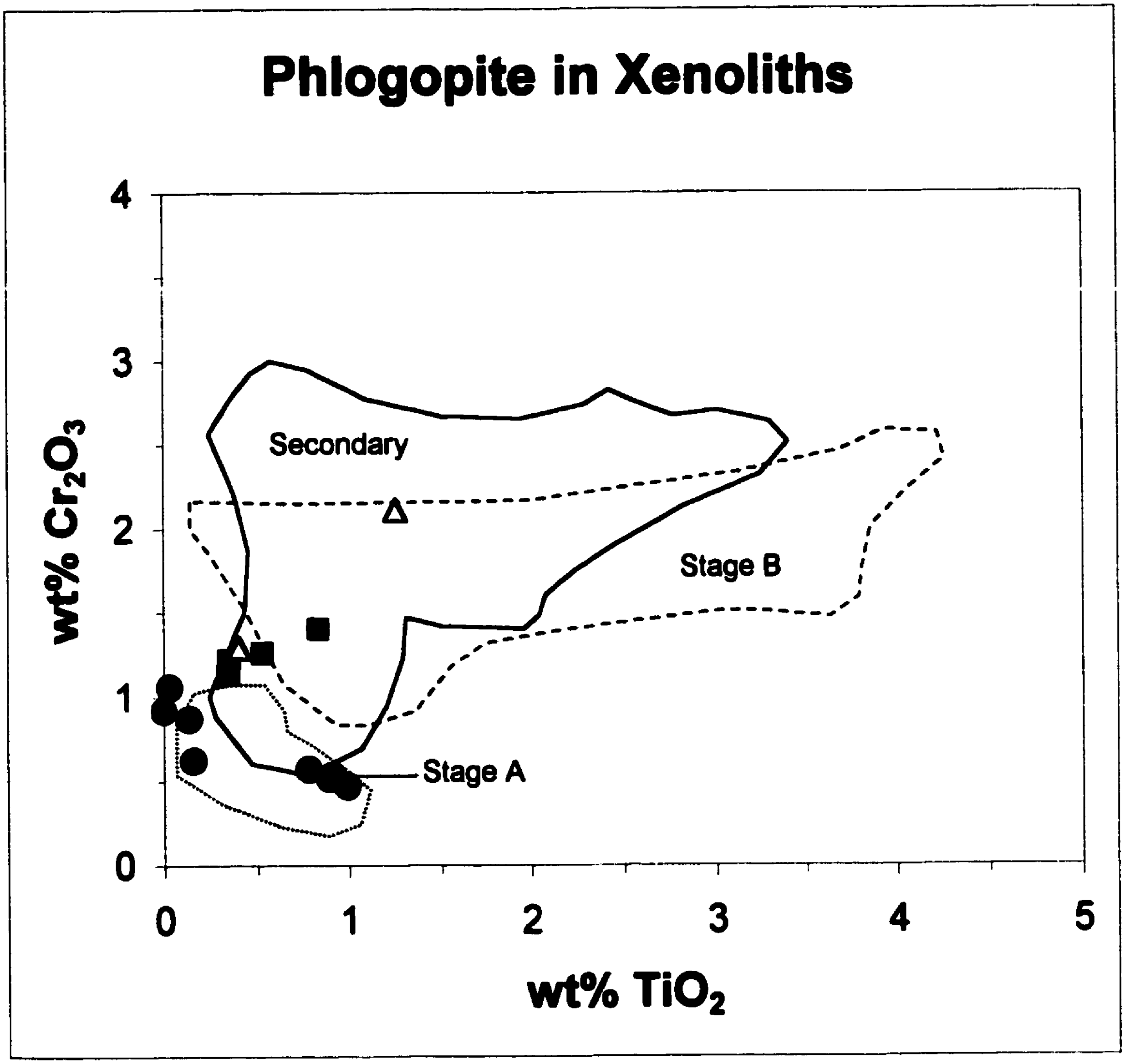

Figure 3-18: Fields of phlogopite compositions from upper mantle sources (after Field et al., 1987): *dotted* – Stage A (paragenetically early, co-existing with amphibole); *dashed* – Stage B (paragenetically late, co-existing with diopside); *solid* – Secondary (due to late-stage metasomatism in the source region). Symbols: *red* – textural type "1" (fine-grained mantles on garnet); *yellow* – textural type "2" (vein filling); *green* – textural type "3" (metasomatically replacing garnet, with or without chromite inclusions). Fields for Stage A, Stage B and Secondary phlogopites based on Erlank et al. (1987), Field et al. (1987) and Haggerty (1995).

Phlogopites occurring with amphibole ± chromite to replace garnet in the Attawapiskat xenoliths fall within or near the "Stage A" field of Erlank et al. (1987) and Field et al. (1989 – Figure 3-18). Two of these phlogopites have low TiO_2 contents (0.032 and 0.0wt% TiO_2, which is below minimum detection for the microprobe analyses), and fall near the "Stage A" field. Phlogopite occurring as textural types "2" and "3" (as mantles on garnets and as vein-filling material, respectively) have higher Cr_2O_3 contents than textural type "1" phlogopites.

Compositions of textural type "2" and "3" phlogopites fall in the "Secondary" and "Stage B" fields in Figure 3-18. None of these phlogopites occur in association with the metasomatic clinopyroxene (see below), so they may be classified as "Secondary" based on Erlank et al. (1987) and Field et al. (1989).

3.2.3.3 Clinopyroxene

Metasomatic clinopyroxenes are Cr-rich (2.7 – 5.0 wt% Cr_2O_3), Ca-rich (14.3 – 16.9 wt% CaO), and Fe-rich (2.6 – 4.4 wt% FeO) compared to primary clinopyroxenes from Lesotho coarse-lherzolites (Figure 3-19). The metasomatic clinopyroxenes have particularly high Na_2O contents compared to primary clinopyroxenes from Lesotho lherzolites (Boyd, 1973; Cox et al., 1973; Nixon and Boyd, 1973). Compositions are similar to those of clinopyroxenes recovered from "V" concentrate (Figure 3-18).

3.2.3.4 Chromite

Chromite compositions have been correlated with the three textural types of chromite occurring in xenoliths as described in Chapter 2.

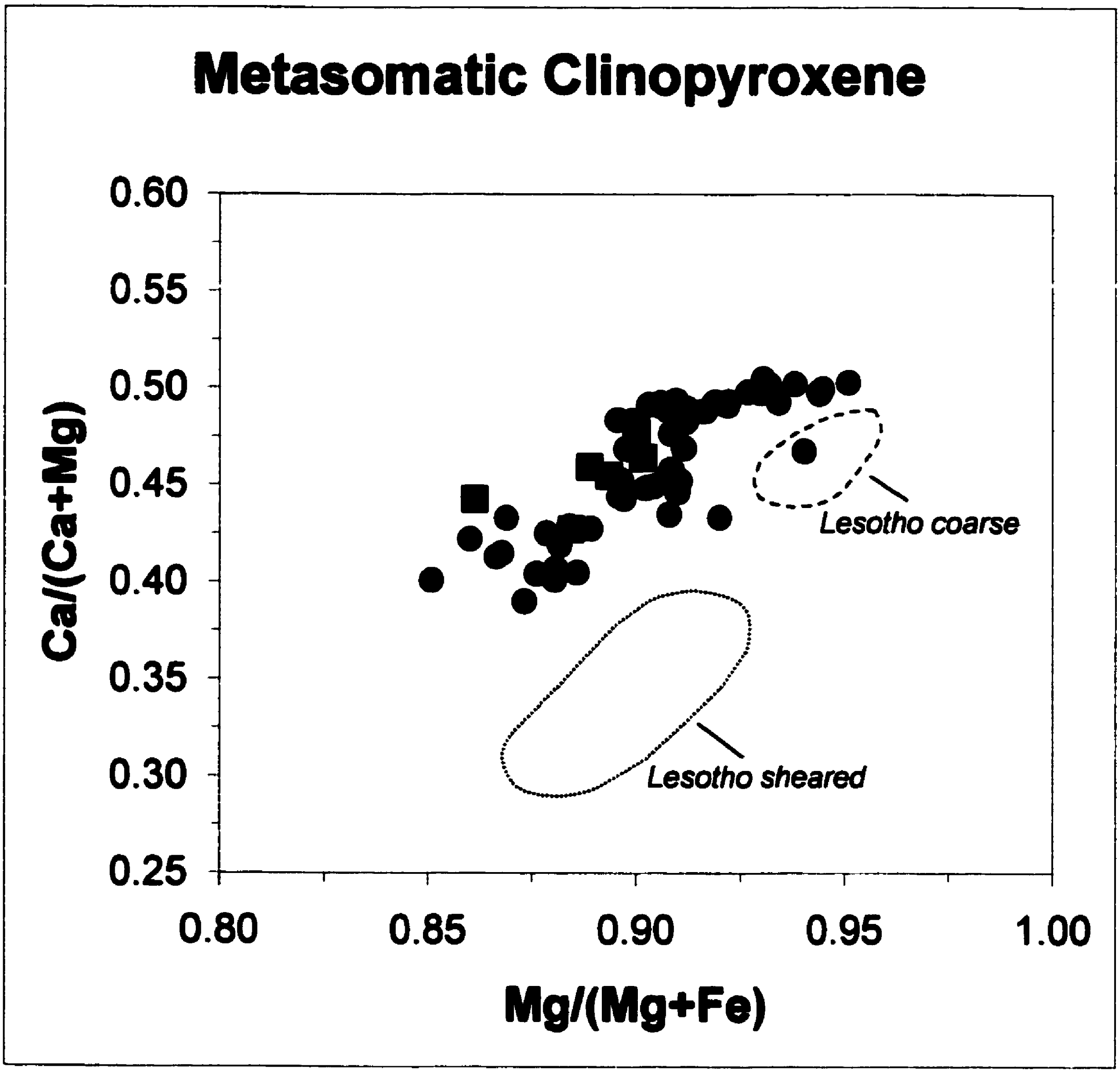

Figure 3-19: Metasomatic clinopyroxene compositions (*red squares*) compared to clinopyroxenes from "V" concentrate (*green circles*). Clinopyroxenes replacing garnet in cognate xenoliths have similar Mg/(Mg+Fe) and Ca/(Ca+Mg) values to those occurring as xenocrysts in the kimberlite. The close compositional correlation between the two groups suggests most of the clinopyroxene xenocrysts may be of metasomatic origin.

A plot of Cr_2O_3 vs TiO_2 content of the Attawapiskat chromites reveals differences in chemistry based on textural occurrence (Figure 3-20). All chromites have 0.0 – 2.2 wt% TiO_2 and 40.1 – 576.7 wt% Cr_2O_3. The primary texture chromites have compositions which overlap secondary texture chromites (Figure 3-20).

With the exception of three outliers, secondary chromites have >0.6 wt% TiO_2 (Figure 3-20). Two of the outliers have 0.02 and 0.01 wt% TiO_2 (at minimum detection for microprobe analyses). The third outlier has low Cr_2O_3 content (40.2 wt% Cr_2O_3) but similar TiO_2 content to the other secondary chromites. The low TiO_2 chromites are from sample 13-95-67 (pipe "G"), and occur as small grains in veins in garnet. The low Cr_2O_3 secondary-texture chromite occurs as a small grain between an inclusion of carbonaceous material in a garnet and the garnet itself (sample 13-102-05, pipe "X").

Chromites occurring as vermicular inclusions in amphibole and phlogopite have very low TiO_2 contents compared to the secondary-textured chromites (Figure 3-20).

Sample 13-97-78 has metasomatic clinopyroxene replacing garnet. The clinopyroxene has three small chromite inclusions, and the garnet it is partially replacing has one chromite inclusion (Plate 6). These inclusions have much higher TiO_2 contents than the vermicular chromite inclusions. The chromite in the garnet in sample 13-97-78 has 41.6 wt% Cr_2O_3, whereas the chromite inclusions in the clinopyroxene replacing the garnet have 54.5 wt% Cr_2O_3 (Figure 3-20).

All of the chromites analyzed fall outside of the field for chromites occurring as inclusions in diamond as defined by Fipke et al. (1995 – Figure 3-21). Chromites in xenoliths from Attawapiskat have a negative Cr_2O_3 - MgO trend compared to chromites from Attawapiskat pipe "V" concentrate (Figure 3-21).

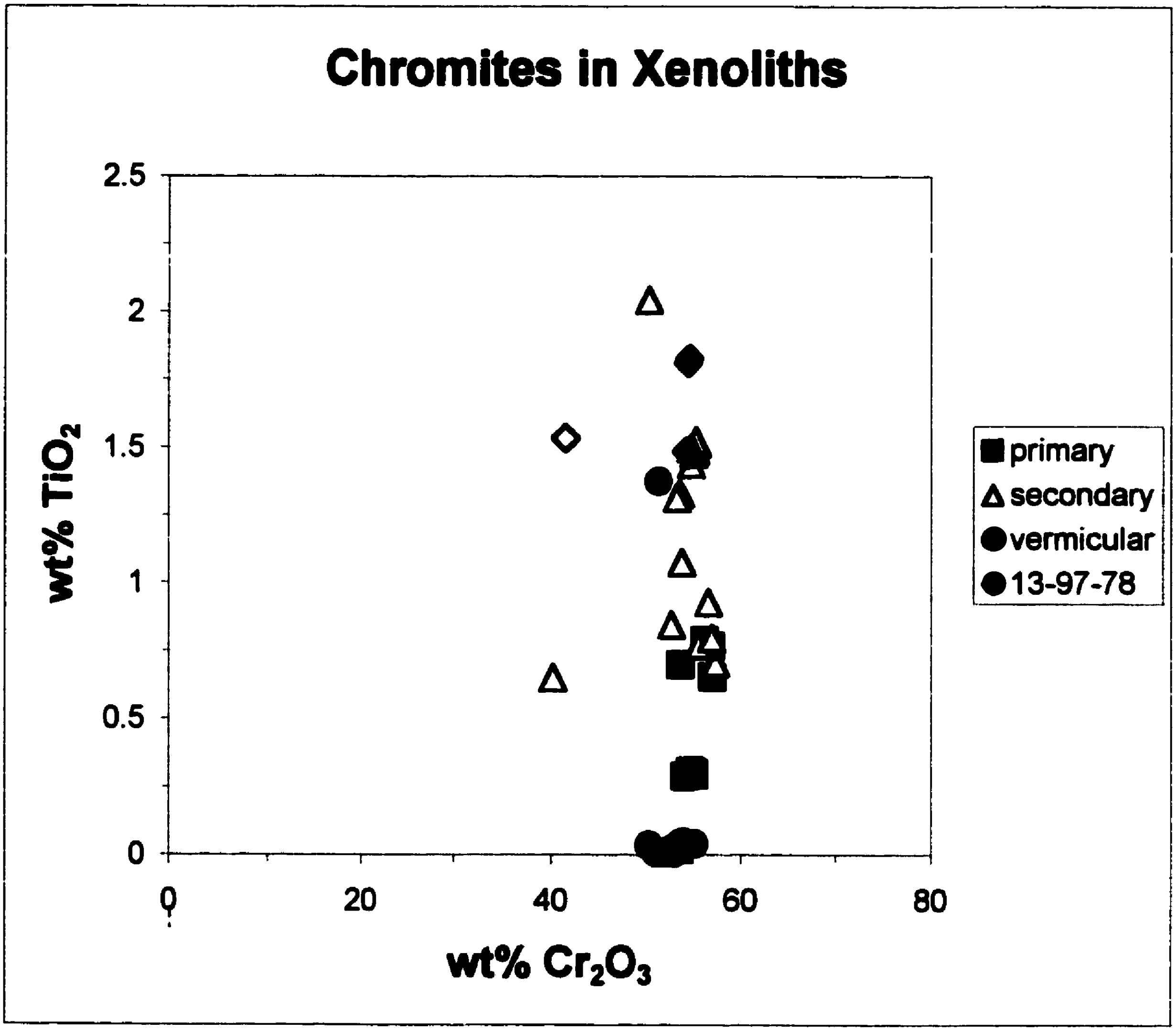

Figure 3-20: Compositions of chromites in xenoliths. Symbols: *red* – textural type "1" (primary); *yellow* – textural type "2" (secondary); *green* – textural type "3" (vermicular inclusions in amphibole and phlogopite); *filled blue* – inclusions in clinopyroxene replacing garnet in garnet harzburgite 13-97-78; *open blue* – inclusion in garnet partially replaced by clinopyroxene in garnet harzburgite 13-97-78.

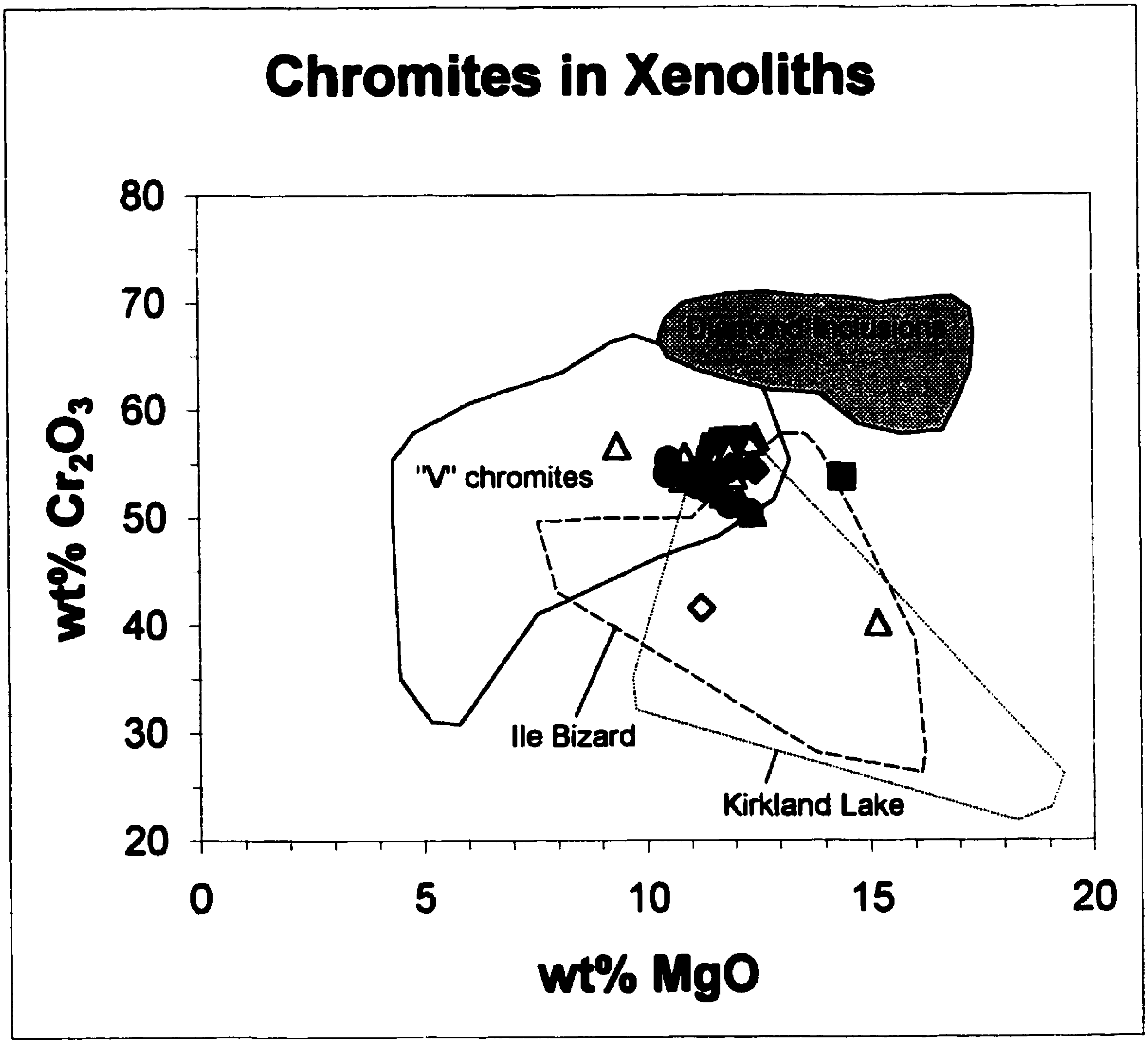

Figure 3-21: Chromites in xenoliths. Compositions fall well outside of the field of diamond inclusions from Fipke et al., (1995). Attawapiskat chromites have a negative trend similar to Ile Bizzard, Quebec and Kirkland Lake, Ontario, but opposite the trend displayed by chromites from "V" concentrate. Kirkland Lake and Ile Bizard data – Fipke et al. (1995). Symbols: *red* – textural type "1" (primary); *yellow* – textural type "2" (secondary); *green* – textural type "3" (vermicular inclusions in amphibole and phlogopite); *filled blue* – inclusions in clinopyroxene replacing garnet in garnet harzburgite 13-97-78; *open blue* – inclusion in garnet partially replaced by clinopyroxene in garnet harzburgite 13-97-78.

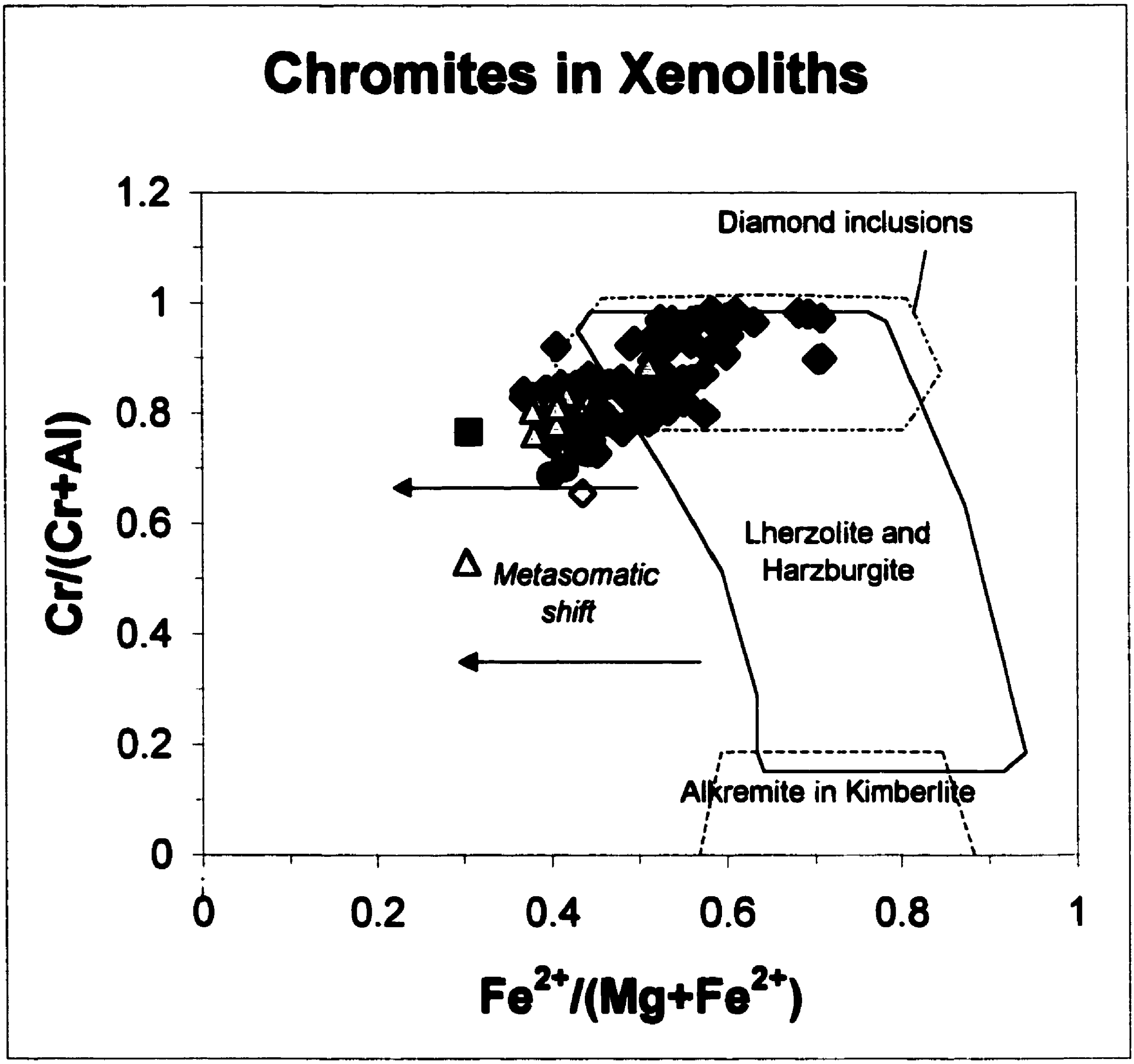

Figure 3-22: Chromites in xenoliths compared to chromites from "V" concentrate Chromite compositions fall towards the Cr/(Cr+Al) axis. Symbols: *red* – textural type "1" (primary); *yellow* – textural type "2" (secondary); *green* – textural type "3" (vermicular inclusions in amphibole and phlogopite); *filled blue* – inclusions in clinopyroxene replacing garnet in garnet harzburgite 13-97-78; *open blue* – inclusion in garnet partially replaced by clinopyroxene in garnet harzburgite 13-97-78. Fields from Haggerty (1995).

Chromite compositions fall outside of all of the fields for mantle chromites as defined by Haggerty (1995 – Figure 3-22) - one secondary-texture chromite falls within the lherzolite-harzburgite and diamond inclusion overlap area. Haggerty (1995) notes that chromites of metasomatic origin should fall towards the Cr/(Cr+Al) axis in Figure 3-22. Attawapiskat chromite compositions are consistent with this observation.

CHAPTER 4: THERMOBAROMETRY

4.1 Introduction

Thermobarometric investigations of mantle xenolith suites place mineral chemistries within a three-dimensional framework that may ultimately reveal local vertical mantle inhomogeneities. Equilibrium pressures and temperatures of mantle assemblages may be estimated using a variety of experimentally calibrated geothermometers and geobarometers (Finnerty and Boyd, 1987). Estimated equilibrium pressures and temperatures of mantle xenoliths may be used to constrain the local subcratonic geothermal gradient at the time of kimberlite eruption. Pressure – temperature values have been calculated for the mantle assemblages at Attawapiskat and have been used to constrain the geothermal gradient below the eastern Sachigo subprovince in the Jurassic.

4.1.1 Geothermometers and Barometers

A variety of thermometers and barometers have been calibrated for mantle assemblages by various authors (reviewed in Finnerty and Boyd, 1987). The thermometers and barometers utilize the experimentally calibrated pressure or temperature dependent molecular or major element exchange between two coexisting phases. The majority of thermometers for the temperature range of the upper mantle are based on the experimentally determined position of the diopside-enstatite miscibility gap (Finnerty and Boyd, 1987). Equilibrium temperatures for garnet-olivine pairs may be determined using the temperature dependant Fe-Mg exchange thermometer of O'Neill and Wood (1979). Estimated temperatures of equilibration of garnet xenocrysts (single garnets for which paragenesis is uncertain) may be calculated using the Ni-in-garnet thermometer of Canil (1999) (assuming equilibration with olivine).

Geobarometers for the pressure range of garnet-bearing mantle assemblages in kimberlites are all based on the pressure-dependant alumina content of enstatite coexisting with olivine plus an garnet, calibrated in either the CMAS (Ca-Mg-Al-Si) system or MAS system (Finnerty and Boyd, 1987). The coexisting aluminous phase for the pressure range defined by the Attawapiskat xenoliths is pyrope garnet (MacGregor, 1974).

Equilibrium P-T pairs may only be calculated for garnet-bearing assemblages using the thermometers and barometers above. Equilibrium temperatures may be calculated for reasonably presumed pressures in orthopyroxene or garnet-free assemblages using either the O'Neill and Wood (1979) thermometer or a two-pyroxene thermometer (Finnerty and Boyd, 1987).

A critical evaluation of various geothermometers and barometers by Finnerty and Boyd (1987) favoured the combination of the pyroxene-miscibility gap thermometer of Lindsley and Dixon (1976) and the alumina-in-enstatite + garnet barometer of MacGregor (1974) for P-T estimates for garnet lherzolites. Harzburgite P-T estimates may be calculated using the garnet-olivine exchange thermometer of O'Neill and Wood (1979) coupled with the MacGregor (1974) barometer.

4.1.2 Required Conditions for Equilibrium Pressure – Temperature Estimations

Estimates of pressures and temperatures for mantle xenoliths may be calculated only for those assemblages in chemical equilibrium (Finnerty and Boyd, 1987). Whereas it is not possible to demonstrate equilibrium has been attained, it is possible to provide evidence that certain conditions of equilibrium are met by a given mineral assemblage.

Mineral homogeneity is an observation that is consistent with chemical equilibrium (Finnerty and Boyd, 1987). Zonation in mantle assemblages is usually manifest as a slight change in minor elements such as TiO_2 or Cr_2O_3 from core to rim (Smith and Boyd, 1992). Most mantle minerals are homogeneous in their MgO, FeO and CaO contents, which are the elements used in temperature and pressure calculations (Finnerty and Boyd, 1987). Heterogeneous distribution of Mg, Fe and Ca is usually restricted to the rims of mineral grains in metasomatized peridotites (Finnerty and Boyd, 1987). These authors argued that the significance of pressures and temperatures calculated using heterogeneous mineral analyses are uncertain.

The presence of metasomatic minerals implies that an assemblage was not at equilibrium prior to kimberlite eruption. Most metasomatism is late-stage, just prior to or related to kimberlite eruption, so the chemical compositions of the cores of the primary minerals may record the equilibrium temperature and pressure prior to the metasomatic event (Erlank et al., 1987). As such, the results of P-T calculations using analyses of the cores of minerals in metasomatized peridotites may represent the equilibrium conditions prevalent immediately before kimberlite eruption.

4.1.3 The Attawapiskat Mantle Xenolith Suite

The mantle sample at Attawapiskat does not readily lend itself to pressure-temperature calculations. Most of the xenoliths are garnet-olivine pairs, so although equilibrium temperatures have been calculated, absolute pressure determinations were not possible. Orthopyroxene grains in most harzburgite fragments are completely altered to serpentine. In only a few xenoliths is fresh orthopyroxene preserved.

Although mantle stratigraphy may be evaluated by relating P-T results to rock type, garnet – olivine pairs cannot be classified into rock types based on modal mineralogy so should not contribute to a three-dimensional model. For the garnet – olivine pairs, rock type classification was done using CaO and Cr_2O_3 contents of the garnets (see Figure 3-15, and Chapter 5 for discussion). Although this method of classification is not as rigorous as that based on modal mineralogy, it does mean that temperatures for garnet – olivine pairs can be related to rock type and used to augment the stratigraphic relations between rock types at depth as determined by the xenoliths.

Analysis of clear, homogeneous grain cores were used for the pressure and temperature calculations for Attawapiskat xenoliths. Temperatures were calculated using the O'Neill and Wood (1979) garnet – olivine Fe-Mg exchange thermometer. Pressures for orthopyroxene-bearing assemblages were calculated using the MacGregor (1974) alumina-in-orthopyroxene coexisting with garnet barometer. T_{equil} for 14 garnets from pipe "V" concentrate were calculated using the Ni-in-garnet (assumed to be in equilibrium with olivine) thermometer of Canil (1999).

4.2 Olivine-Garnet Thermometry, Garnet-Enstatite Barometry

Estimated equilibrium temperatures of Attawapiskat xenoliths were calculated using the O'Neill and Wood (1979) thermometer (with the O'Neill (1980) correction, the combination of which will hereafter be referred to as OW79).

Partitioning of Fe and Mg between high-Mg olivine and coexisting garnet may be represented by the exchange equation;

$$\underset{\text{(olivine)}}{3\ Fe_2SiO_4} + \underset{\text{(garnet)}}{2\ Mg_3Al_2Si_3O_{12}} \equiv \underset{\text{(garnet)}}{2\ Fe_3Al_2Si_3O_{12}} + \underset{\text{(olivine)}}{3\ Mg_2SiO_4} \qquad (1)$$

as defined by O'Neill and Wood (1979).

The thermometer is dependant on olivine and garnet compositions, temperature and Ca content of the garnet, with minor dependence on pressure. The equilibrium temperature is calculated by;

$$T = \frac{902 + DV + (X^{ol}_{Mg} - X^{ol}_{Fe})(498 + 1.5(P - 30)) - 98(X^{gt}_{Mg} - X^{gt}_{Fe}) + 1347\, X^{gt}_{Ca}}{\text{Ln}\, K_D + 0.357} \qquad (2)$$

where X^i_j is the mole fraction of component j in phase i, P is pressure in kbar at which the phases are in equilibrium, and T is in K (O'Neill and Wood, 1979). K_D is the partition coefficient between olivine and garnet, given by;

$$K_D = \frac{X^{ol}_{Mg} \cdot X^{gt}_{Fe}}{X^{ol}_{Fe} \cdot X^{gt}_{Mg}} \qquad (3)$$

where,

$$X^{ol}_{Mg} = \left(\frac{Mg}{Mg + Fe}\right)_{Olivine}$$

$$X^{gt}_{Mg} = \left(\frac{Mg}{Mg + Fe + Ca}\right)_{Garnet} \qquad (4)$$

and so on for components Fe (olivine and garnet) and Ca (garnet) (O'Neill and Wood, 1979). DV is the term,

$$\begin{aligned} DV = &\ 462.5\,[1.0191 + (T - 1073)(2.87 \cdot 10^{-5})] \cdot (P - 2.63 \cdot 10^{-4} P^2 - 29.76) \\ &- 262.4\,[1.0292 + (T - 1073)(4.5 \cdot 10^{-5})] \cdot (P - 3.9 \cdot 10^{-4} P^2 - 29.65) \\ &+ 454\,[1.020 + (T - 1073)(2.84 \cdot 10^{-5})] \cdot (P - 2.36 \cdot 10^{-4} P^2 - 29.79) \\ &+ 278.3\,[1.0234 + (T - 1073)(2.3 \cdot 10^{-5})] \cdot (P - 4.5 \cdot 10^{-4} P^2 - 29.6) \end{aligned} \qquad (5)$$

which is used to incorporate the pressure dependant volume change of the Fe-Mg exchange (O'Neill and Wood, 1979). Equation (2) may be solved iteratively with a geobarometer to arrive at a P-T pair for the assemblage. A first approximation of the pressure and temperature of formation must be made and entered into eq. (2) for the first iteration. The thermometer is most sensitive at high temperatures ($\leq$1300 °C), where two-pyroxene thermometers become spurious due to the decrease in size of the pyroxene miscibility gap (O'Neill and Wood, 1979). Pressure effects on K_D lead to slight increases in the calculated temperature, from 6 °C/ kbar at 10 kbar, to 3 °C/ kbar at 70 kbar (O'Neill and Wood, 1979). Error in the calculated temperature is ± 60 °C for values between 600 °C and 1300 °C (O'Neill and Wood, 1979).

The pressure of equilibration for the Attawapiskat samples was estimated using the equation derived by Finnerty and Boyd (1984) for the alumina-in-enstatite geobarometer of MacGregor (1974) for use in the program TEMPEST (F.R. Boyd, personal communication to D. Schulze). The equilibrium between enstatite and coexisting olivine and garnet may be represented by the exchange reaction,

$$\underset{\text{(garnet)}}{x\,Mg_3Al_2Si_3O_{12}} + \underset{\text{(enstatite)}}{3(1-x)\,MgSiO_3} \equiv \underset{\text{(Mg-Tschermaks)}}{3\,MgSiO_3 \cdot x\,Al_2O_3} \qquad (6)$$

as experimentally determined by MacGregor (1974). Isopleths of Al_2O_3 in enstatite projected onto P-T space may be used to determine the pressure of equilibration a given temperature. Finnerty and Boyd (1984) derived an equation for calculating a MacGregor (1974) equilibrium pressure for a known temperature for the computer program TEMPEST. Pressure may be calculated by,

$$P\,(\text{kbar}) = \left(\frac{1.46 - \ln Al_2O_3}{97.1}\right) \cdot T - 38.5 \qquad (7)$$

where Al_2O_3 is the weight fraction of Al_2O_3 in enstatite, and T is in K (F.R. Boyd, personal communication to D.J. Schulze).

Equation (7) may be solved iteratively with a geothermometer to arrive at a P-T pair for the mantle assemblage. Error in eq. (7) is partially dependant on the error in the geothermometer with which the pressure determination is coupled. Error in eq. (7) solved iteratively with eq. (2) is ±3.0 kbar (O'Neill and Wood, 1979).

4.3 Pressure-Temperature Results

Pressures and temperatures of equilibration were calculated for seven coarse garnet + olivine + orthopyroxene assemblages, one chromite + garnet + olivine + orthopyroxene assemblage, and one deformed garnet lherzolite. The garnet + olivine + orthopyroxene assemblages are modally classified as harzburgite. Garnet analyses for four of these assemblages plot in the CaO-rich field in Figure 3-15, so they are chemically classified as lherzolites. Those garnet + olivine + orthopyroxene assemblages for which garnet compositions fall to the left of the discriminant line in Figure 3-15 are considered harzburgites; those with garnets compositions to the right of the discriminant line lherzolites. Lherzolites were recovered from pipes "A1", "G" and "V". Harzburgites were recovered from pipes "A1" and "G". A chromite-garnet harzburgite was recovered from pipe "G". The single deformed garnet lherzolite was recovered from pipe "A1". Results of T – P calculations are summarized in Table 4-1.

Calculated T_{OW79} and P_{MC74} indicate the garnet lherzolites equilibrated in the range 782.9 °C/31.4 kbar to 937.4 °C/42.4 kbar. Garnet harzburgites equilibrated in the range 1036 °C/47.4 kbar to 1045 °C/47.9 kbar. The chromite-garnet harzburgite has calculated equilibrium T-P values of 681.7 °C/25 kbar. The deformed garnet lherzolite from pipe "G" has calculated equilibrium temperature and pressure of 927.0 °C/42.9 kbar.

Attawapiskat xenolith equilibrium pressures and temperatures fall along a 40mWm^{-2} conductive subcratonic steady-state geothermal gradient in Figure 4-1 (Pollack and Chapman, 1977). Garnet lherzolites equilibrated at pressures below the graphite-diamond univariant curve of Kennedy and Kennedy (1976). Two of the harzburgite samples equilibrated within the diamond stability field, the other two within the graphite stability field. The chromite-garnet harzburgite has equilibrium pressure and temperature that places it well within the graphite stability field in Figure 4-1. Error in the P-T results of ± 60 °C and ● 3 kbar preserves the relationship between rock type and the diamond-graphite univariant.

There is a slight "gap" in the Attawapiskat P-T results, between 937 °C/42.4 kbar and 1036 °C/47.7 kbar (Figure 4-1). The gap roughly corresponds to a division between lower pressure and temperature lherzolitic assemblages and higher pressure and temperature harzburgitic assemblages.

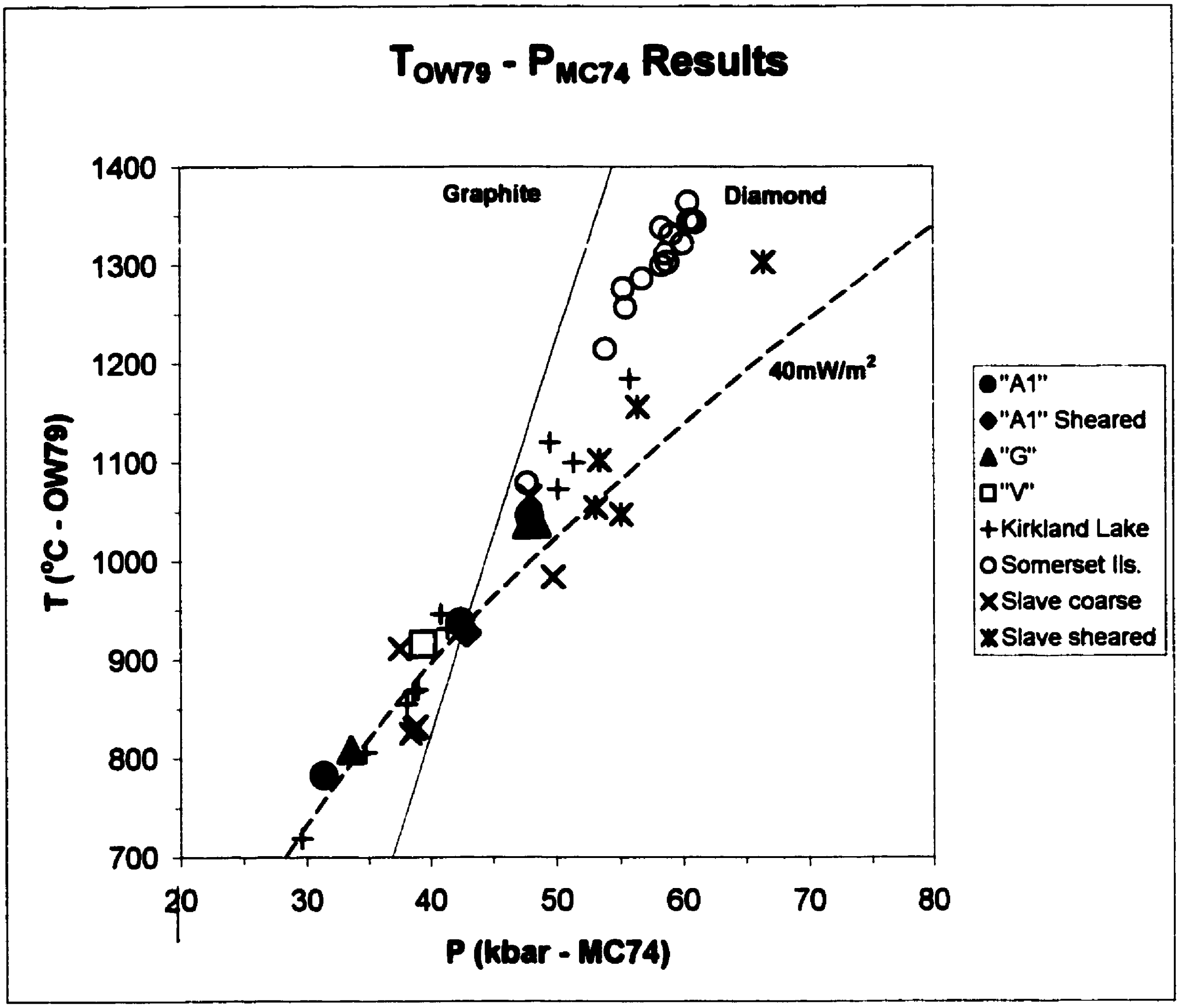

Figure 4-1: Pressure – Temperature results for Attawapiskat xenoliths. The xenoliths have equilibrium pressures and temperatures that fall along a 40mWm^{-2} conductive subcratonic steady-state geothermal gradient. Graphite – diamond stability, Kennedy and Kennedy (1976); 40mWm-2 geothermal gradient, Pollack and Chapman, (1977); Kirkland Lake data, Vicker (1997); Somerset Island data, Jago (personal communication); Slave data, Kopylova et al. (1999) and MacKenzie and Canil (1999).

Attawapiskat xenoliths equilibrated at lower temperatures and pressures compared to coarse garnet peridotites from other Canadian localities. Some Slave craton coarse peridotites equilibrated at higher temperatures, at pressures within the diamond stability field (Figure 4-1; Kopylova et al., 1999; MacKenzie and Canil, 1999). These samples equilibrated on a slightly hotter geothermal gradient than those at Attawapiskat ($42mWm^{-2}$ - Kopylova et al., 1999; MacKenzie and Canil, 1999). Somerset Island peridotites define a geothermal gradient that inflects to high temperatures at pressures > 45 kbar (Mitchell, 1978). Coarse peridotites from Kirkland Lake have a broad range of equilibrium temperatures and pressures, but generally yield equilibrium temperatures above the $40mWm^{-2}$ geothermal gradient at pressures above 50 kbar (Vicker, 1997).

4.4 Thermometry Results

4.4.1 T_{OW79} for Coarse Garnet Peridotites

Temperatures of equilibration for garnet-olivine pairs were calculated using T_{OW79} at an assumed equilibrium pressure of 40 kbar (which is consistent with the calculated pressures discussed above). Results of the temperature calculations are summarized in Table 4-1. Calculated equilibrium temperatures were projected to a reference $40mWm^{-2}$ geothermal gradient in Figure 4-2 by drawing horizontal tie-lines from T_{OW79} at 40 kbar to the reference geothermal gradient (see Figure 4-2 for a graphical explanation). Temperatures were then recalculated using the pressure on the $40mWm^{-2}$ geothermal gradient. The difference between T_{OW79} (at 40 kbar) and T_{OW79} (assumed pressure) was 3 – 10 °C for all of the samples. Projection of calculated equilibrium temperatures to a known geothermal gradient in this manner allows for spatial comparison of garnet –

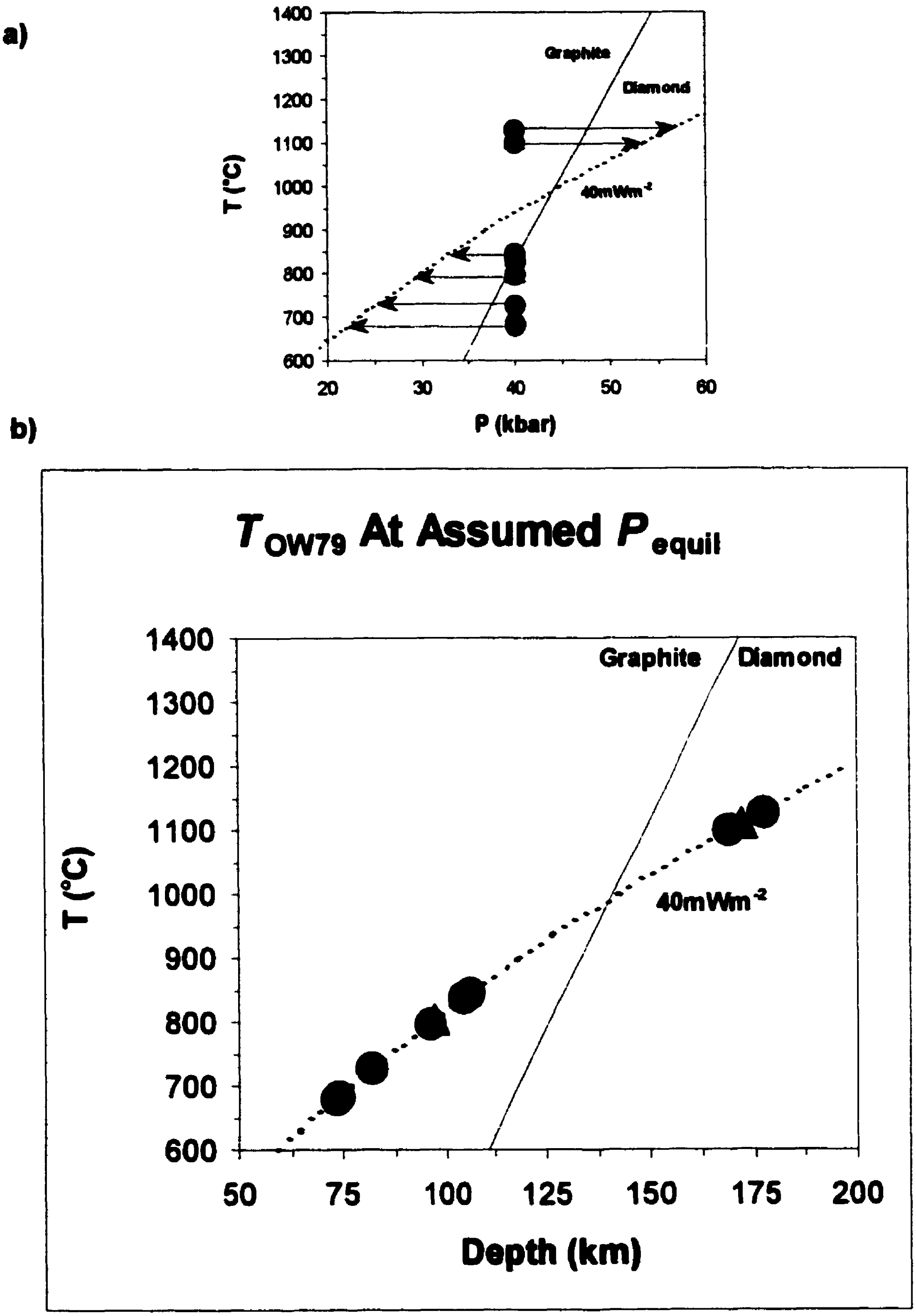

Figure 4-2: Equilibrium temperatures for garnet - olivine pairs, calculated using OW79 at an assumed pressure of 40 kbar. a) Temperature results were horizontally projected to a 40 mWm^{-2} geothermal gradient (arrows). Temperatures were then recalculated at the pressure corresponding to the geothermal gradient. This procedure was repeated until a final P-T pair was attained. b) Results of recalculation process in (a). There is a "gap" in the results from ~850 - 1100 °C. *Symbols: red - lherzolite, blue - harzburgite.*

olivine chemistries with those of the composite xenoliths. Although absolute depths of equilibration for the garnet – olivine pairs are somewhat uncertain, relative stratigraphy between the samples is preserved

Calculated T_{OW79} for garnet-olivine pairs ranges from 680 °C to 1129 °C at an assumed pressure of 40 kbar, with a slight "gap" from ~850 – 1100 °C (Figure 4-2). Seven of the samples that lie below the 40 mWm^{-2} geothermal gradient in Figure 4-2 contain garnets with compositions that fall in the lherzolite field in Figure 3-15. The eighth sample contains garnet with harzburgite composition. Three samples plot above the 40mWm^{-2} geothermal gradient in Figure 4-2. They may be classified as lherzolite (two samples) and harzburgite (one sample) based on CaO and Cr_2O_3 content of the garnets.

4.4.2 Ni-in-garnet Thermometer

Trace element analyses of 14 low-CaO (harzburgitic) garnets from "V" concentrate were used to determine T_{equil} using the Ni-in-garnet thermometer of Canil (1999). The Ni-in-garnet thermometer is based on the temperature sensitive partitioning of Ni between Mg-rich olivine (forsterite) and garnet. Ni strongly prefers partitions into the octahedral site in olivine over the distorted cubic site in garnet due to a large difference in stabilization energy (Ross et al., 1996; Canil, 1999). The thermometer was calibrated using experimentally derived partition coefficients between coexisting olivine and garnet and natural garnets occurring in lherzolite and harzburgite xenoliths (Ryan et al., 1996; Canil, 1994; Canil, 1999). However, the thermometer is applicable to single garnets by assuming the garnet was in equilibrium with a Mg-rich (forsteritic) mantle

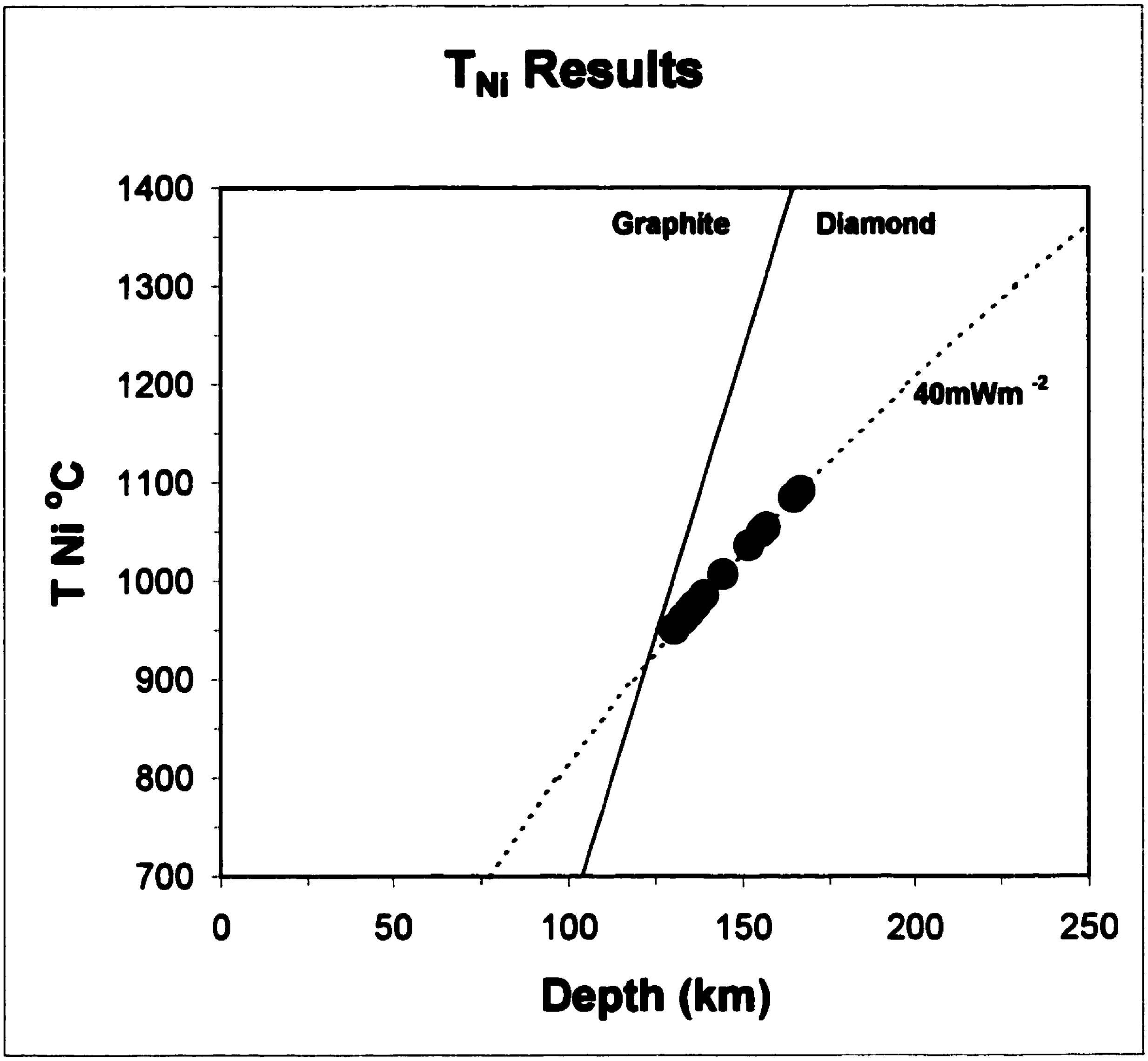

Figure 4-3: Equilibrium temperatures calculated using the Ni-in-garnet thermometer. Temperatures have been projected to the 40 mWm^{-2} geothermal gradient in a similar manner to those results in Figure 4-2. T_{Ni} span the "gap" in temperature seen in Figures 4-1 and 4-2.

olivine. Mantle olivines have Ni contents which typically range from 2700 – 3100 ppm. The average Ni content for mantle olivines (2900 ppm) Griffin et al. (1989) may be used to calculate T_{Ni} for single garnets of peridotite affinity. T_{Ni} is calculated by,

$$T = 8772 / (2.53 - \ln D_{Ni}^{gt/ol}) \quad (8)$$

where T is temperature in K, and $D^{gt/ol}{}_{Ni} = [Ni]_{gt} / [Ni]_{ol}$ (ppm) (Canil, 1999). $[Ni]_{ol}$ is assumed to be 2900 ppm. Error in eq. (8) is ±50 °C (Canil, 1994; Canil, 1999).

Results of T_{Ni} for the 14 "V" garnets have been projected to the 40 mWm^{-2} geothermal gradient using the same method for T_{OW79} results discussed above (Figure 4-3). Relative stratigraphy of the source rocks is preserved whereas true depths of equilibration are uncertain. The temperatures cluster between 950 – 1091 °C. Calculated T_{Ni} span the temperature "gap" in the T_{OW79} and T_{OW79}-P_{MC74} results. The range in T_{Ni}, and their approximate depths of origin, coincide with the higher P-T group (harzburgite) of xenoliths.

4.4.3 Comparison of T_{OW79} and T_{Ni}

The temperature dependant exchange of Fe and Mg between coexisting olivine and garnet calibrated for the OW79 thermometer has a slight dependence on Ca content of garnet and a slight pressure dependence, related to volume expansion in the exchange reaction as pressure increases (O'Neill and Wood, 1979). The "DV" term (eq. 4) corrects for most of this dependence, but error in eq. (1) is somewhat greater at higher pressure because of the dependence (above 60kbar (approximately equivalent to temperatures >1400 °C) and below 600 °C, error is ±90 °C – O'Neill and Wood, 1979). For the temperature range 600-1300 °C, T_{OW79} is within ±60 °C of the Wells (1977) two-pyroxene thermometer (O'Neill and Wood, 1979). Error in OW79 is comparable to error in experimentally calibrated two-pyroxene thermometers (O'Neill and Wood, 1979; Finnerty and Boyd, 1987).

The Ni-in-garnet thermometer has several advantages over conventional two-phase thermometers. It is applicable to single grains recovered from diamond exploration samples, or for garnets from heavy mineral concentrates. T_{Ni} is independent of pressure, so no correction terms are necessary (Canil, 1999). The Ni-in-garnet thermometer of Canil (1999) assumes garnet coexisted with olivine with 2900 ppm Ni, so it is only applicable to peridotitic garnets. Application of the Ni-in-garnet thermometer to Fe-rich deformed peridotites and fertile lherzolites has not been tested.

Results of OW79 and the Ni-in-garnet thermometer for this study yield very similar results (Figures 4-2 and 4-3). Calculated equilibrium temperatures using T_{Ni} for harzburgitic garnets are somewhat more restricted than those for garnet harzburgite garnets calculated using OW79 (T_{Ni} – 950 °C to 1091 °C, T_{OW79} – 808 °C to1129 °C).

4.5 Deformed Lherzolites

One deformed lherzolite sample from pipe "A1" yields T_{OW79} = 927.0 °C and P_{MC74} = 42.9 kbar. This point plots just into the diamond stability field, on the 40mWm^{-2} geothermal gradient in Figure 4-1. Error of ±60 °C and ±3 kbar would place the sample further into the diamond stability field or below the graphite-diamond univariant in the graphite stability field (Figures 4-1).

The single deformed lherzolite from pipe "A1" has a low calculated T_{equil}. Deformed lherzolites from Kimberley South Africa (Boyd and Nixon, 1977), Matsoku, Lesotho

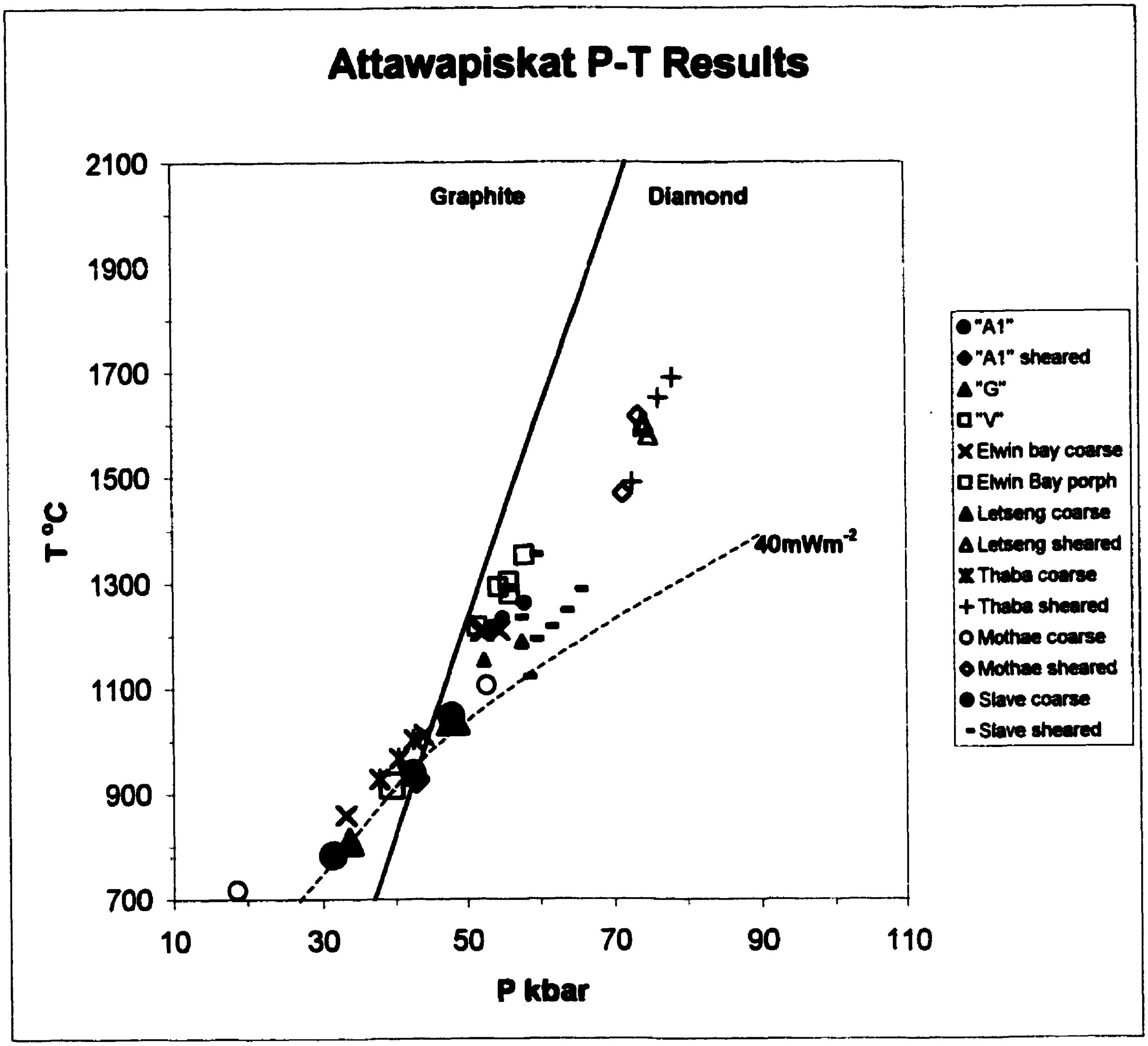

Figure 4-4: Pressure – Temperature results from Attawapiskat compared to sheared garnet lherzolite pressures and temperatures from worldwide sources. Data for Elwin Bay, Northwest Territories, Mitchell (1977); Letseng, Lesotho, Boyd (1973); Thaba Putsoa and Mothae, Lesotho, Nixon (1973) and Nixon and Boyd (1973); Slave province, Northwest Territories, Kopylova et al. (1999) and MacKenzie and Canil (1999).

(Cox et al., 1973) and the Thumb minnette, New Mexico (Harte, 1983) have similarly low equilibration temperatures. Worldwide, however, deformed lherzolites typically have calculated equilibration temperatures above a 40 mWm^{-2} steady – state geothermal gradient (Nixon and Boyd, 1973; Boyd and Nixon, 1978; Boyd, 1987; Harte, 1983).

Table 4-1: Pressure - Temperature Results

Pipe	SAMPLE	Rock Type		T_{OW79} (°C)	P_{MC74} (kbar)
		garnet chemistry classification	modal classification		
G	13-95-33	gnt. lherzolite	gnt. harzburgite	808.8	33.5
G	13-95-67	gnt. harzburgite	gnt. harzburgite	1036.4	47.7
G	13-95-35	gnt. harzburgite	gnt. harzburgite	1037.7	48.5
G	13-95-42	gnt-chr harzburgite	gnt-chr harzburgite	681.7	25
A1	13-97-78	gnt. harzburgite	gnt. harzburgite	1045.9	47.9
A1	13-97-83	gnt. lherzolite	gnt. lherzolite	937.4	42.4
A1	Att-A1-P1	disrupted gnt. lherzolite	gnt. lherzolite	927.0	42.9
A1	Att-A1-P2	coarse gnt. lherzolite	gnt. lherzolite	782.9	31.4
V	13-99-18	gnt. lherzolite	gnt. lherzolite	915.0	39.4
	Temperature only			*T_{OW79} (°C)*	*P(assumed)*
G	13-95-34	gnt. lherzolite	gnt-oliv pair	1100	40
G	13-95-48	gnt. lherzolite	gnt-oliv pair	827	40
G	13-95-50	gnt. lherzolite	gnt-oliv pair	726	40
G	13-95-52	gnt. lherzolite	gnt-oliv pair	844	40
G	13-95-56	gnt. lherzolite	gnt-oliv pair	683	40
G	13-95-59	gnt. harzburgite	gnt-oliv pair	802	40
G	13-95-70	gnt. lherzolite	gnt-oliv pair	680	40
A1	13-97-81	gnt. lherzolite	gnt-oliv pair	1100	40
A1	13-97-82	gnt. lherzolite	gnt-oliv pair	797	40
X	13-102-09	gnt. harzburgite	gnt-oliv pair	1129	40

CHAPTER 5: DISCUSSION

5.1 Introduction

Results of analysis of ultramafic xenoliths from the Attawapiskat kimberlites have been used to determine vertical heterogeneity in the mantle beneath the eastern Sachigo subprovince during the late to middle Jurassic. The results of this study represent the first conductive subcratonic steady-state geothermal gradient determination for the Sachigo subprovince, and for that portion of the Superior Province which is covered by the Palaeozoic sedimentary rocks of the Hudson Bay Platform.

5.2 Mineral Chemistry

Ultramafic mantle xenoliths from the Attawapiskat kimberlites are small, and typically occur as garnet – olivine pairs. Modal classification of the xenolith suite indicates that the mantle below Attawapiskat consists of harzburgite, with minor volumes of lherzolite and eclogite. Rock type classification of the composite xenoliths based on mineral chemistry indicates that the mantle below Attawapiskat is approximately bimodal, consisting of abundant lherzolite with significant amounts of harzburgite. Eclogite is volumetrically insignificant at Attawapiskat. Garnet-olivine pairs are predominantly lherzolite-derived, however, harzburgite fragments contribute considerably to the suite.

Classification of composite mantle assemblages based on garnet chemistry is problematic, as the divisions in Figures 3-1, 3-2, 3-3 and 3-15 are based on statistical analyses of garnets included in diamond and not on garnets from xenoliths. Fipke et al.

(1995) use the "G9", "G10" and "Eclogite" fields of Gurney (1984) to relate the chemical composition of garnet xenocrysts to parent rock type. In the case of the Attawapiskat ultramafic xenolith suite, modal classification has been augmented by chemical classification, particularly for the garnet – olivine pairs.

Analysis of garnets from heavy mineral separates expands the data suite from the cognate xenoliths. Garnet xenocrysts indicate that the mantle below Attawapiskat is predominantly lherzolitic, with subordinate amounts of harzburgite. The paucity of eclogite at depth indicated by the xenolith suite is corroborated by xenocryst analyses.

Cr-diopsides recovered from pipe "V" are ferroan compared to Cr-diopsides from coarse and sheared lherzolites from Lesotho (Boyd, 1973; Cox et al., 1973; Nixon and Boyd, 1973 – Figure 3-19). Xenocryst compositions correspond closely to those for metasomatic clinopyroxenes in the xenoliths, indicating the xenocryst population is dominated by metasomatic clinopyroxene. It is unknown why primary clinopyroxene did not survive in the xenolith and xenocryst populations.

5.3 Geothermobarometry

5.3.1 Pressure – Temperature Results

Subcratonic conductive steady-state geothermal gradients equal to 40 mWm^{-2} have been calculated for the Kaapvaal craton, southern Africa, Siberia (Finnerty and Boyd, 1987), and for the Superior Craton, Canada (Meyer, 1994; Vicker, 1997). A 40 mWm^{-2} geothermal gradient is considered typical of deep, cool peridotitic roots at the centres of cratons (Finnerty and Boyd, 1987). Meyer (1994) and Vicker (1997) both showed that the Kirkland Lake suite of xenoliths from the Abitibi subprovince correspond to a central

– cratonic geothermal gradient. Results of this study are consistent with the location of these kimberlites in the Sachigo subprovince in the central region of the Superior Craton. The equilibration depths of the samples corroborates the estimate of 150 km depth to the lithosphere-asthenosphere boundary by Grand (1987).

Calculated equilibrium pressures and temperatures indicate that the mantle below Attawapiskat is layered. Garnet lherzolite xenoliths typically equilibrated at shallower depths than garnet harzburgites. The majority of garnet lherzolites equilibrated at pressures within graphite stability. Harzburgites typically equilibrated at higher pressures and temperatures than the lherzolites, and two of three harzburgite samples equilibrated at pressures within the diamond stability field.

5.3.2 Temperature Results

Temperatures of equilibration calculated for garnet-olivine pairs using OW79, and T_{Ni} coincide with the temperature range of the xenoliths for which both equilibrium pressure and temperature were determined. OW79 results indicate that the majority of lherzolite xenoliths equilibrated at pressures and temperatures within the graphite stability field. Two garnet – olivine pairs of lherzolite affinity equilibrated within the diamond stability field. Harzburgitic garnet – olivine pairs equilibrated at pressures within both diamond and graphite stability. T_{Ni} for harzburgitic garnets do not extend below ~ 940 °C, consistent with the higher T_{equil} established for garnet harzburgite samples using OW79.

5.3.3 The Attawapiskat P-T "Gap"

Thermobarometry on composite xenoliths indicates there is a segment of the mantle, near 45 – 50 kbar (140 – 160 km depth)/ 950 – 1000 °C that is not represented by the mantle xenolith suite. Results for for T_{OW79} for garnet – olivine pairs have the same "gap" in data. T_{Ni} for low-CaO garnets extend into the gap, suggesting that there may be a layer of harzburgite between 140 – 160 km depth that was sampled but did not survive as composite xenoliths during kimberlite eruption.

5.4 Metasomatism

Metasomatism is the *in situ* enrichment of a mantle peridotite by an LIL- and LREE-enriched fluid or volatile-rich silicate magma, resulting in an enrichment/depletion reaction between the host rock and infiltrating fluid (Harte 1983; Spera, 1987; Menzies and Hawksworth, 1987). The result of the interaction may be 1) the introduction of one or more new hydrous phases, such as phlogopite and amphibole (modal metasomatism), or 2) LREE enrichment and major element depletion in the host rock phases, without any accompanying change in the modal mineralogy (cryptic metasomatism – Harte, 1983; Spera, 1987; Menzies and Hawksworth, 1987). Secondary minerals are the product of reactions between the mantle assemblage and the volatile-rich kimberlite magma as the xenoliths are transported to and sit at the surface (Harte, 1983).

Excess chrome from the breakdown of Cr-pyrope is accommodated as vermicular chromite inclusions in the phlogopite and amphibole replacing the garnet. It may be inferred that small "clots" of phlogopite + amphibole ● chromite in some xenoliths are completely replaced garnets (Erlank et al., 1987). It is possible to extend this inference to several phlogopite + amphibole ± chromite fragments in the kimberlite – they may be fragments of completely replaced garnet from coarse-grained metasomatized lherzolites (Erlank et al., 1987). Garnet harzburgites and garnet – olivine pairs of harzburgite affinity have garnet which is partially replaced by metasomatic clinopyroxene only. The metasomatic assemblage at Attawapiskat is similar to that at Monastery, South Africa, where Summers (1987) showed that metasomatism took place in stages, with gradual replacement of garnet by clinopyroxene → amphibole → amphibole + phlogopite with decreasing depth. Vicker (1997) noted clinopyroxene metasomatism in the Kirkland Lake, Ontario xenoliths, but not amphibole metasomatism. Metasomatism at Attawapiskat appears to have penetrated to greater depths than that at Kirkland Lake.

Petrographic, chemical and thermobarometric evidence suggests two different types of metasomatism occurred at Attawapiskat: 1) Modal metasomatism of garnet lherzolite between ~120 - 140 km, where garnet consumed by phlogopite + amphibole, and 2) Modal metasomatism of a dominantly harzburgite mantle at depths greater than ~160km, where garnet was partially replaced by clinopyroxene. A similar relationship was observed in mantle xenoliths from Kimberley, South Africa by Erlank et al. (1987). Phlogopite and amphibole metasomatism is restricted to shallow samples, whereas clinopyroxene metasomatism occurred at deeper intervals. The same relationship between depth and type of metasomatism is evident at Attawapiskat, however, parent rock type seems to have played a roll as well. Shallow lherzolites have amphibole + phlogopite metasomatism whereas deeper harzburgite fragments have undergone clinopyroxene metasomatism. Compositions of the phlogopite, amphibole and clinopyroxene indicate that the metasomatising fluid was TiO_2- and K_2O- poor.

Dawson (1987) and Lloyd (1987) argue that replacement of relatively dense garnet by light oxides in garnet peridotite may create a density contrast in the mantle that could lead to gravitational instabilities at depth, contributing to local buoyancy of the overlying craton. The result of large-scale metasomatism could lead to the creation of craton-scale basin and dome structures, and associated rifting. The degree to which metasomatic alteration of the lithospheric mantle contributes to craton buoyancy will typically be small but may make an important contribution to craton buoyancy when coupled with larger instability influences such as isostatic rebound after glacial retreat (Lloyd, 1987). Amphibole and phlogopite metasomatism was only a small component of the total metasomatic event at Attawapiskat, and will likely have had a negligible role in Superior Craton buoyancy. Cr-diopside and pyrope garnet have very similar densities (Deer et al., 1966), and clinopyroxene metasomatism will not have had any effect on the gravitational stability of the upper mantle

5.5 Deformed Peridotites

One deformed lherzolite sample was recovered from the Attawapiskat kimberlite. Calculated pressure and temperature of equilibration for this sample place it near the $40 mWm^{-2}$ geothermal gradient. This is similar to Bultfontein, Kimberley, South Africa (Dawson et al., 1975; Boyd and Nixon, 1978), Matsoku, Lesotho (Harte et al., 1975), and the Thumb minnette in New Mexico, (Harte, 1983), where deformed peridotites have pressures and temperatures of equilibration that fall on or near the local geothermal gradient.

Worldwide, deformed peridotites may be correlated with high estimated equilibrium temperatures, and define high-temperature inflections in the local geothermal gradient at depths > 150 km (Finnerty and Boyd, 1987). This is particularly pronounced in xenoliths from northern Lesotho (Finnerty and Boyd, 1987). Finnerty and Boyd (1987) and Boyd (1987) argue that high-temperature deformed lherzolites form in regions where the lithosphere – asthenosphere boundary is shallow, particularly in circum-cratonic mobile belts. The low-temperature deformed lherzolites at Attawapiskat are typical of regions where cool craton roots penetrate to depths > 150 km (Boyd and Nixon, 1987; Boyd, 1987).

5.6 Diamond Potential

Diamonds from eclogite are not expected at Attawapiskat. Gurney (1984) showed that 85% of peridotite garnet diamond inclusions have compositions that fall on the CaO-poor portion of Figure 3-15, the "harzburgite" field. Harzburgite xenoliths at Attawapiskat equilibrated at pressures and temperatures near or in the diamond stability field (Figure 4-1). The presence of diamonds at Attawapiskat is consistent with the high P-T harzburgite xenolith suite.

Results of T_{Ni} for garnet xenocrysts indicate that a layer of harzburgite, which equilibrated at temperatures corresponding to the diamond stability field, was sampled by the Attawapiskat kimberlites but did not survive as cognate xenoliths. If this layer of harzburgite contained diamonds, there is a high possibility that the diamonds survived kimberlite eruption and are recoverable from the kimberlite.

CHAPTER 6: CONCLUSIONS

6.1 The Attawapiskat Mantle Xenolith Suite

The Attawapiskat mantle xenolith suite is representative of a dominantly lherzolitic mantle, with subordinate amounts of harzburgite and eclogite. Estimated pressures and temperatures of equilibrium for xenoliths define a $40 mWm^{-2}$ conductive steady-state subcratonic geothermal gradient below the Sachigo subprovince of the Superior Province of the Canadian Shield.

The xenolith assemblage at Attawapiskat includes deformed peridotites with estimated equilibration temperatures and pressures which fall near the $40 mWm^{-2}$ geothermal gradient. This is similar to the cold, sheared peridotites from Kimberley, South Africa, Matsoku, Lesotho, and Thumb, New Mexico. This appears to be unique within Canada, as all other Canadian localities report some high-temperature sheared peridotites.

Lherzolite and harzburgite xenoliths have different metasomatic assemblages. Modal metasomatism of shallow-derived lherzolites resulted in the introduction of phlogopite + amphibole (pargasite) ± chromite at the expense of garnet. Deeper harzburgite xenoliths have undergone modal metasomatism where garnet is consumed by clinopyroxene only. The identity and source of the fluid remains undetermined.

The presence of harzburgite xenoliths with calculated equilibrium pressures and temperatures within the diamond stability field is consistent with the presence of diamond in the Attawapiskat kimberlite pipes.

REFERENCES

Brummer, J.J., Mac Fayden, D.A., and Pegg, C.C. (1992a). Discovery of Kimberlites in the Kirkland Lake Area, Northern Ontario, Canada Part I: Early Surveys and Surficial Geology. Explor. Mining Geol., 1: 339 – 350.

Brummer, J.J., MacFayden, D.A., and Pegg, C.C. (1992). Discovery of Kimberlites in the Kirkland Lake Area, Northern Ontario, Canada Part II: Kimberlite Discoveries, Sampling, Diamond Content, Ages and Emplacement. Explor. Mining Geol., 1: 351 – 370.

Boyd, F.R. (1973). Appendix of mineral analyses (Letseng-la-terae kimberlite pipes). *in* Nixon, P.H. (ed.). Lesotho Kimberlites. Lesotho National Development Corporation Maseur, p. 33 – 36.

Boyd, F.R. (1987). High- and low-temperature garnet peridotite xenoliths and their possible relation to the lithosphere-asthenosphere boundary beneath southern Africa. *in* Nixon, P.H. (ed.). Mantle Xenoliths. John Wiley and Sons. p. 402 – 412.

Boyd, F.R. and Nixon, P.H. (1978). Ultramafic nodules from the Kimberley pipes, South Africa. Geochim. Cosmochim. Acta, 42: 1367 – 1382.

Card, K.D. and Ciesielski, André (1986). DNAG#1. Subdivisions of the Superior Province of the Canadian Shield. Geoscience Canada, 13: 5 – 13.

Canil, D. (1994). An experimental calibration of the 'Nickel in Garnet' geothermometer with applications. Contrib. Min. Petrol. 117: 410 – 420.

Canil, Dante (1999). The Ni-in-garnet geothermometer: calibration at natural abundances. Contrib. Min. Petrol., 136: 240 – 246.

Cox, K.G. and Gurney, J.J. (1973). Xenoliths from the Matsoku pipe: Appendix of rock and mineral analyses. *in* Nixon, P.H. (ed.). Lesotho Kimberlites. Lesotho National Development Corporation Maseur, p. 93 – 100.

Dawson, J. Barry. Kimberlites and their Xenoliths. New York: Springer-Verlag. 1980. 252p.

Dawson, J.B. (1987). Metasomatized Harzburgites in Kimberlite and Alkaline Magmas: Enriched Restites and "Flushed" Lherzolites. *in* Menzies, M.A. and Hawksworth, C.J. (eds.). Mantle Metasomatism, Academic Press. p. 125 – 144.

Dawson, J.B. and Carswell, D.A. (1990). High temperature and ultra-high pressure eclogites. *in* Carswell D.A. (ed.). Eclogite Facies Rocks. Glasgow: Blackie and Sons Ltd.. p. 315 – 349.

Dawson, J.B., Gurney, J.J., and Lawless, P.J. (1975). Paleogeothermal gradients derived from xenoliths in kimberlite. Nature, 275: 299 – 300.

Deer, W.A., Howie, R.A., and Zussman, J.. An Introduction to the Rock Forming Minerals. New York: John Wiley and Sons Ltd.. 1966.

Erlank, A.J., Waters, F.G., Hawksworth, C.J., Haggerty, S.E., Allsopp, H.L., Rickard, R.S., and Menzies, M. (1987). Evidence for Mantle Metasomatism in peridotite Nodules from the Kimberley Pipes, South Africa. *in* Menzies, M.A. and Hawksworth, C.J. (eds.). Mantle Metasomatism, Academic Press. p. 221 – 311.

Field, S.W., Haggerty, S.E., and Erlank, A.J. (1989). Subcontinental metasomatism in the region of Jagersfonetin, South Africa. *in* Ross, J. (ed.) Kimberlites and related rocks 2. Geol. Soc. Australia Special Publication 14, Blackwell Scientific. p. 771 – 783.

Fipke, C.E., Gurney, J.J., and Moore, R.O. (1995). Diamond Exploration Techniques Emphasizing Indicator Mineral Geochemistry and Canadian Examples. Geological Survey of Canada Bulletin 423.

Finnerty, A.A. and Boyd, F.R. (1984). Evaluation of thermobarometers for garnet peridotites. Geochim. Cosmochim. Acta, 48: 15 – 27.

Finnerty, A.A. and Boyd, F.R. (1987). Thermobarometry for garnet peridotites: basis for the determination of thermal and compositional structure of the upper mantle. *in* Nixon, P.H. (ed.). Mantle Xenoliths. John Wiley and Sons. p. 381 – 402.

Grand, Stephen P. (1987). Tomographic Inversion for Shear Velocity Beneath the North American Plate. J. Geophys. Research, 90 (B-13): 14,065 – 14,090.

Griffin, W.L., Cousens, D.R., Ryan, C.G., Sie, S.H., and Suter, G.F. (1989). Ni in chrome pyrope garnets: a new geothermometer. Contrib. Min. Petrol, 103: 199 – 202.

Gurney, J.J. (1984). A correlation between garnets and diamonds. *in* Glover, J.E. and Harris, P.G. (ed.'s). Kimberlite Occurrence and Origin: A basis for Conceptual Models in Exploration. University of Western Australia Publication 8, p. 376 – 383.

Haggerty, Stephen E. (1995). Upper Mantle Mineralogy. J. Geodynamics, 20: 331 – 364.

Harte, Ben (1977). Rock nomenclature with particular relation to deformation and recrystallization textures in olivine-bearing xenoliths. J. Geol., 85: 279 – 288.

Harte, B. (1983). Mantle peridotites and processes – the kimberlite sample. *in* Hawksworth and Norry (eds.). Continental basalts and mantle xenoliths. Shiva Publishing Ltd.. p. 46 – 91.

Harte, B., Cox, K.G., and Gurney, J.J. (1975). Petrography and geological history of upper mantle xenoliths from the Matsoku kimberlite pipe. *in* Physics and Chemistry of the Earth, First International Conference on Kimberlite. Oxford: Pergamon Press, p. 477 – 506.

Henry, Phillipe, Stevenson, Ross K., Larbi, Youcef and Gariepy, Clement (1997). Use of Nd isotopes to quantify 700 Ma crustal growth from 3.4 – 2.7 Ga in the western Superior Privince. in *in*, Harrap, R., and Helmstaedt, H. (eds.). Lithoprobe; Western Superior Transect Third Annual Workshop. Lithoprobe Report 63: 27 – 36.

Hetman, Casey M. (1996). The Ilmenite Association of the Attawapiskat Kimberlite Cluster, Ontario, Canada. Unpublished Masters Thesis, University of Toronto.

Janse, A.J.A., Downie, I.F., Reed, L.E., and Sinclair, I.G.L. (1989). Alkaline Intrusions in the Hudson Bay Lowlands, Canada: Exploration methods, petrology and geochemistry. *in* Ross, J. (ed.). Kimberlites and Related Rocks. Geological Society of Australia Special Publication No. 14, vol. 2, p 1192 – 1203.

Johnson, M.D., Armstrong, D.K., Sanford, B.V., Telford, P.G., and Rutka, M.A. (1991). Paleozoic and Mesozoic Geology of Ontario. *in* Geology of Ontario, Ontario Geological Survey, Special Volume 4, Part 2, 907 – 1008.

Kennedy, C. Scott and Kennedy, George C. (1976). The Equilibrium Boundary Between Graphite and Diamond. J. Geophys. Research. 81: 2467 – 2470.

Kong, J.M., Boucher, D.R., and Scott Smith, B.H. (1999). Exploration and Geology of the Attawapiskat Kimberlites, James Bay Lowland, Northern Ontario, Canada. *in* Dawson, J.B. (ed.). Proceedings of the 7th International Kimberlite Conference.

Kopylova, M.G., Russell, J.K., and Cookenboo, H. (1999). Petrology of Peridotite and Pyroxenite Xenoliths from the Jericho Kimberlite: Implications for the Thermal State of the Mantle beneath the Slave Craton, Northern Canada. J. Petrol., 40: 79 – 104.

Leake, Bernard E. (Chairman), Woolley, Alan R. (Secretary), Arps, Charles E.S., Birch, William D., Gilbert, M. Charles, Grice, Joel D., Hawthorne, Frank C., Kato, Akira, Kisch, Hanan J., Krivovichev, Vladimir G., Linthout, Kees, Laird, Jo, Mandarino, Joseph A., Maresch, Walter V., Nickel, Ernest H., Rock, Nicholas, S., Schumacher, John C., Smith, David C., Stephenson, Nick C.N., Ungaretti, Luciano, Whittaker, Eric J.W., and Youzhi, Guo. (1997). Nomenclature of amphiboles: Report of the Subcommittee on Amphiboles of the International Mineralogical Association, Commission on New Minerals and Mineral Names. Am. Min., 82: 1019-1037.

Lindsley, D.H. and Dixon, S.A. (1976). Diopside-enstatite equilibria at 850 °C to 1400 °C, 5 to 35 kbar. Am. J. Sci., 276: 1285 – 1301.

Lloyd, F.E. (1987). Characterization of Mantle Metasomatic Fluids in Spinel Lherzolites and Alkali Clinopyroxenites from the West Eifel and South West Uganda. *in* Menzies, M.A. and Hawksworth, C.J. (eds). Mantle Metasomatism, Academic press. p. 91 – 123.

MacGregor, Ian D. (1974). The System $MgO - Al_2O_3 - SiO_2$: Solubility of Al_2O_3 in Enstatite for Spinel and Garnet Peridotite Compositions. Am. Min., 59: 110 – 119.

MacKenzie, J.M. and Canil, D. (1999). Composition and thermal evolution of cratonic mantle beneath the central Archean Slave Province, NWT, Canada. Contrib. Min. Petrol., 134: 313 – 324.

Meyer, Henry O.A., Waldman, Michael A., and Garwood, Blaine L. (1994). Mantle xenoliths from kimberlite near Kirkland Lake, Ontario. Can. Min., 32: 295 – 306.

Mitchell, Roger H. (1977). Ultramafic xenoliths from the Elwin Bay kimberlite: the first Canadian paleogeotherm. Can. J. Earth Sci., 14: 1202 – 1210.

Mitchel, Roger H. (1978). Garnet Lherzolites From Somerset Island, Canada and Aspects of the Nature of Perturbed Geotherms. Contrib. Min. Petrol., 67: 341 – 347.

Mitchell, Roger H.. Kimberlites; Mineralogy, Geochemistry, and Petrology. Plenum Press, 1986. 442p.

Moser, D.E., and Krogh, T.E. (1995). A U-Pb dating study of lower crustal xenoliths from the Attawapiskat kimberlite pipes, Sachigo subprovince. *in* Lithoprobe Western Superior Transect, Second Annual Workshop, Lithoprobe Report no. 53, p. 54.

Moser, D., Amelin, Y., Schulze, D., and Krogh, T. (1997). Progress in Understanding the Geology of the Lithosphere beneath the Eastern Sachigo Subprovince. *in*, Harrap, R., and Helmstaedt, H. (eds.). Lithoprobe; Western Superior Transect Third Annual Workshop. Lithoprobe Report 63: 102-103.

Nixon, P.H. (1987). Kimberlite xenoliths and their cratonic setting. *in* Nixon, P.H. (ed). Mantle Xenoliths. Chichester: Wiley and Sons Ltd., p. 216 – 239.

Nixon, P.H. and Boyd, F.R. (1973). Petrogenesis of the Granular and Sheared Ultrabasic Nodule Suite in Kimberlite. *in* Nixon, P.H. (ed.). Lesotho Kimberlites. Lesotho National Development Corporation Maseur, p. 48 – 56.

O'Neill, Hugh St.C. and Wood, B.J.,(1979). An Experimental Study of Fe – Mg Partitioning Between Garnet and Olivine and Its Calibration as a Geothermometer. Contrib. Min. Petrol., 70: 59 – 70.

O'Neill, Hugh St. C. (1980). An Experimental Study of Fe – Mg Partitioning Between Garnet and Olivine and Its Calibration as a Geothermometer: Corrections. Contrib. Min. Petrol., 72: 337.

Pollack, Henry N. and Chapman, David S. (1977). On the regional variation of heat flow, geotherms, and lithospheric thickness. Tectonophysics, 38: 279 – 296.

Ross, C.R.I.I., Keppler, H., Canil, D., and O'Neill, H.StC. (1996). Structure and crystal field spectra of $Co_3Al_2(SiO_4)_3$ and $(Mg,Ni)_3Al_2(SiO_4)_3$ garnet. Am. Min. 81: 61 – 66.

Ryan, C.G., Griffin, W.L., and Pearson, N.L. (1996). Garnet geotherms: pressure-temperature data from Cr-pyrope garnet xenocrysts in volcanic rocks. J.G.R., 101 (B3): 5611 – 5625.

Sage, R.P. (1996). Kimberlites in Ontario. Ontario Geological Survey Open File Report 5236.

Sanford, B.V. and Norris, A.W. (1975). Devonian Stratigraphy of the Hudson Platform, Parts I & II. Geological Survey of Canada Memoir 379.

Schulze, D.J. (1993). Constraints on the abundance of eclogite in the upper mantle. J.G.R., 94: 4205 – 4212.

Schulze, Daniel J. (1995). Low-Ca garnet harzburgites from Kimberley, South Africa: Abundance and bearing on the structure and evolution of the lithosphere. J.G.R. 100(B7): 12,513 – 12,526.

Schulze, Daniel J. (1997). The Significance of Eclogite and Cr-poor Megacryst Garnets in Diamond Exploration. Explor. Mining Geol., 6: 349 – 366.

Schulze, Daniel J. and Hetman, Casey M. (1997). Mantle Xenoliths from the Attawapiskat Kimberlites. in Harrap, R.M. and Helmstaedt, H. (eds.). 1997 Western Superior Transect Third Annual Workshop, April 11-12, 1997. Lithoprobe Report #63, Lithoprobe Secretariat, University of British Columbia, p. 62 – 66.

Shee, S.R., Gurney, J.J., and Robinson, D.N. (1982). Two diamond-bearing peridotite xenoliths from Finsch kimberlite, South Africa. Contrib. Min. Petrol. 81: 79 – 87.

Smith, Douglas and Boyd, Francis R. (1992). Compositional zonation in garnets in peridotite xenoliths. Contrib. Min. Petrol., 112: 134 – 147.

Spera, F.J. (1987). Dynamics of Translithospheric Migration of Metasomatic Fluid and Alkaline Magma. *in* Menzies, M.A. and Hawksworth, C.J. (eds.). Mantle Metasomatism, Academic Press. p. 1 – 20.

Suchy, Daniel R. and Stearn, Colin W. (1993). Evidence of a continent-wide fault system on the Attawapiskat River, Hudson Bay Platform, northern Ontario. Can. J. Earth Sci., 30: 1668 – 1673.

Summers, R.W. (1989). A study of the petrography and geochemistry of metasomatized garnets in xenoliths from the Monastery kimberlite pipe. Unpublished B.Sc. thesis, Queens University. 76 p.

Thurston, P.C., Osmani, I.A., and Stone, D. (1991). Northwestern Superior Province: Review and Terrain Analysis. *in* Geology of Ontario, Ontario Geological Survey, Special Volume 4, Part 1, p. 81-144.

Wells, P.R.A. (1977). Pyroxene thermometry in simple and complex systems. Contrib. Min. Petrol. 62: 129 – 139.

Williams, H.R., Stott, G.M., Thurston, P.C., Sutcliff, R.H., Bennett, G., Easton, R.M., and Armstrong, D.K. (1991). Tectonic Evolution of Ontario: Summary and Synthesis. *in* Geology of Ontario, Ontario Geological Survey, Special Volume 4, Part 2, 1255 – 1334.

Vicker, Philip A. (1997). Garnet Peridotite Xenoliths from Kimberlite Near Kirkland Lake, Canada. Unpublished Masters Thesis, University of Toronto.

Appendix A: Electron Microprobe Standards and Operations Specifications

APPENDIX I

MICROPROBE STANDARDS

All minerals

Mineral	PYROPE	OLIVINE (Fo85)	CPX/OPX	CPX [+]	CHROMITE	PHLOGOPITE	AMPHIBOLE
Accelerating voltage (kv)	15	20	15	15	20	15	15
Beam current (nA)	30	30	25	25	20	8	25
Na	albite	n/a	albite	albite	n/a	albite	albite
Mg	pyrope	olFo85**	enstatite	MgOsx1*	chromite	phlogopite	pyrope
Al	pyrope	n/a	pxTiAlsx1*	Al2O3sx1*	ghanite	phlogopite	pyrope
Si	pyrope	olFo85**	kakaugite^ (cpx) hypersthene (opx)	wollastonite	bustamite	phlogopite	pyrope
Mn	bustamite	bustamite	bustamite	rhodochrosite	bustamite	bustamite	bustamite
Ni	n/a	pentlandite	pentlandite	pentlandite	pentlandite	pentlandite	n/a
Fe	pyrope	olFo85**	hypersthene	hematite	chromite	GARsx2*	pyrope
Ca	bustamite	bustamite	bustamite	wollastonite	bustamite	bustamite	bustamite
Ti	pxTiAlsx1*	n/a	pxTiAlsx1*	TiO2sx2*	TiO2sx2*	pxTiAlsx1*	pxTiAlsx1*
Cr	chromite	chromite	chromite	Cr2O3sx1*	n/a	Cr2O3sx1*	chromite
K	n/a	n/a	sanidine	sanadine	n/a	phlogopite	microcline
Cl	n/a	n/a	n/a	n/a	n/a	tugtapite	tugtapite
F	n/a	n/a	n/a	n/a	n/a	phlogopite	CaF2sx2*

* - synthetic oxides, University of Toronto

** - synthetic olivine, forsterite content 85

^ - augite from kakanui basalt, New Zealand

[+] - Due to mechanical problems with the microprobe, clinopyroxenes from heavy mineral concentrate from pipe V-1 were analyzed using this routine.

Appendix B: Mineral Analysis Results

SAMPLE	MgO	SiO2	CaO	Cr2O3	MnO	FeO	NiO	Total
13-95-33/1	50.391	41.283	0.005	0.004	0.110	7.733	0.334	99.860
13-95-33/2	50.537	41.350	0.003	0.013	0.099	7.825	0.360	100.187
13-95-33/a	50.390	41.284	0.006	0.004	0.110	7.733	0.333	99.860
13-95-33/b	50.536	41.350	0.003	0.013	0.098	7.826	0.360	100.186
13-95-34/1	49.502	41.365	0.031	0.032	0.087	8.576	0.347	99.939
13-95-34/3	49.369	41.143	0.017	0.010	0.147	8.644	0.374	99.704
13-95-34/4	49.747	41.057	0.043	0.022	0.146	8.653	0.389	100.058
13-95-38	50.270	40.190	0.030	0.010	0.100	9.030	0.380	100.050
13-95-42	52.150	40.870	0.010	0.000	0.110	7.080	0.350	100.580
13-95-48/ol-3	50.080	41.192	0.021	0.070	0.081	8.188	0.370	100.003
13-95-48/ol-4	50.046	41.209	0.011	0.023	0.103	8.151	0.370	99.913
13-95-48/ol-6	49.885	40.672	0.021	0.056	0.139	8.114	0.354	99.241
13-95-48/ol-7	50.070	41.102	0.011	0.037	0.110	8.235	0.331	99.895
13-95-48/a	50.153	41.301	0.014	0.073	0.126	8.304	0.329	100.301
13-95-48/b	50.135	41.349	0.014	0.030	0.122	8.106	0.330	100.087
13-95-48/c	50.259	41.373	0.014	0.047	0.119	8.136	0.349	100.297
13-95-48/d	50.137	41.252	0.017	0.027	0.109	8.068	0.327	99.938
13-95-48/e	50.152	41.316	0.006	0.021	0.124	7.995	0.340	99.954
13-95-48/f	50.141	41.448	0.021	0.022	0.109	8.052	0.359	100.152
13-95-48/g	49.717	40.989	0.023	0.023	0.109	7.987	0.370	99.217
13-95-48/1	50.063	41.208	0.014	0.007	0.092	8.084	0.333	99.800
13-95-48/2	49.975	41.284	0.014	0.024	0.118	8.057	0.315	99.787
13-95-48/3	50.057	41.319	0.016	0.004	0.084	8.028	0.326	99.835
13-95-48/4	49.990	41.350	0.013	0.008	0.127	8.016	0.282	99.786
13-95-48/5	50.215	41.555	0.013	0.015	0.133	8.089	0.349	100.369
13-95-48/6	49.810	41.479	0.019	0.065	0.129	8.680	0.274	100.457
13-95-50/1	50.906	41.607	0.013	0.018	0.101	7.499	0.328	100.470
13-95-50/2	50.099	41.008	0.001	0.006	0.075	7.460	0.375	99.025
13-95-50/7	50.666	41.436	0.004	0.000	0.096	7.310	0.380	99.891

Appendix B **Mineral Analysis Results** **Olivine**

SAMPLE	MgO	SiO2	CaO	Cr2O3	MnO	FeO	NiO	Total
13-95-52/1	50.500	41.275	0.004	0.015	0.114	7.728	0.380	100.015
13-95-52/2	50.274	41.267	0.017	0.038	0.118	7.822	0.383	99.919
13-95-56/1	51.287	41.646	0.012	0.021	0.114	7.158	0.344	100.582
13-95-56/2	50.640	41.480	0.010	0.015	0.091	7.052	0.360	99.648
13-95-56/3	50.465	41.390	0.007	0.000	0.084	7.036	0.337	99.320
13-95-56/a	50.070	40.984	0.000	0.010	0.111	7.728	0.363	99.267
13-95-59/1	50.429	41.432	0.010	0.004	0.112	7.799	0.350	100.136
13-95-59/2	49.898	41.017	0.007	0.001	0.097	7.689	0.344	99.053
13-95-59/3	50.211	41.265	0.000	0.013	0.084	7.876	0.358	99.807
13-95-59/a	50.429	41.432	0.010	0.004	0.112	7.799	0.350	100.136
13-95-59/b	49.898	41.017	0.007	0.001	0.097	7.689	0.344	99.053
13-95-59/c	50.211	41.265	0.000	0.013	0.084	7.876	0.358	99.807
13-95-67/1	49.623	40.773	0.029	0.039	0.115	8.438	0.354	99.371
13-95-67/2	50.027	41.196	0.057	0.013	0.115	8.338	0.354	100.100
13-95-67/3	49.755	41.068	0.010	0.028	0.081	8.514	0.366	99.823
13-95-67/4	50.007	41.151	0.008	0.034	0.155	8.374	0.355	100.084
13-95-67/5	50.196	41.470	0.046	0.026	0.092	8.190	0.355	100.375
13-97-78/a	50.062	41.111	0.020	0.076	0.110	8.845	0.426	100.648
13-97-78/c	49.686	41.081	0.042	0.045	0.143	9.317	0.406	100.720
13-97-78/e	50.873	41.802	0.010	0.000	0.099	7.339	0.364	100.488
13-97-78/1	49.044	41.068	0.053	0.086	0.107	9.546	0.365	100.270
13-97-78/2	49.331	40.989	0.027	0.051	0.108	8.677	0.389	99.573
13-97-78/4	49.628	41.175	0.014	0.058	0.108	8.601	0.387	99.972
13-97-78/5	49.653	41.248	0.028	0.057	0.108	8.596	0.401	100.090
13-97-78/6	49.600	41.124	0.018	0.054	0.106	8.594	0.402	99.896
13-97-81/1	49.691	40.891	0.029	0.034	0.129	9.072	0.425	100.272
13-97-81/2	49.917	41.215	0.046	0.029	0.078	8.957	0.409	100.652
13-97-81/a	49.691	40.890	0.028	0.034	0.129	9.072	0.425	100.270
13-97-81/b	49.918	41.215	0.046	0.029	0.079	8.958	0.410	100.654
13-97-82/1	50.260	41.426	0.011	0.023	0.133	8.178	0.364	100.395
13-97-82/2	50.337	41.622	0.014	0.019	0.065	8.184	0.364	100.604

Appendix B **Mineral Analysis Results** **Olivine**

SAMPLE	MgO	SiO2	CaO	Cr2O3	MnO	FeO	NiO	Total
13-97-82/3	50.222	41.651	0.012	0.020	0.116	8.228	0.336	100.585
13-97-82/4	50.343	41.573	0.018	0.022	0.119	8.177	0.339	100.591
13-97-82/5	50.255	41.659	0.040	0.011	0.132	8.147	0.374	100.617
13-97-82/6	49.820	41.716	0.020	0.018	0.103	8.215	0.364	100.254
13-97-82/7	50.349	41.666	0.012	0.017	0.091	8.216	0.378	100.728
13-97-82/8	50.358	41.622	0.015	0.035	0.068	8.174	0.379	100.651
13-97-82/9	50.664	41.731	0.043	0.019	0.092	8.106	0.330	100.984
13-97-83/1	50.326	41.233	0.018	0.009	0.165	8.326	0.330	100.407
13-97-83/2	50.617	41.476	0.040	0.007	0.159	8.144	0.328	100.771
13-97-83/3	50.426	41.198	0.047	0.019	0.142	8.327	0.334	100.494
13-97-83/a	50.326	41.233	0.018	0.009	0.165	8.326	0.331	100.408
13-97-83/b	50.618	41.476	0.039	0.007	0.160	8.143	0.328	100.772
13-97-83/c	50.427	41.198	0.048	0.019	0.142	8.327	0.333	100.494
13-102-09/b	50.274	41.329	0.018	0.029	0.084	8.457	0.379	100.572
13-102-09/c	50.311	41.194	0.011	0.003	0.127	8.317	0.363	100.325
ATT-A1-P2	51.840	40.670	0.000	0.010	0.110	6.790	0.340	99.770
ATT-A1-P1	49.970	40.220	0.020	0.020	0.120	8.750	0.380	99.520

SAMPLE	Na2O	MgO	Al2O3	SiO2	MnO	FeO	CaO	TiO2	Cr2O3	Total
13-95-28/g1	0.022	10.985	22.327	39.177	0.510	21.766	5.567	0.033	0.650	101.037
13-95-28/g2	0.018	11.051	22.626	39.423	0.489	21.752	5.343	0.040	0.500	101.242
13-95-29/g3	0.016	10.975	22.171	39.496	0.522	21.641	5.678	0.045	0.716	101.259
13-95-28/g4	0.019	10.691	22.390	39.412	0.523	22.296	5.507	0.047	0.665	101.549
13-95-28/g5	0.011	10.913	22.571	39.350	0.493	21.945	5.369	0.048	0.500	101.200
13-95-32/g1	0.043	21.500	23.884	41.776	0.390	7.314	4.053	0.140	0.468	99.568
13-95-32/g2	0.054	21.862	24.336	42.491	0.373	7.410	3.960	0.137	0.314	100.936
13-95-32/g3	0.043	21.797	23.962	42.561	0.376	7.435	3.992	0.162	0.472	100.798
13-95-32/g4	0.047	21.882	23.994	42.576	0.373	7.429	3.939	0.152	0.479	100.872
13-95-32/g5	0.044	21.633	23.705	42.003	0.378	7.431	3.869	0.145	0.482	99.689
13-95-32/g6	0.047	21.941	24.088	42.405	0.395	7.454	3.989	0.157	0.497	100.973
13-95-33/core1	0.022	19.562	21.823	42.195	0.652	8.260	5.044	0.000	3.227	100.785
13-95-33/rim1	0.036	19.756	22.042	42.195	0.652	8.167	4.935	0.015	2.906	100.704
13-95-33/core2	0.024	19.449	21.691	41.844	0.675	8.158	5.157	0.000	3.191	100.190
13-95-33/rim2	0.034	19.892	22.121	42.174	0.622	8.271	4.767	0.000	2.952	100.833
13-95-34/g1(r)	0.082	20.398	20.496	41.181	0.402	8.047	4.074	0.357	4.119	99.156
13-95-34/g2(c)	0.090	20.169	20.591	41.017	0.405	8.062	4.490	0.297	4.050	99.172
13-95-34/g3	0.070	19.849	20.718	40.925	0.376	8.017	5.125	0.300	3.720	99.100
13-95-35/g1	0.066	20.726	22.269	41.911	0.354	8.095	4.372	0.320	2.394	100.507
13-95-35/g3	0.055	20.411	21.341	41.014	0.360	8.334	4.368	0.372	2.831	99.087
13-95-35/g4	0.070	20.500	21.505	41.410	0.377	8.302	4.343	0.365	3.120	99.993
13-95-42	0.020	19.620	21.720	41.480	0.550	8.150	5.100	0.000	3.300	99.940
13-95-47/g-a	0.065	20.546	22.425	42.022	0.395	7.689	4.525	0.123	2.498	100.223
13-95-47/g-b	0.068	20.600	22.505	41.809	0.472	7.878	4.129	0.123	2.280	99.796
13-95-47/g-c	0.077	20.507	22.298	41.619	0.451	7.731	4.422	0.100	2.494	99.622
13-95-47/g-e	0.053	20.595	22.372	41.766	0.403	7.709	4.444	0.124	2.517	99.930
13-95-47/g-f	0.062	20.695	22.446	42.084	0.415	7.716	4.466	0.114	2.478	100.414
13-95-47/g-g	0.075	20.584	22.503	41.999	0.421	7.780	4.544	0.093	2.506	100.430
13-95-48/g-b	0.086	19.737	19.710	41.588	0.450	7.712	5.215	0.263	5.275	99.950

SAMPLE	Na2O	MgO	Al2O3	SiO2	MnO	FeO	CaO	TiO2	Cr2O3	Total
13-95-48/g-c	0.092	19.620	19.154	41.411	0.452	7.796	5.462	0.267	6.563	100.725
13-95-48/g-d	0.070	19.683	19.062	41.288	0.440	7.857	5.274	0.263	6.431	100.298
13-95-48/g-e	0.080	19.571	18.935	41.419	0.455	7.799	5.318	0.253	6.684	100.434
13-95-48/g-f	0.080	19.281	19.082	41.307	0.470	7.752	5.808	0.283	6.737	100.720
13-95-49/g-a	0.040	19.440	21.716	41.767	0.477	8.226	5.367	0.125	3.460	100.578
13-95-49/g-b	0.043	19.476	21.697	41.658	0.509	8.332	5.406	0.118	3.439	100.635
13-95-49/g-c	0.038	19.369	21.645	41.799	0.458	8.395	5.417	0.147	3.524	100.754
13-95-49/g-d	0.040	19.392	21.748	41.601	0.450	8.231	5.336	0.146	3.494	100.398
13-95-49/g-e	0.042	19.294	21.759	41.559	0.468	8.425	5.326	0.113	3.508	100.452
13-95-49/g-f	0.036	19.303	21.538	41.650	0.451	8.336	5.433	0.129	3.603	100.443
13-95-49/g-g	0.040	19.307	21.528	41.688	0.505	8.369	5.364	0.142	3.604	100.507
13-95-50/g-a	0.031	19.834	21.874	41.688	0.583	8.429	4.828	0.004	3.274	100.514
13-95-50/g-b	0.025	20.584	21.715	41.895	0.600	8.432	3.721	0.006	3.638	100.591
13-95-50/g-c	0.021	19.742	22.171	41.812	0.598	8.313	5.183	0.006	2.960	100.785
13-95-50/g-d	0.027	19.641	21.760	41.690	0.539	8.188	5.084	0.024	3.699	100.625
13-95-50/g-e	0.037	20.344	22.035	41.919	0.549	8.288	4.273	0.005	3.214	100.627
13-95-50/g-f	0.021	19.975	21.871	41.797	0.588	8.338	4.645	0.000	3.482	100.696
13-95-50/g-g	0.035	21.104	22.591	42.441	0.569	8.380	3.538	0.000	3.037	101.660
13-95-50/g-h	0.032	20.101	21.699	41.751	0.543	8.350	4.428	0.006	3.436	100.314
13-95-50/g-i	0.038	21.033	22.918	41.813	0.567	8.296	3.194	0.006	2.114	99.941
13-95-52/g-a	0.079	19.527	18.487	40.981	0.421	7.248	5.455	0.183	7.430	99.732
13-95-52/g-b	0.072	19.509	18.537	40.871	0.390	7.352	5.439	0.193	7.393	99.684
13-95-52/g-c	0.075	19.624	18.492	41.034	0.424	7.331	5.400	0.194	7.410	99.909
13-95-52/g-d	0.061	19.776	18.802	40.734	0.438	7.254	5.037	0.171	6.546	98.758
13-95-52/g-e	0.073	19.685	18.820	41.361	0.388	7.418	5.423	0.181	7.339	100.615
13-95-52/g-f	0.096	19.770	18.720	41.275	0.434	7.336	5.239	0.167	7.197	100.138
13-95-54/g-a	0.070	16.585	23.556	40.976	0.412	14.404	4.176	0.159	0.095	100.363
13-95-54/g-b	0.076	16.584	23.495	40.790	0.425	14.539	4.232	0.136	0.114	100.315
13-95-54/g-c	0.070	16.470	23.541	41.072	0.446	14.620	4.225	0.133	0.118	100.625
13-95-54/g-e	0.043	16.891	23.768	41.008	0.414	14.136	3.968	0.120	0.121	100.426
13-95-54/g-f	0.058	16.852	23.755	41.066	0.401	14.440	4.023	0.070	0.097	100.704

Appendix B **Mineral Analysis Results** **Garnet**

SAMPLE	Na2O	MgO	Al2O3	SiO2	MnO	FeO	CaO	TiO2	Cr2O3	Total
13-95-54/g-g	0.044	16.923	23.856	41.187	0.391	14.247	4.012	0.061	0.091	100.768
13-95-54/g-i	0.062	17.231	23.801	41.220	0.403	13.633	3.869	0.076	0.107	100.340
13-95-54/g-l	0.061	16.893	23.583	41.010	0.425	14.100	4.178	0.137	0.065	100.391
13-95-56/g1	0.012	20.034	22.053	41.421	0.536	8.348	4.925	0.007	3.142	100.480
13-95-56/g2	0.004	19.749	21.870	41.521	0.514	8.334	5.201	0.003	3.427	100.624
13-95-56/g3	0.020	19.714	21.562	40.905	0.536	8.370	4.491	0.000	3.135	98.735
13-95-59/g1	0.023	21.558	23.017	42.108	0.640	8.789	2.419	0.005	1.923	100.482
13-95-59/g2	0.031	21.470	23.253	41.697	0.640	8.774	2.415	0.002	1.545	99.827
13-95-59/g3	0.024	21.754	23.350	42.080	0.622	8.869	2.328	0.005	1.635	100.668
13-95-59/g4	0.030	21.679	23.414	42.080	0.671	8.792	2.454	0.005	1.915	101.039
13-95-63/g1	0.024	19.444	21.296	41.173	0.584	8.420	5.199	0.000	3.737	99.877
13-95-63/g2	0.011	19.633	21.479	41.399	0.515	8.245	5.209	0.005	3.696	100.193
13-95-63/g3	0.020	20.674	22.016	41.744	0.567	8.635	3.863	0.000	3.356	100.875
13-95-63/g4	0.028	20.426	21.917	41.472	0.591	8.572	3.751	0.000	3.278	100.037
13-95-66/g1	0.058	20.185	21.604	41.778	0.597	8.290	4.267	0.025	3.744	100.549
13-95-66/g2	0.038	20.340	21.317	41.444	0.560	8.170	4.456	0.040	4.065	100.429
13-95-67/g1	0.062	21.251	20.413	41.519	0.438	7.772	3.543	0.192	5.153	100.344
13-95-67/g2	0.075	21.237	20.207	41.417	0.407	7.781	3.585	0.207	5.316	100.231
13-95-67/g3	0.071	20.751	19.584	40.790	0.430	7.832	3.667	0.219	5.577	98.921
13-95-67/g4	0.073	21.157	20.069	41.457	0.371	7.781	3.634	0.203	5.305	100.050
13-95-67/g5	0.071	21.041	19.966	41.515	0.416	7.819	3.799	0.212	5.529	100.367
13-95-70/g1	0.024	20.069	22.269	42.148	0.569	8.457	4.998	0.000	3.367	101.902
13-95-70/g2	0.019	19.270	21.509	41.421	0.586	8.480	5.307	0.000	3.679	100.271
13-95-70/g3	0.005	19.530	21.764	40.858	0.519	8.412	5.022	0.000	2.946	99.057
13-97-78/core1	0.089	19.763	17.113	40.169	0.377	7.805	4.459	0.459	8.022	98.256
13-97-78/rim1	0.106	19.875	16.786	40.178	0.389	7.993	4.417	0.509	8.372	98.624
13-97-78/rim3	0.058	19.741	18.497	40.390	0.353	8.065	4.917	0.360	6.833	99.213
13-97-78/core3	0.112	19.975	17.315	40.191	0.403	7.918	4.398	0.472	7.974	98.757
13-97-81/core1	0.039	19.186	18.692	40.276	0.363	8.129	5.546	0.240	6.331	98.803
13-97-81/rim1	0.030	19.219	18.953	40.584	0.381	8.128	5.395	0.229	6.024	98.943
13-97-81/core2	0.042	19.300	18.885	40.578	0.395	8.277	5.483	0.224	6.055	99.239

SAMPLE	Na2O	MgO	Al2O3	SiO2	MnO	FeO	CaO	TiO2	Cr2O3	Total
13-97-81/rim2	0.046	19.199	18.766	40.300	0.439	8.214	5.441	0.244	5.938	98.585
13-97-82/1	0.030	19.103	19.374	41.072	0.434	7.854	6.040	0.115	6.266	100.288
13-97-78/2	0.012	19.081	19.369	41.299	0.452	7.893	5.920	0.085	6.387	100.498
13-97-78/3	0.013	18.927	19.514	41.331	0.452	7.885	6.004	0.102	6.412	100.638
13-97-78/4	0.024	19.006	19.461	41.293	0.457	7.903	5.910	0.108	6.228	100.391
13-97-78/5	0.022	18.919	19.389	41.282	0.420	7.884	5.938	0.108	6.331	100.292
13-97-78/6	0.027	18.930	19.365	41.387	0.429	7.968	5.931	0.090	6.355	100.482
13-97-78/7	0.013	18.852	19.433	41.410	0.420	7.938	5.942	0.075	6.280	100.365
13-97-78/8	0.023	18.927	19.495	41.376	0.449	7.877	5.962	0.102	6.273	100.484
13-97-78/9	0.024	18.932	19.387	41.151	0.440	7.860	5.896	0.080	6.232	100.004
13-97-78/10	0.026	19.040	19.591	41.410	0.413	7.961	5.941	0.122	6.147	100.650
13-97-83/core1	0.020	19.884	21.165	41.173	0.507	8.132	4.697	0.033	4.005	99.616
13-97-83/gar?	0.032	19.975	21.152	40.978	0.527	8.026	4.672	0.028	3.902	99.294
13-97-83/core2	0.028	20.102	21.241	41.312	0.535	8.057	4.570	0.025	3.633	99.504
13-97-83/rim1	0.034	20.605	22.314	41.434	0.513	7.918	4.046	0.020	2.813	99.697
13-97-83/rim2	0.028	20.706	22.267	41.810	0.496	7.947	4.034	0.022	2.813	100.122
13-99-18/core1	0.042	19.602	21.715	40.888	0.568	8.329	4.823	0.047	3.267	99.280
13-99-18/rim1	0.034	19.663	21.613	40.875	0.634	8.282	4.876	0.040	3.199	99.217
13-99-18/core2	0.036	19.569	21.386	40.967	0.573	8.312	4.896	0.040	3.473	99.252
13-99-18/core3	0.034	19.375	21.335	40.689	0.576	8.165	4.931	0.063	3.332	98.500
13-99-18/rim2	0.036	19.617	21.528	40.768	0.591	8.325	4.938	0.067	3.259	99.130
13-99-18/rim3	0.038	19.532	21.303	40.790	0.544	8.227	4.886	0.025	3.104	98.449
13-102-04/rim1	0.070	21.232	19.676	41.583	0.427	7.741	3.464	0.297	5.703	100.195
13-102-04/core2	0.078	21.228	19.845	41.857	0.431	7.728	3.417	0.264	5.560	100.408
13-102-04/rim2	0.078	21.333	19.724	41.874	0.393	7.584	3.450	0.260	5.614	100.311
13-102-05/core1	0.071	19.831	18.273	41.307	0.420	8.019	4.676	0.275	7.498	100.368
13-102-05/rim1	0.078	20.228	18.726	41.380	0.399	8.046	4.385	0.329	6.564	100.136
13-102-05/core2	0.063	19.927	18.225	41.314	0.389	8.187	4.567	0.282	7.512	100.466
13-102-05/rim3	0.066	19.990	18.634	41.344	0.449	8.070	4.468	0.265	6.635	99.921
13-102-09/core1	0.053	20.555	19.992	40.865	0.424	7.952	4.007	0.150	5.288	99.285
13-102-09/rim1	0.053	20.568	19.950	40.927	0.435	7.844	3.930	0.145	5.425	99.277

SAMPLE	Na2O	MgO	Al2O3	SiO2	MnO	FeO	CaO	TiO2	Cr2O3	Total
13-102-09/core2	0.050	20.522	19.546	40.828	0.424	7.833	4.041	0.115	5.602	98.961
13-102-09/rim2	0.053	20.476	19.508	40.593	0.442	7.868	4.174	0.153	5.596	98.863
13-102-12/core1	0.086	21.094	19.871	41.996	0.448	7.683	3.474	0.279	5.799	100.730
13-102-12/core1y	0.062	19.706	19.025	41.633	0.451	7.772	5.629	0.130	6.467	100.874
13-102-12/rim1	0.059	20.691	19.565	41.774	0.417	7.930	4.122	0.158	5.871	100.587
13-102-12/core2	0.057	19.749	18.443	41.346	0.434	7.858	5.145	0.190	7.191	100.413
13-102-12/rim2	0.067	20.562	18.875	41.770	0.411	7.917	4.343	0.227	6.739	100.910
102-15/g1	0.059	20.023	18.157	41.151	0.399	7.293	4.985	0.202	7.970	100.240
102-15/g4	0.051	20.038	18.072	40.957	0.455	7.332	5.149	0.180	7.897	100.129
102-15/g5	0.032	20.522	19.756	41.395	0.435	7.220	4.732	0.162	6.276	100.530
102-15/g6	0.050	19.784	18.445	41.500	0.374	7.368	4.911	0.152	7.277	99.861
102-15/g7	0.051	19.981	18.186	41.357	0.399	7.458	5.068	0.183	7.765	100.448
102-15/g8	0.105	19.998	18.290	41.288	0.394	7.274	4.920	0.187	7.800	100.255
ATT-A1-P2	0.050	20.490	21.210	41.100	0.450	7.420	4.050	0.030	3.860	98.660
ATT-A1-P1	0.060	19.290	20.530	40.650	0.410	8.390	4.880	0.250	3.790	98.250

SAMPLE	Na2O	Al2O3	MgO	SiO2	NiO	FeO	MnO	Cr2O3	K2O	CaO	TiO2	Total
13-95-33/1	0.070	0.682	36.325	57.581	0.101	4.660	0.112	0.221	0.000	0.273	0.000	100.025
13-95-33/2	0.059	0.695	36.604	58.122	0.079	4.748	0.107	0.257	0.001	0.218	0.007	100.899
13-95-33/3	0.078	0.699	36.350	57.609	0.062	4.751	0.098	0.257	0.000	0.161	0.008	100.074
13-95-33/4	0.059	0.688	36.816	58.129	0.041	4.823	0.143	0.259	0.000	0.169	0.000	101.126
13-95-33/5	0.073	0.667	36.410	57.686	0.080	4.716	0.148	0.235	0.007	0.173	0.000	100.197
13-95-33/6	0.085	0.690	36.487	57.812	0.083	4.669	0.134	0.227	0.000	0.200	0.000	100.385
13-95-35/1	0.148	0.697	36.252	57.598	0.099	5.416	0.114	0.168	0.006	0.444	0.117	101.059
13-95-35/2	0.142	0.690	36.415	58.219	0.092	5.482	0.101	0.171	0.000	0.459	0.117	101.885
13-95-35/4	0.133	0.712	35.889	57.078	0.101	5.464	0.134	0.210	0.000	0.437	0.097	100.254
13-95-35/3	0.137	0.722	36.149	57.123	0.097	5.523	0.128	0.203	0.000	0.467	0.125	100.675
13-95-42	0.030	0.700	37.160	57.780	0.090	4.510	0.130	0.220	0.000	0.170	0.010	100.800
13-95-67/1	0.213	0.739	36.259	57.737	0.095	4.840	0.127	0.403	0.000	0.364	0.042	100.819
13-95-67/2	0.205	0.754	36.221	57.333	0.074	4.868	0.133	0.373	0.000	0.376	0.047	100.383
13-97-78/1	0.317	0.805	35.821	57.731	0.116	5.435	0.119	0.643	0.000	0.497	0.075	101.559
13-97-78/2-core	0.286	0.761	35.697	58.000	0.078	5.280	0.132	0.558	0.001	0.486	0.068	101.348
13-97-78/2-rim	0.295	0.782	35.703	58.084	0.106	5.444	0.170	0.649	0.000	0.500	0.085	101.818
13-97-83/2	0.057	0.673	37.398	58.229	0.076	4.766	0.077	0.251	0.000	0.192	0.037	101.757
13-97-83/3	0.050	0.661	37.123	58.334	0.106	4.629	0.147	0.257	0.000	0.199	0.027	101.531
13-97-83/4	0.054	0.667	37.323	58.189	0.074	4.727	0.141	0.241	0.000	0.194	0.002	101.612
13-97-83/5	0.051	0.684	37.094	58.112	0.094	4.748	0.112	0.212	0.000	0.171	0.028	101.307
13-99-18	0.050	0.740	36.670	56.860	0.070	4.650	0.140	0.290	0.010	0.300	0.050	99.830
ATT-A1-P2	0.100	0.720	36.120	56.680	0.080	4.170	0.130	0.350	0.000	0.210	0.030	98.590
ATT-A1-P1	0.100	0.610	35.370	56.460	0.090	5.340	0.130	0.220	0.000	0.400	0.090	98.810

Primary Clinopyroxene

SAMPLE	Na2O	Al2O3	MgO	SiO2	NiO	FeO	MnO	Cr2O3	K2O	CaO	TiO2	Total
13-95-35	2.290	2.680	16.180	53.290	0.040	2.820	0.070	1.560	0.010	18.570	0.300	97.810
13-102-05/3	3.919	3.777	13.911	55.487	0.069	2.851	0.085	4.744	0.010	15.609	0.264	100.725
13-102-05/4	3.950	3.711	14.070	55.459	0.066	2.919	0.063	4.744	0.007	15.650	0.257	100.896
13-102-12/1	3.972	4.060	14.148	55.606	0.013	2.851	0.083	3.940	0.000	15.832	0.187	100.693
13-102-12/2	4.034	4.212	14.118	55.761	0.075	2.950	0.110	4.021	0.013	15.639	0.220	101.153
ATT-A1-P2	3.550	3.940	13.960	53.710	0.040	2.150	0.070	3.240	0.010	17.000	0.070	97.740
ATT-A1-P1	2.270	2.390	16.220	53.850	0.070	2.830	0.080	1.540	0.010	18.790	0.180	98.230

Metasomatic Clinopyroxene (not nalyzed for Ni)

SAMPLE	Na2O	Al2O3	MgO	SiO2	FeO	MnO	Cr2O3	K2O	CaO	TiO2	Total
13-95-34/1	4.200	4.412	13.916	54.999	2.988	0.112	2.841	0.010	16.235	0.359	100.072
13-95-34/2	4.003	4.434	14.147	54.229	2.959	0.132	2.523	0.002	16.331	0.344	99.123
13-97-78/1	4.549	3.709	13.954	53.482	3.202	0.108	5.124	0.019	14.038	0.369	98.555
13-97-78/2	4.393	3.507	13.772	54.013	3.203	0.119	4.902	0.000	14.490	0.329	98.732
13-97-78/3	4.464	3.418	13.724	54.323	3.216	0.084	5.006	0.024	14.342	0.339	98.944
13-97-78/4	4.274	3.418	13.785	54.107	3.158	0.067	4.963	0.033	14.567	0.300	98.673
13-97-78/5	4.350	3.463	13.739	54.282	3.225	0.107	4.915	0.028	14.470	0.284	98.863
13-97-78/6	4.566	3.569	13.835	54.528	3.196	0.012	4.873	0.008	14.407	0.379	99.385
13-97-78/7	2.797	2.590	15.345	53.848	4.405	0.107	2.664	0.014	16.945	0.274	98.991
13-97-78/9	4.660	3.788	13.721	54.485	3.309	0.119	5.067	0.031	14.077	0.309	99.593
13-97-78/11	4.654	3.777	13.818	54.150	3.112	0.103	5.114	0.023	14.049	0.345	99.145
13-102-05/1	4.490	3.718	13.268	54.485	2.902	0.173	4.668	0.020	15.862	0.259	99.867
13-102-05/2	4.413	3.875	13.523	54.421	3.008	0.111	4.411	0.013	15.923	0.230	99.937
13-102-05/3	4.641	4.127	13.386	54.667	3.016	0.097	4.382	0.033	15.667	0.282	100.296
13-102-12/1	4.486	4.077	12.988	54.524	2.561	0.107	4.652	0.011	16.484	0.145	100.051
13-102-15/1	4.150	3.535	13.508	53.966	2.696	0.019	4.673	0.000	16.167	0.135	98.850
13-102-15/2	4.215	3.579	13.739	54.513	2.591	0.146	4.494	0.024	16.608	0.137	100.047

Appendix B **Mineral Analysis Results** **Amphibole**

SAMPLE	Na2O	MgO	Al2O3	SiO2	Cr2O3	MnO	FeO	Cl	K2O	TiO2	CaO	Total
13-95-49/a1	4.508	18.428	13.041	45.259	2.303	0.081	3.232	0.009	0.41	0.143	10.036	97.45
13-95-49/a2	4.482	18.275	13.366	44.934	2.422	0.08	3.391	0.014	0.341	0.153	9.978	97.435
13-95-49/a3	4.501	18.514	13.266	45.742	1.91	0.137	3.493	0.022	0.341	0.122	9.868	97.916

SAMPLE	F	Na2O	SiO2	MgO	Al2O3	Cr2O3	MnO	FeO	Cl	NiO	K2O	CaO	TiO2	Total
13-95-33/1	0.008	0.818	41.986	24.821	11.711	1.004	0.032	2.892	0.130	0.106	8.568	0.116	0.048	92.241
13-95-33/2	0.291	0.783	40.385	25.853	11.816	0.748	0.019	3.145	0.065	0.033	7.503	0.099	0.304	91.046
13-95-33/3	0.399	1.438	41.693	24.919	12.272	0.851	0.077	3.299	0.076	0.000	8.118	0.186	0.063	93.390
13-95-34/1-rim	0.184	0.802	41.992	24.841	13.126	0.554	0.032	3.369	0.043	0.025	7.923	0.071	0.946	93.909
13-95-34/1-core	0.053	1.627	42.125	25.153	12.905	0.475	0.039	2.949	0.108	0.000	6.667	0.210	0.844	93.153
13-95-34/2-rim	0.269	1.647	41.671	24.629	12.684	0.468	0.000	2.787	0.102	0.000	7.474	0.129	0.994	92.855
13-95-34/2-core	0.072	0.539	42.041	24.931	12.916	0.531	0.000	2.910	0.091	0.000	9.355	0.085	0.906	94.378
13-95-34/2-rim2	0.404	1.432	41.892	25.102	12.869	0.570	0.045	3.291	0.022	0.000	9.008	0.053	0.781	95.466
13-95-47/1-rim	0.211	0.829	40.045	23.788	16.153	1.371	0.090	4.149	0.037	0.000	8.769	0.176	0.507	96.126
13-95-47/1-core	0.266	0.588	41.806	25.058	14.244	1.257	0.026	3.283	0.000	0.000	9.220	0.046	0.385	96.180
13-95-47/1-core1	0.000	0.297	40.756	24.898	12.614	1.716	0.045	4.375	0.096	0.000	8.469	0.119	1.298	94.682
13-95-47/1-core2	0.227	0.470	42.095	24.709	14.539	1.187	0.084	3.106	0.022	0.000	9.737	0.000	0.297	96.471
13-95-47/1-core3	0.402	0.419	41.592	25.163	14.567	1.210	0.052	3.248	0.022	0.000	9.735	0.067	0.374	96.852
13-95-47/1-rim1	0.075	0.621	40.009	24.765	13.676	0.845	0.013	3.705	0.005	0.081	6.625	0.090	0.472	90.983
13-95-47/1-rim2	0.058	0.714	40.026	23.744	16.107	1.567	0.019	4.221	0.022	0.043	8.902	0.147	0.614	96.184
13-95-47/2-core	0.120	0.403	38.407	23.699	15.890	1.403	0.097	5.574	0.064	0.000	6.956	0.206	0.834	93.652
13-95-47/vein1	0.193	1.763	38.434	21.240	17.993	2.004	0.000	4.627	0.053	0.000	7.702	0.046	1.149	95.206
13-95-47/vein2	0.153	1.434	37.684	21.054	17.462	2.157	0.032	4.998	0.022	0.000	8.154	0.000	1.231	94.381
13-95-47/vein3	0.072	1.064	38.599	21.270	17.037	2.178	0.090	4.477	0.043	0.011	8.891	0.018	1.393	95.142
13-95-49/1	0.045	1.909	39.645	24.311	15.820	0.535	0.026	2.359	0.027	0.000	7.358	0.011	0.123	92.168
13-95-49/2	0.112	1.826	40.259	24.579	15.686	0.383	0.045	2.497	0.005	0.000	7.414	0.000	0.157	92.965
13-95-49/4	0.000	1.945	39.391	24.135	16.077	0.734	0.052	2.473	0.022	0.009	7.294	0.064	0.142	92.336
13-95-49/5	0.085	1.870	39.908	24.526	16.268	0.837	0.000	2.442	0.005	0.020	7.176	0.018	0.220	93.376
13-95-59/1	0.000	1.841	40.753	25.015	15.182	0.975	0.143	2.241	0.016	0.053	7.191	0.077	0.000	93.488
13-95-59/2	0.194	1.868	41.008	24.876	15.023	0.864	0.000	2.309	0.000	0.000	6.872	0.078	0.000	93.093
13-95-59/3	0.185	1.348	39.448	25.506	14.594	1.093	0.032	2.461	0.033	0.000	5.754	0.060	0.027	90.542
13-95-59/4	0.049	1.605	40.704	25.233	15.051	1.023	0.006	2.406	0.033	0.000	6.463	0.092	0.037	92.701
13-99-18/filling vein	0.146	0.156	36.719	27.262	11.520	1.292	0.174	6.341	0.027	0.032	1.339	0.235	0.404	85.647
13-99-18/2	0.180	0.516	38.244	27.091	12.083	1.133	0.045	5.689	0.016	0.073	5.298	0.125	0.349	90.841

SAMPLE	SiO2	Al2O3	MgO	MnO	FeO	NiO	TiO2	Cr2O3	CaO	ZnO	Total
13-95-33/1	0.000	10.362	10.940	0.279	21.716	0.060	0.040	53.713	0.001	0.158	97.269
13-95-33/2	0.019	10.904	11.354	0.280	21.163	0.064	0.045	53.997	0.025	0.167	98.018
13-95-33/3	0.000	10.050	10.474	0.300	21.694	0.060	0.035	54.029	0.006	0.137	96.784
13-95-33/4	0.043	9.506	10.501	0.358	21.093	0.057	0.038	55.233	0.080	0.148	97.057
13-95-42	0.020	10.820	10.820	0.200	21.200	0.000	0.010	54.700	0.000	n/a	97.770
13-95-52/1	0.045	10.823	11.471	0.364	21.681	0.089	1.313	53.272	0.025	0.037	99.120
13-95-52/2	0.379	9.234	12.396	0.283	19.051	0.095	0.797	56.993	0.070	0.132	99.430
13-95-59/1-core	0.034	13.294	11.200	0.311	19.942	0.056	0.007	52.952	0.004	0.193	97.992
13-95-59/1-rim	0.002	14.634	11.888	0.302	19.875	0.079	0.010	51.096	0.034	0.193	98.111
13-95-59/2-core	0.011	12.888	11.177	0.312	19.901	0.038	0.020	52.898	0.000	0.203	97.448
13-95-59/2-rim	0.011	15.391	12.358	0.294	19.912	0.066	0.035	50.315	0.043	0.209	98.635
13-95-67/vermicular in amph	0.000	12.793	11.490	0.315	19.948	0.041	0.017	53.403	0.024	0.159	98.190
13-95-67/2-core	0.009	12.421	11.399	0.254	19.969	0.070	0.020	53.560	0.021	0.167	97.890
13-95-67/2-rim	0.034	13.171	11.739	0.298	19.504	0.051	0.010	52.094	0.062	0.162	97.126
13-97-78/1	0.150	7.509	12.477	0.248	21.778	0.145	1.485	54.311	0.208	0.049	98.358
13-97-78/2	0.111	6.787	11.933	0.275	22.754	0.177	1.811	54.514	0.122	0.090	98.574
13-97-78/3	0.173	6.889	12.411	0.254	22.088	0.190	1.826	54.624	0.238	0.111	98.803
13-97-78/4	0.246	14.615	11.247	0.460	27.209	0.034	1.536	41.572	0.066	0.057	97.043
13-97-83/3-core	0.019	10.398	11.497	0.247	20.343	0.056	0.300	55.181	0.000	0.185	98.225
13-97-83/3-rim	0.006	10.887	11.709	0.270	20.334	0.093	0.307	54.752	0.018	0.110	98.486
13-97-83/4-core	0.021	10.339	11.492	0.243	20.374	0.076	0.294	55.238	0.000	0.169	98.246
13-97-83/4-rim	0.032	11.066	11.885	0.288	20.361	0.122	0.289	54.200	0.022	0.095	98.361
13-99-18/1-core	0.024	11.718	11.540	0.307	22.026	0.073	0.847	52.715	0.000	0.184	99.434
13-99-18/1-rim	0.045	4.818	9.347	0.544	26.485	0.074	0.929	56.617	0.083	0.171	99.112
13-102-05/1-core	0.081	7.486	11.805	0.266	22.654	0.143	1.488	55.270	0.000	0.097	99.289
13-102-05/1-rim	0.105	7.756	12.036	0.258	22.953	0.102	1.438	54.836	0.039	0.108	99.631
13-102-05/2-core	0.053	7.408	11.693	0.271	22.692	0.154	1.516	55.490	0.000	0.083	99.362
13-102-05/2-rim	0.075	7.656	12.013	0.293	22.513	0.076	1.476	55.075	0.028	0.068	99.274
13-102-05/3-core	0.077	7.365	11.562	0.312	22.796	0.131	1.523	55.286	0.010	0.092	99.154
13-102-05/4-core	0.064	7.456	11.829	0.278	22.616	0.102	1.496	54.761	0.064	0.141	98.807
13-102-05/vermicular in amph	0.233	10.290	12.139	0.271	21.969	0.130	1.374	51.391	0.266	0.060	98.123
13-102-09/1-core	0.041	7.868	11.552	0.280	21.100	0.109	0.787	56.252	0.010	0.077	98.076
13-102-12/1-core	0.101	8.737	11.902	0.240	20.909	0.093	0.771	56.255	0.007	0.055	99.068
13-102-12/1-rim	0.066	8.219	10.870	0.289	21.087	0.102	0.771	55.600	0.035	0.103	97.143
13-102-12/2-core	0.208	8.162	11.749	0.249	21.151	0.097	0.766	56.972	0.017	0.105	99.475
13-102-12/2-rim	0.473	10.995	14.402	0.404	20.782	0.053	0.699	53.704	0.102	0.072	101.687
13-102-12/3-core	0.287	8.922	10.826	0.329	22.875	0.088	1.328	53.592	0.108	0.106	98.460
13-102-15/1	0.053	8.026	12.079	0.256	20.335	0.103	0.652	57.094	0.007	0.100	98.706
13-102-15/2	0.079	23.848	15.168	0.236	18.475	0.171	0.651	40.195	0.105	0.019	98.947
13-102-15/3	0.094	7.888	12.477	0.231	20.388	0.143	0.706	57.409	0.011	0.076	99.423
13-102-15/4	0.152	10.498	12.432	0.252	22.463	0.140	2.042	50.327	0.087	0.088	98.480
13-102-15/5	0.083	10.184	11.996	0.303	21.560	0.097	1.076	53.794	0.007	0.088	99.188

Appendix B **Mineral Analysis Results** **Garnets from "A1" Concentrate**

POINT	Na2O	MgO	Al2O3	SiO2	MnO	FeO	CaO	TiO2	Cr2O3	Total
1	0.016	15.961	23.837	41.029	0.252	8.796	9.735	0.107	0.086	99.819
2	0.031	18.458	23.623	41.021	0.324	10.827	5.083	0.479	0.091	99.936
3	0.012	16.189	23.820	41.076	0.243	8.848	9.632	0.083	0.094	99.997
4	0.018	16.141	23.911	41.057	0.311	8.780	9.600	0.103	0.101	100.023
5	0.031	9.303	22.206	38.648	0.514	22.603	6.978	0.065	0.110	100.458
6	0.018	16.145	23.882	41.177	0.263	9.008	9.649	0.147	0.115	100.404
7	0.081	19.855	22.503	41.553	0.394	10.090	4.031	0.432	1.193	100.133
8	0.096	20.366	22.569	41.761	0.411	9.408	3.995	0.340	1.235	100.180
9	0.101	19.356	22.176	41.344	0.369	10.234	4.624	0.367	1.250	99.823
10	0.078	19.668	22.269	41.365	0.408	10.282	3.990	0.420	1.267	99.747
11	0.092	19.399	22.280	41.408	0.385	10.152	4.617	0.404	1.282	100.018
12	0.101	19.429	22.182	41.263	0.408	10.157	4.441	0.392	1.299	99.673
13	0.101	19.456	22.320	41.258	0.381	10.225	4.517	0.399	1.317	99.974
14	0.075	20.034	22.496	41.485	0.409	9.718	3.782	0.362	1.339	99.701
15	0.053	19.799	22.581	41.532	0.338	9.348	4.307	0.350	1.388	99.695
16	0.077	19.703	22.280	41.278	0.411	10.095	4.009	0.389	1.434	99.674
17	0.093	19.786	22.505	41.573	0.399	9.997	4.074	0.347	1.542	100.316
18	0.084	20.187	22.108	41.483	0.393	9.659	3.974	0.385	1.564	99.837
19	0.034	20.343	22.741	41.626	0.435	8.510	4.258	0.210	1.587	99.745
20	0.059	19.804	22.473	41.447	0.334	9.350	4.249	0.360	1.627	99.704
21	0.044	19.655	22.359	41.678	0.332	9.459	4.574	0.290	1.641	100.034
22	0.096	20.340	22.140	41.487	0.395	9.638	3.844	0.360	1.644	99.944
23	0.043	19.235	22.061	41.363	0.403	10.038	4.777	0.394	1.660	99.975
24	0.039	19.965	22.588	41.367	0.393	9.197	4.584	0.207	1.694	100.033
25	0.042	19.242	22.072	41.166	0.382	10.406	4.787	0.415	1.694	100.205
26	0.039	20.318	22.979	41.299	0.451	8.414	4.388	0.197	1.704	99.789
27	0.036	19.670	22.416	41.387	0.386	9.107	4.517	0.225	1.710	99.454
28	0.081	19.532	22.199	41.258	0.467	10.527	3.739	0.344	1.726	99.873
29	0.092	19.948	22.014	41.464	0.413	9.591	4.133	0.405	1.732	99.791
30	0.047	19.118	21.915	41.250	0.413	10.182	4.726	0.437	1.748	99.836

Appendix B — Mineral Analysis Results — Garnets from "A1" Concentrate

POINT	Na2O	MgO	Al2O3	SiO2	MnO	FeO	CaO	TiO2	Cr2O3	Total
31	0.044	19.675	22.388	41.316	0.400	9.353	4.570	0.299	1.751	99.796
32	0.093	19.554	22.033	41.243	0.427	10.144	4.058	0.427	1.751	99.730
33	0.049	19.603	22.416	41.183	0.411	9.438	4.538	0.259	1.752	99.647
34	0.035	20.083	22.548	41.517	0.417	8.448	4.433	0.209	1.942	99.633
35	0.088	19.419	22.171	41.282	0.455	10.536	3.799	0.350	1.951	100.050
36	0.034	20.290	22.718	41.532	0.404	8.444	4.470	0.180	1.951	100.024
37	0.031	20.102	22.592	41.648	0.424	8.424	4.326	0.190	1.966	99.702
38	0.101	20.016	22.025	41.367	0.372	9.686	4.007	0.419	1.966	99.959
39	0.074	20.175	21.891	41.528	0.396	9.646	3.964	0.365	1.972	100.011
40	0.077	20.535	21.946	41.432	0.319	9.066	4.067	0.322	1.982	99.745
41	0.035	19.103	21.683	41.076	0.408	10.164	4.668	0.397	2.040	99.575
42	0.067	20.379	22.395	41.462	0.433	8.648	4.184	0.178	2.058	99.804
43	0.038	20.267	22.692	41.451	0.380	8.100	4.475	0.113	2.068	99.582
44	0.047	19.272	21.730	41.134	0.362	10.009	4.676	0.442	2.108	99.780
45	0.046	19.373	21.649	41.190	0.376	9.888	4.654	0.410	2.122	99.707
46	0.035	20.593	22.590	41.500	0.377	8.037	4.344	0.165	2.151	99.794
47	0.054	19.343	21.573	41.057	0.386	9.517	4.759	0.427	2.159	99.275
48	0.089	19.423	20.852	41.143	0.322	8.616	5.969	0.752	2.175	99.339
49	0.040	20.560	22.601	41.750	0.443	8.149	4.402	0.200	2.178	100.324
50	0.078	19.562	21.454	40.835	0.394	9.421	4.885	0.412	2.242	99.282
51	0.047	19.602	21.700	41.256	0.386	9.511	4.711	0.420	2.271	99.904
52	0.039	19.638	21.664	41.307	0.387	9.532	4.778	0.400	2.279	100.025
53	0.053	19.207	21.598	41.196	0.402	9.655	4.680	0.392	2.286	99.468
54	0.044	19.774	21.727	41.265	0.389	9.345	4.732	0.382	2.287	99.945
55	0.057	19.633	21.674	41.391	0.371	9.353	4.673	0.367	2.318	99.835
56	0.061	19.464	21.572	41.072	0.374	9.485	4.672	0.430	2.334	99.464
57	0.049	19.441	21.377	41.051	0.394	9.497	4.746	0.432	2.340	99.325
58	0.044	19.492	21.515	41.183	0.390	9.467	4.767	0.424	2.357	99.641
59	0.042	19.580	21.590	41.175	0.374	9.381	4.788	0.374	2.359	99.663
60	0.047	19.497	21.534	41.278	0.396	9.423	4.812	0.437	2.363	99.788
61	0.042	19.388	21.585	41.190	0.371	9.526	4.768	0.379	2.363	99.612

POINT	Na2O	MgO	Al2O3	SiO2	MnO	FeO	CaO	TiO2	Cr2O3	Total
62	0.034	19.661	21.555	41.138	0.389	9.548	4.777	0.375	2.365	99.843
63	0.036	20.371	22.463	41.688	0.487	8.134	4.309	0.170	2.368	100.028
64	0.040	19.328	21.436	41.034	0.387	9.523	4.827	0.415	2.369	99.359
65	0.044	19.714	21.802	41.322	0.351	9.403	4.585	0.380	2.372	99.976
66	0.055	19.655	21.551	41.224	0.403	9.340	4.574	0.377	2.374	99.551
67	0.046	19.602	21.473	41.427	0.378	9.525	4.785	0.405	2.374	100.016
68	0.049	19.615	21.479	41.263	0.386	9.372	4.782	0.404	2.376	99.726
69	0.047	19.398	21.507	41.265	0.356	9.441	4.816	0.369	2.384	99.583
70	0.042	19.496	21.422	41.265	0.389	9.461	4.736	0.389	2.384	99.583
71	0.040	19.457	21.426	40.995	0.362	9.475	4.837	0.395	2.385	99.372
72	0.046	19.506	21.581	41.269	0.391	9.544	4.794	0.374	2.388	99.893
73	0.043	19.660	21.451	41.267	0.383	9.443	4.796	0.405	2.391	99.840
74	0.044	19.413	21.347	41.384	0.378	9.408	4.817	0.407	2.400	99.599
75	0.044	19.380	21.411	41.042	0.350	9.517	4.801	0.389	2.406	99.338
76	0.059	19.535	21.543	41.278	0.383	9.521	4.526	0.410	2.406	99.663
77	0.059	19.570	21.453	41.087	0.422	9.555	4.575	0.377	2.414	99.512
78	0.036	19.399	21.383	41.226	0.381	9.434	4.710	0.402	2.416	99.387
79	0.044	19.341	21.556	41.124	0.382	9.580	4.880	0.379	2.419	99.706
80	0.044	19.570	21.539	41.203	0.372	9.475	4.805	0.389	2.431	99.829
81	0.040	19.428	21.400	41.318	0.387	9.432	4.829	0.377	2.432	99.643
82	0.044	19.501	21.436	40.972	0.362	9.407	4.777	0.414	2.432	99.342
83	0.038	19.583	21.494	41.100	0.350	9.524	4.812	0.400	2.435	99.736
84	0.039	19.570	21.761	41.372	0.325	9.520	4.829	0.405	2.438	100.260
85	0.036	19.307	21.487	41.201	0.420	9.430	4.851	0.425	2.441	99.596
86	0.042	19.623	21.558	41.526	0.385	9.559	4.770	0.389	2.450	100.300
87	0.043	19.416	21.456	41.012	0.333	9.472	4.843	0.427	2.451	99.454
88	0.038	19.308	21.564	41.081	0.409	9.436	4.803	0.407	2.458	99.505
89	0.043	19.210	21.265	41.087	0.346	9.429	4.771	0.395	2.460	99.007
90	0.038	19.429	21.420	41.100	0.360	9.565	4.871	0.427	2.460	99.669
91	0.031	19.436	21.477	41.166	0.393	9.439	4.747	0.390	2.461	99.541
92	0.065	19.089	21.141	41.109	0.404	10.018	5.036	0.525	2.466	99.852

Appendix B **Mineral Analysis Results** **Garnets from "A1" Concentrate**

POINT	Na2O	MgO	Al2O3	SiO2	MnO	FeO	CaO	TiO2	Cr2O3	Total
93	0.040	19.366	21.553	41.316	0.416	9.475	4.714	0.415	2.466	99.761
94	0.039	19.743	21.422	41.025	0.354	9.259	4.496	0.414	2.467	99.219
95	0.036	19.535	21.386	41.113	0.402	9.525	4.855	0.405	2.474	99.732
96	0.042	19.915	21.638	41.248	0.403	9.270	4.372	0.382	2.479	99.748
97	0.032	19.529	21.426	41.363	0.389	9.475	4.732	0.370	2.482	99.798
98	0.047	19.985	21.077	41.419	0.332	8.929	4.847	0.484	2.486	99.605
99	0.042	19.411	21.479	41.203	0.383	9.418	4.885	0.424	2.490	99.734
100	0.042	19.549	21.351	41.282	0.367	9.602	4.763	0.417	2.496	99.868
101	0.043	20.020	21.422	41.215	0.341	8.846	4.722	0.404	2.501	99.514
102	0.042	19.638	21.366	41.194	0.407	9.533	4.816	0.422	2.507	99.924
103	0.047	19.607	21.430	41.061	0.382	9.508	4.782	0.415	2.511	99.745
104	0.036	19.152	21.341	41.053	0.371	9.511	4.820	0.439	2.528	99.252
105	0.023	20.354	22.318	41.432	0.435	8.016	4.552	0.160	2.536	99.825
106	0.042	20.000	21.334	41.269	0.337	8.956	4.798	0.434	2.543	99.711
107	0.069	19.734	21.912	41.380	0.504	8.731	4.582	0.234	2.549	99.695
108	0.027	19.749	22.061	41.241	0.413	8.542	4.690	0.145	2.641	99.511
109	0.061	19.456	21.218	41.124	0.433	9.561	4.802	0.399	2.727	99.779
110	0.050	20.345	21.870	41.427	0.386	7.836	4.746	0.215	2.787	99.662
111	0.057	19.729	21.279	41.089	0.385	9.144	4.600	0.354	2.797	99.435
112	0.053	19.497	21.169	41.183	0.403	9.414	4.693	0.414	2.797	99.623
113	0.049	19.474	21.167	41.096	0.386	9.547	4.729	0.405	2.799	99.652
114	0.047	19.501	21.029	41.186	0.405	9.429	4.715	0.464	2.828	99.604
115	0.047	19.419	21.434	41.280	0.416	9.611	4.837	0.385	2.884	100.313
116	0.035	19.832	21.761	41.320	0.405	8.591	4.907	0.175	2.904	99.932
117	0.034	20.404	22.180	41.573	0.395	7.862	4.600	0.123	2.948	100.119
118	0.035	18.856	21.494	41.027	0.500	9.797	4.946	0.254	2.974	99.882
119	0.036	20.000	21.670	41.201	0.400	8.399	4.718	0.162	3.077	99.663
120	0.031	19.608	21.462	40.952	0.358	8.554	4.788	0.257	3.210	99.218
121	0.044	20.036	21.477	41.412	0.420	8.188	4.880	0.240	3.243	99.942
122	0.028	19.467	21.014	41.143	0.325	9.000	4.952	0.325	3.296	99.552
123	0.027	20.008	21.562	41.355	0.381	7.505	5.212	0.112	3.588	99.749

Appendix B Mineral Analysis Results Garnets from "A1" Concentrate

POINT	Na2O	MgO	Al2O3	SiO2	MnO	FeO	CaO	TiO2	Cr2O3	Total
124	0.026	19.787	21.400	41.228	0.524	8.199	4.672	0.020	3.600	99.456
125	0.020	20.157	21.513	41.314	0.456	7.732	4.428	0.025	3.601	99.247
126	0.028	20.293	21.473	41.618	0.501	7.766	4.759	0.013	3.796	100.247
127	0.038	20.029	21.122	41.220	0.349	7.655	4.953	0.072	3.949	99.387
128	0.047	17.148	20.680	40.546	0.714	10.256	5.920	0.085	4.024	99.419
129	0.024	19.709	21.194	41.245	0.502	8.080	4.816	0.025	4.028	99.626
130	0.035	19.776	21.133	41.252	0.509	7.995	4.882	0.018	4.108	99.709
131	0.031	19.696	20.725	41.055	0.429	8.284	5.230	0.153	4.236	99.839
132	0.027	19.651	20.920	41.094	0.523	8.324	4.810	0.007	4.295	99.651
133	0.026	19.837	21.052	41.391	0.496	8.096	4.815	0.020	4.301	100.033
134	0.038	19.398	20.559	40.848	0.390	8.546	5.209	0.235	4.345	99.567
135	0.039	19.457	20.716	41.273	0.365	8.525	5.212	0.147	4.369	100.102
136	0.028	19.797	20.993	41.312	0.484	7.927	5.030	0.023	4.461	100.057
137	0.026	19.592	20.752	40.944	0.554	8.182	4.879	0.037	4.464	99.428
138	0.024	19.641	20.905	41.156	0.408	8.028	5.058	0.085	4.499	99.803
139	0.046	19.569	20.531	41.164	0.495	8.083	5.107	0.182	4.611	99.787
140	0.031	19.613	20.718	41.207	0.505	8.089	4.981	0.047	4.645	99.836
141	0.047	19.262	20.428	41.004	0.462	8.442	5.212	0.185	4.661	99.703
142	0.036	19.191	20.546	40.888	0.507	8.168	5.180	0.058	4.776	99.349
143	0.022	19.240	20.124	40.895	0.369	8.410	5.336	0.180	4.896	99.473
144	0.024	19.648	20.453	40.999	0.422	7.719	5.198	0.173	4.956	99.593
145	0.046	19.123	19.905	40.766	0.466	8.605	5.192	0.265	4.958	99.326
146	0.028	19.018	19.975	40.661	0.475	8.131	5.545	0.135	5.153	99.123
147	0.036	19.547	20.221	41.032	0.442	8.003	5.390	0.158	5.266	100.095
148	0.028	19.074	19.794	40.916	0.435	8.161	5.548	0.145	5.411	99.513
149	0.038	19.326	19.984	40.984	0.462	8.033	5.251	0.203	5.419	99.701
150	0.032	19.454	20.049	40.895	0.407	7.872	5.362	0.068	5.427	99.565
151	0.043	18.842	19.676	40.721	0.455	8.607	5.517	0.259	5.431	99.551
152	0.024	20.036	19.569	41.303	0.302	7.135	5.695	0.185	5.433	99.682
153	0.044	19.799	19.886	40.871	0.399	7.435	5.280	0.183	5.538	99.436
154	0.119	19.996	19.981	40.959	0.434	7.988	4.593	0.098	5.554	99.721

Appendix B **Mineral Analysis Results** **Garnets from "A1" Concentrate**

POINT	Na2O	MgO	Al2O3	SiO2	MnO	FeO	CaO	TiO2	Cr2O3	Total
155	0.040	19.709	19.864	40.753	0.422	7.913	4.866	0.128	5.650	99.347
156	0.018	19.179	19.975	41.074	0.448	7.876	5.660	0.087	5.661	99.976
157	0.049	19.351	19.701	40.961	0.447	7.700	5.325	0.168	5.814	99.516
158	0.084	18.224	18.879	40.428	0.433	10.198	5.050	0.477	5.839	99.612
159	0.036	19.076	19.486	40.753	0.449	8.128	5.496	0.190	5.868	99.483
160	0.044	19.844	19.898	41.222	0.396	7.891	4.806	0.163	5.887	100.152
161	0.036	19.310	19.595	40.730	0.430	7.931	5.486	0.177	5.897	99.593
162	0.031	19.003	19.737	40.948	0.448	7.977	5.872	0.083	5.925	100.025
163	0.038	18.967	19.461	40.796	0.456	8.116	5.602	0.163	6.005	99.605
164	0.039	19.177	19.580	40.961	0.422	7.849	5.590	0.123	6.146	99.887
165	0.058	20.015	19.372	40.920	0.395	7.653	4.725	0.125	6.299	99.563
166	0.035	19.290	19.365	40.717	0.417	7.647	5.415	0.177	6.302	99.364
167	0.038	18.987	19.297	40.809	0.430	8.132	5.821	0.175	6.312	100.000
168	0.051	19.121	19.102	40.873	0.465	8.132	5.496	0.219	6.365	99.823
169	0.043	19.277	19.248	40.957	0.435	7.658	5.703	0.178	6.383	99.882
170	0.030	19.718	19.153	40.920	0.373	7.350	5.321	0.103	6.393	99.362
171	0.040	19.108	19.136	40.653	0.439	7.657	5.727	0.203	6.399	99.363
172	0.030	19.325	19.251	40.623	0.438	7.714	5.518	0.058	6.422	99.379
173	0.031	18.980	19.174	40.927	0.457	8.177	5.781	0.153	6.438	100.118
174	0.019	18.542	19.214	40.608	0.435	8.183	6.226	0.075	6.447	99.749
175	0.038	19.255	19.138	40.854	0.413	7.836	5.990	0.225	6.511	100.261
176	0.030	18.821	18.943	40.546	0.473	8.093	5.723	0.225	6.549	99.402
177	0.039	18.832	18.815	40.426	0.523	8.237	5.819	0.162	6.586	99.439
178	0.015	18.557	19.095	40.708	0.488	8.145	6.257	0.038	6.592	99.894
179	0.030	18.831	18.853	40.790	0.396	8.181	5.749	0.138	6.619	99.588
180	0.043	19.254	19.172	40.644	0.471	7.185	5.861	0.193	6.627	99.451
181	0.015	18.270	18.883	40.332	0.436	8.254	6.403	0.023	6.684	99.300
182	0.031	19.071	18.902	40.428	0.409	7.880	5.842	0.122	6.711	99.396
183	0.019	18.605	18.928	40.661	0.448	8.142	6.440	0.030	6.739	100.014
184	0.054	18.887	18.811	40.518	0.487	8.107	5.819	0.173	6.746	99.604
185	0.020	18.539	18.866	40.687	0.465	8.118	6.335	0.028	6.774	99.832

POINT	Na2O	MgO	Al2O3	SiO2	MnO	FeO	CaO	TiO2	Cr2O3	Total
186	0.049	19.398	18.845	40.661	0.400	7.859	5.155	0.188	6.919	99.474
187	0.085	19.701	18.265	40.236	0.394	8.060	4.760	0.384	6.935	98.819
188	0.058	19.564	18.804	40.766	0.488	8.353	4.799	0.100	6.988	99.919
189	0.032	19.358	18.588	40.867	0.347	7.666	5.542	0.135	7.002	99.538
190	0.051	18.963	18.683	40.589	0.426	7.760	5.937	0.178	7.012	99.599
191	0.030	19.661	18.994	40.882	0.451	7.352	5.159	0.062	7.058	99.648
192	0.055	18.983	18.545	40.552	0.489	7.490	6.099	0.172	7.189	99.575
193	0.044	18.700	18.424	40.454	0.457	8.019	5.998	0.172	7.202	99.470
194	0.038	18.441	18.528	40.458	0.470	8.097	6.287	0.120	7.223	99.661
195	0.040	18.569	18.428	40.567	0.462	7.927	6.184	0.173	7.277	99.628
196	0.013	18.209	18.465	40.582	0.469	7.912	6.488	0.048	7.277	99.464
197	0.027	18.754	18.227	40.435	0.445	7.918	6.299	0.165	7.423	99.695
198	0.026	18.484	18.324	40.550	0.474	7.869	6.119	0.108	7.426	99.379
199	0.080	19.346	18.174	40.674	0.386	7.972	5.038	0.310	7.435	99.416
200	0.038	18.390	18.150	40.377	0.479	8.095	6.154	0.202	7.457	99.340
201	0.008	17.952	18.237	40.370	0.519	8.250	6.806	0.027	7.520	99.689
202	0.030	18.602	18.174	40.584	0.471	7.939	6.398	0.083	7.533	99.815
203	0.026	18.360	18.208	40.373	0.444	7.913	6.324	0.092	7.547	99.288
204	0.028	18.481	18.227	40.460	0.452	7.948	6.274	0.087	7.585	99.543
205	0.019	18.473	17.961	40.345	0.456	7.945	6.295	0.125	7.599	99.217
206	0.024	18.378	18.191	40.422	0.456	7.947	6.259	0.083	7.683	99.443
207	0.030	18.333	18.295	40.480	0.436	7.953	6.342	0.123	7.711	99.705
208	0.039	18.434	18.155	40.364	0.453	7.907	6.354	0.082	7.789	99.577
209	0.020	17.587	18.029	40.278	0.471	8.236	6.883	0.032	7.990	99.527
210	0.018	18.703	17.609	40.625	0.400	7.674	6.282	0.147	8.147	99.605
211	0.030	18.385	17.592	40.542	0.429	7.643	6.492	0.115	8.179	99.407
212	0.008	18.348	17.717	40.525	0.373	7.725	6.904	0.060	8.202	99.862
213	0.027	18.431	17.865	40.394	0.469	7.889	6.393	0.120	8.224	99.811
214	0.027	18.454	17.643	40.197	0.431	7.592	6.677	0.160	8.256	99.439
215	0.015	18.240	17.167	40.161	0.380	7.700	6.674	0.068	8.885	99.291
216	0.027	17.930	16.992	40.011	0.471	7.959	6.960	0.148	9.054	99.552

Appendix B | Mineral Analysis Results | Garnets from "G" Concentrate

POINT	SiO2	TiO2	Al2O3	Cr2O3	FeO	MnO	MgO	CaO	Na2O	Total
1	39.309	0.125	22.351	0.055	17.693	0.493	10.652	9.218	0.039	99.935
2	39.217	0.158	22.400	0.060	18.524	0.455	10.337	8.714	0.046	99.911
3	37.733	0.103	21.570	0.000	28.111	0.683	5.848	6.709	0.024	100.781
4	38.895	0.057	22.408	0.060	19.532	0.438	8.196	10.642	0.026	100.254
5	38.069	1.184	22.166	0.026	24.582	0.442	7.764	6.541	0.015	100.789
6	39.451	0.129	22.450	0.081	18.261	0.469	10.669	8.763	0.054	100.327
7	41.260	0.268	20.931	3.832	8.122	0.371	20.127	4.668	0.049	99.628
8	41.385	0.190	20.586	4.682	7.489	0.344	20.133	5.130	0.035	99.974
9	41.428	0.383	22.480	1.505	9.195	0.343	20.023	4.253	0.069	99.679
10	41.648	0.259	22.467	1.806	8.510	0.364	20.310	4.479	0.036	99.879
11	40.729	0.312	18.705	6.430	7.680	0.384	19.367	5.675	0.045	99.327
12	41.632	0.182	21.405	3.385	8.251	0.422	20.144	4.666	0.053	100.140
13	41.243	0.052	22.188	2.722	9.141	0.515	19.113	5.066	0.016	100.056
14	41.321	0.000	21.705	3.341	8.501	0.568	19.511	4.843	0.021	99.811
15	41.520	0.355	22.452	1.567	9.230	0.353	19.954	4.410	0.062	99.903
16	41.632	0.009	21.842	3.260	8.361	0.584	20.592	3.640	0.025	99.945
17	41.654	0.208	22.147	2.628	8.101	0.357	20.254	4.667	0.040	100.056
18	40.815	0.026	20.331	5.109	8.302	0.572	18.538	6.434	0.007	100.134
19	41.573	0.171	20.885	4.483	7.762	0.410	20.790	4.192	0.073	100.339
20	40.630	0.219	17.344	8.564	7.322	0.404	19.637	5.199	0.058	99.377
21	40.839	0.148	18.871	6.904	7.462	0.442	19.364	5.750	0.051	99.831
22	41.230	0.001	21.534	3.859	8.014	0.488	19.668	5.079	0.014	99.887
23	41.617	0.389	22.459	1.605	9.332	0.342	20.048	4.407	0.067	100.266
24	41.111	0.757	21.659	1.766	10.591	0.520	18.767	4.841	0.143	100.155
25	40.778	0.144	19.170	6.345	7.971	0.447	19.111	5.778	0.032	99.776
26	41.429	0.379	21.683	2.221	9.556	0.393	19.706	4.542	0.052	99.961
27	41.410	0.270	20.984	4.014	7.769	0.431	20.029	5.079	0.053	100.039
28	40.381	0.337	16.842	9.170	7.482	0.392	18.778	6.288	0.055	99.725
29	41.389	0.011	21.896	3.216	8.166	0.540	19.982	4.589	0.017	99.806
30	40.991	0.302	18.786	6.485	7.661	0.376	19.477	5.694	0.044	99.816

Appendix B **Mineral Analysis Results** **Garnets from "G" Concentrate**

POINT	SiO2	TiO2	Al2O3	Cr2O3	FeO	MnO	MgO	CaO	Na2O	Total
31	40.981	0.130	19.659	5.720	7.804	0.414	19.546	5.463	0.046	99.763
32	41.094	0.236	20.371	4.593	7.844	0.430	19.692	5.300	0.031	99.591
33	40.955	0.026	20.913	4.189	8.131	0.550	19.103	5.584	0.011	99.462
34	40.918	0.826	21.407	1.823	10.644	0.489	18.518	5.061	0.167	99.853
35	41.430	0.193	21.858	2.789	8.135	0.394	20.092	4.773	0.029	99.693
36	41.013	0.339	20.741	3.592	10.437	0.437	18.712	4.549	0.098	99.918
37	41.003	0.260	19.621	5.614	7.430	0.407	19.520	5.513	0.057	99.425
38	41.278	0.187	20.367	4.509	7.677	0.378	20.058	5.136	0.040	99.630
39	41.530	0.237	22.436	1.877	8.473	0.400	20.209	4.588	0.048	99.798
40	40.831	0.297	18.888	6.580	7.725	0.380	19.417	5.626	0.053	99.797
41	41.798	0.251	22.474	1.876	8.465	0.367	20.307	4.531	0.041	100.110
42	40.846	0.300	18.747	6.519	7.655	0.422	19.461	5.601	0.041	99.592
43	41.315	0.414	20.270	4.751	7.693	0.398	20.170	5.078	0.060	100.149
44	41.412	0.243	20.632	4.485	7.793	0.406	20.095	5.029	0.054	100.149
45	41.518	0.430	22.430	1.569	9.234	0.358	20.113	4.262	0.071	99.985
46	41.287	0.229	20.936	4.080	7.884	0.396	20.074	4.879	0.062	99.827
47	41.011	0.188	19.624	5.890	7.498	0.400	19.798	5.209	0.046	99.664
48	40.905	0.228	18.178	7.544	7.929	0.405	20.005	4.532	0.070	99.796
49	41.629	0.231	22.154	2.448	8.558	0.413	20.048	4.559	0.042	100.082
50	41.715	0.289	22.826	1.405	8.392	0.378	20.397	4.446	0.052	99.900
51	41.032	0.368	20.375	4.337	7.749	0.422	20.192	4.825	0.077	99.377
52	41.712	0.231	21.671	3.039	8.153	0.377	20.224	4.820	0.040	100.267
53	41.672	0.227	22.138	2.554	8.108	0.398	20.437	4.622	0.030	100.186
54	41.432	0.273	21.128	3.575	8.392	0.341	20.081	4.651	0.063	99.936
55	41.128	0.021	20.290	5.153	7.878	0.528	19.782	4.691	0.030	99.501
56	40.553	0.114	18.234	7.232	7.978	0.406	18.598	6.446	0.022	99.583
57	41.198	0.144	19.965	5.141	8.067	0.422	19.693	5.593	0.037	100.260
58	41.420	0.179	20.740	4.354	7.705	0.371	20.098	5.051	0.037	99.955
59	41.317	0.126	21.327	3.607	8.061	0.389	20.025	4.997	0.026	99.875
60	41.090	0.134	20.011	5.068	8.106	0.437	19.622	5.466	0.031	99.965
61	41.756	0.306	22.082	2.475	7.467	0.360	20.706	4.619	0.084	99.855
62	41.091	0.005	21.494	3.644	8.615	0.613	19.398	4.964	0.014	99.838
63	40.898	0.126	18.806	6.952	7.416	0.418	20.118	4.678	0.043	99.455

POINT	SiO2	TiO2	Al2O3	Cr2O3	FeO	MnO	MgO	CaO	Na2O	Total
64	41.463	0.389	22.338	1.487	9.260	0.370	19.929	4.368	0.050	99.654
65	41.550	0.000	21.393	3.891	8.172	0.493	19.765	5.123	0.007	100.394
66	41.072	0.000	21.111	3.877	7.980	0.536	19.525	5.044	0.006	99.151
67	41.440	0.383	22.061	2.128	9.513	0.461	19.971	3.934	0.090	99.981
68	41.810	0.246	22.106	2.479	8.054	0.346	20.916	3.952	0.077	99.986
69	41.168	0.287	19.928	5.485	7.201	0.350	20.161	5.239	0.039	99.858
70	41.439	0.020	21.163	4.177	8.269	0.502	19.687	5.105	0.025	100.387
71	41.331	0.159	21.687	3.134	8.323	0.411	19.803	4.890	0.039	99.777
72	41.524	0.389	22.345	1.937	8.833	0.357	20.171	4.421	0.063	100.040
73	41.409	0.211	20.603	4.654	7.388	0.412	20.160	5.207	0.036	100.080
74	41.589	0.368	22.475	1.541	9.228	0.369	20.087	4.365	0.067	100.089
75	40.770	0.284	18.957	6.610	7.609	0.428	19.212	5.789	0.054	99.713
76	41.521	0.000	22.369	2.806	8.345	0.564	20.412	4.146	0.008	100.171
77	41.406	0.161	20.797	4.441	7.698	0.362	20.061	5.026	0.037	99.989
78	40.796	0.206	18.660	6.947	7.804	0.416	19.058	6.028	0.035	99.950
79	41.933	0.255	23.207	1.166	8.486	0.377	20.793	3.993	0.077	100.287
80	40.702	0.333	19.155	5.916	10.405	0.431	18.249	4.921	0.098	100.210
81	41.628	0.000	22.202	3.074	8.193	0.538	20.510	3.970	0.008	100.123
82	41.187	0.451	19.297	6.617	7.436	0.422	20.426	4.469	0.101	100.406
83	41.405	0.000	21.214	4.114	8.036	0.527	19.371	5.667	0.009	100.343
84	40.835	0.216	19.368	6.153	7.977	0.420	19.465	5.414	0.054	99.902
85	41.335	0.180	20.210	5.164	7.619	0.405	20.309	4.724	0.060	100.006
86	41.292	0.188	20.019	5.009	7.622	0.357	19.922	5.195	0.037	99.641
87	41.742	0.218	22.290	2.423	8.021	0.387	21.005	3.806	0.068	99.960
88	41.146	0.304	18.913	6.630	7.404	0.391	19.744	5.402	0.063	99.997
89	40.233	0.152	16.531	9.743	7.094	0.436	18.424	6.682	0.046	99.341
90	40.572	0.229	17.659	8.114	7.627	0.398	19.908	6.202	0.046	100.755
91	41.371	0.247	21.594	3.076	8.065	0.379	20.158	4.839	0.045	99.774
92	40.915	0.255	19.039	6.482	7.668	0.413	19.524	5.800	0.043	100.139
93	40.845	0.239	18.094	7.772	7.381	0.390	19.190	6.081	0.033	100.025
94	40.836	0.256	19.294	5.695	7.830	0.392	19.631	5.377	0.038	99.349
95	40.740	0.242	18.980	6.349	8.007	0.449	19.278	5.466	0.054	99.565
96	41.480	0.237	22.501	1.823	8.588	0.362	20.206	4.494	0.040	99.731

POINT	SiO2	TiO2	Al2O3	Cr2O3	FeO	MnO	MgO	CaO	Na2O	Total
97	41.544	0.197	22.228	2.566	8.215	0.395	20.282	4.695	0.040	100.162
98	41.659	0.252	20.472	4.696	7.550	0.388	20.361	5.063	0.040	100.481
99	41.470	0.264	21.046	3.677	8.124	0.404	19.844	4.984	0.048	99.861
100	41.422	0.247	21.147	3.364	8.177	0.357	20.031	4.989	0.036	99.770
101	41.429	0.228	21.974	2.658	8.587	0.398	19.949	4.646	0.048	99.917
102	40.119	0.090	16.088	10.041	7.734	0.424	17.335	7.798	0.018	99.647
103	41.527	0.219	20.738	4.316	7.830	0.380	20.085	5.016	0.042	100.153
104	41.245	0.032	20.933	4.308	8.207	0.596	18.997	5.800	0.008	100.126
105	40.922	0.294	18.885	6.424	7.737	0.389	19.519	5.745	0.044	99.959
106	40.732	0.184	17.542	8.320	7.317	0.405	19.544	5.604	0.057	99.705
107	41.504	0.389	22.434	1.673	9.187	0.348	20.110	4.255	0.062	99.962
108	41.640	0.248	22.407	1.852	8.550	0.379	20.286	4.557	0.042	99.961
109	41.106	0.161	18.288	7.733	7.520	0.437	20.014	4.867	0.065	100.191
110	41.426	0.218	20.539	4.589	7.413	0.324	20.304	5.141	0.047	100.001
111	41.150	0.207	19.087	6.355	8.193	0.440	20.210	4.186	0.075	99.903
112	41.475	0.395	22.055	2.217	9.703	0.463	19.819	3.999	0.094	100.220
113	41.474	0.243	21.016	3.984	7.762	0.407	20.173	5.023	0.051	100.133
114	41.677	0.393	22.386	1.719	9.242	0.353	20.024	4.407	0.064	100.265
115	41.240	0.020	21.028	4.251	8.240	0.588	19.086	5.669	0.021	100.143
116	41.083	0.048	20.640	4.693	8.228	0.519	19.302	5.538	0.024	100.075
117	41.325	0.219	20.624	4.381	7.802	0.413	19.995	5.001	0.045	99.805
118	41.113	0.241	20.370	4.702	7.793	0.401	19.819	5.321	0.041	99.801
119	41.125	0.231	19.880	5.055	7.885	0.381	19.740	5.307	0.052	99.656
120	42.022	0.268	23.205	1.149	8.356	0.348	20.909	3.963	0.085	100.305
121	41.354	0.187	20.853	4.233	7.981	0.421	20.058	4.916	0.054	100.057
122	41.560	0.032	20.768	4.611	7.983	0.511	19.987	4.992	0.020	100.464
123	41.524	0.388	22.471	1.588	9.261	0.380	19.946	4.379	0.074	100.011
124	41.834	0.387	22.613	1.802	9.146	0.456	20.430	3.895	0.089	100.652
125	41.570	0.258	21.288	3.577	8.150	0.395	20.266	4.645	0.050	100.199
126	41.550	0.451	22.109	2.086	9.225	0.474	20.131	4.055	0.084	100.165
127	41.386	0.265	21.182	3.621	8.146	0.398	20.086	4.969	0.044	100.097
128	41.035	0.282	18.923	6.670	7.411	0.387	19.728	5.597	0.063	100.096
129	41.468	0.219	20.036	5.282	7.731	0.411	19.982	5.300	0.038	100.467

Appendix B | Mineral Analysis Results | Garnets from "V" Concentrate

POINT	Na2O	MgO	Al2O3	SiO2	MnO	FeO	CaO	TiO2	Cr2O3	Total
1	0.043	19.630	19.729	41.342	0.391	7.694	5.394	0.163	5.618	100.006
2	0.047	19.696	19.336	41.207	0.371	7.575	5.170	0.275	5.884	99.561
3	0.013	19.744	20.568	42.018	0.333	7.698	5.204	0.232	4.160	99.970
4	0.050	18.895	21.539	41.553	0.399	10.383	4.785	0.544	1.763	99.912
5	0.022	19.824	21.256	41.737	0.416	8.158	5.024	0.112	3.613	100.161
6	0.023	16.433	23.508	41.361	0.325	13.714	5.103	0.038	0.126	100.632
7	0.053	18.982	18.526	41.004	0.395	8.257	5.676	0.379	6.654	99.925
8	0.024	16.557	23.423	41.228	0.482	13.962	4.626	0.068	0.126	100.497
9	0.032	20.923	23.278	42.636	0.333	7.824	4.249	0.205	1.000	100.481
10	0.081	19.859	20.918	41.881	0.374	8.949	4.433	0.472	3.307	100.274
11	0.066	19.570	19.607	41.534	0.421	7.963	5.173	0.290	5.868	100.493
12	0.031	18.793	18.227	41.040	0.382	7.406	6.478	0.092	7.641	100.090
13	0.036	20.296	21.577	41.740	0.381	7.938	4.792	0.193	3.144	100.097
14	0.044	19.305	18.505	40.952	0.414	7.505	5.413	0.183	7.055	99.378
15	0.051	19.794	19.703	41.284	0.372	7.675	5.052	0.279	5.452	99.661
16	0.034	19.607	20.364	41.468	0.386	7.983	5.227	0.188	4.746	100.003
17	0.036	19.612	18.658	40.967	0.383	7.370	5.573	0.188	7.072	99.860
18	0.058	19.540	21.783	41.560	0.405	9.744	4.300	0.394	1.958	99.743
19	0.024	19.718	19.909	41.530	0.334	7.612	5.563	0.152	5.136	99.978
20	0.077	19.585	19.083	41.282	0.363	8.276	5.041	0.494	5.823	100.024
21	0.101	20.041	21.628	41.994	0.337	9.435	4.004	0.375	2.026	99.942
22	0.036	18.587	21.834	41.325	0.442	10.773	4.675	0.492	1.536	99.698
23	0.042	18.955	21.390	41.506	0.409	10.108	4.998	0.509	2.033	99.950
24	0.050	19.147	18.641	41.115	0.402	7.700	5.627	0.272	6.976	99.930
25	0.049	20.306	21.655	41.904	0.343	8.706	4.466	0.340	2.371	100.140
26	0.063	20.165	21.573	41.896	0.354	8.612	4.403	0.330	2.409	99.805
27	0.024	19.338	19.639	41.337	0.331	7.894	5.443	0.349	5.351	99.705
28	0.044	18.766	17.419	40.942	0.412	7.438	6.025	0.235	8.483	99.765

Appendix B

Mineral Analysis Results

Garnets from "V" Concentrate

POINT	Na2O	MgO	Al2O3	SiO2	MnO	FeO	CaO	TiO2	Cr2O3	Total
29	0.038	20.124	22.958	42.090	0.372	8.482	4.277	0.158	1.660	100.160
30	0.051	19.381	18.892	41.404	0.385	7.347	5.899	0.317	6.520	100.196
31	0.038	19.753	19.792	41.744	0.331	7.454	5.286	0.167	5.297	99.861
32	0.054	19.933	21.366	41.851	0.372	9.202	4.361	0.362	2.803	100.304
33	0.084	19.441	22.851	41.620	0.442	10.787	3.621	0.352	0.956	100.153
34	0.086	18.536	20.495	41.421	0.413	9.359	5.755	0.699	3.191	99.953
35	0.059	19.467	23.314	42.165	0.355	9.375	4.852	0.397	0.377	100.362
36	0.085	18.940	16.788	40.732	0.374	7.974	5.835	0.704	8.265	99.696
37	0.093	20.043	22.371	42.257	0.354	9.602	3.941	0.329	1.210	100.200
38	0.080	19.583	22.267	41.804	0.448	10.081	3.913	0.389	1.542	100.106
39	0.047	18.303	23.017	41.258	0.350	12.165	4.156	0.264	0.332	99.892
40	0.054	18.741	22.581	41.449	0.420	10.743	4.498	0.270	1.241	99.997
41	0.089	19.782	22.265	41.800	0.387	9.851	3.948	0.335	1.299	99.758
42	0.049	20.137	20.659	41.391	0.369	7.679	4.816	0.299	4.187	99.587
43	0.038	20.646	23.030	42.221	0.398	8.156	4.118	0.175	1.106	99.888
44	0.036	20.076	22.000	41.821	0.400	8.250	4.599	0.207	2.676	100.066
45	0.049	19.368	17.742	40.937	0.407	7.247	5.516	0.290	8.300	99.855
46	0.011	18.439	23.729	41.797	0.320	8.950	6.425	0.027	0.446	100.144
47	0.090	19.690	21.124	41.941	0.389	9.430	4.118	0.362	3.052	100.195
48	0.030	19.675	19.244	41.596	0.309	7.908	5.683	0.282	5.498	100.226
49	0.038	18.824	18.458	41.081	0.345	7.590	6.397	0.053	7.150	99.935
50	0.012	18.124	23.675	41.669	0.270	8.344	7.167	0.023	0.409	99.694
51	0.032	20.361	21.573	42.003	0.398	7.792	4.584	0.215	2.850	99.808
52	0.067	19.953	20.914	41.945	0.355	8.859	4.413	0.464	3.207	100.177
53	0.061	18.827	21.556	41.675	0.414	10.505	4.894	0.614	1.559	100.108
54	0.094	19.814	22.297	42.050	0.383	9.921	3.839	0.374	1.204	99.977
55	0.042	19.582	19.378	41.333	0.408	7.594	5.257	0.210	5.789	99.593
56	0.012	19.118	19.028	41.089	0.394	7.402	5.821	0.092	6.535	99.491
57	0.038	19.378	17.490	41.085	0.413	7.152	5.704	0.145	8.588	99.994
58	0.071	19.764	20.872	41.836	0.390	8.857	4.465	0.490	3.195	99.940
59	0.066	19.963	20.831	41.645	0.346	7.947	4.862	0.389	3.772	99.821

Appendix B **Mineral Analysis Results** **Garnets from "V" Concentrate**

POINT	Na2O	MgO	Al2O3	SiO2	MnO	FeO	CaO	TiO2	Cr2O3	Total
60	0.069	19.260	18.480	41.423	0.346	8.421	5.122	0.444	6.264	99.830
61	0.063	19.670	21.154	41.917	0.409	9.030	4.435	0.432	3.037	100.147
62	0.046	20.499	21.162	41.998	0.364	7.332	4.675	0.260	3.429	99.764
63	0.051	19.670	19.540	41.367	0.353	7.679	5.343	0.212	5.785	100.000
64	0.086	18.866	22.303	41.635	0.398	10.493	4.760	0.369	0.873	99.780
65	0.085	19.947	22.167	41.958	0.394	9.771	3.918	0.325	1.498	100.062
66	0.073	19.618	17.447	41.344	0.377	7.391	5.345	0.374	8.169	100.137
67	0.067	19.948	18.926	41.455	0.390	7.341	5.068	0.342	6.537	100.074
68	0.049	20.131	21.613	42.078	0.386	8.515	4.434	0.410	2.581	100.196
69	0.008	18.313	21.009	41.412	0.532	8.945	5.696	0.013	4.084	100.012
70	0.065	19.436	21.666	41.626	0.377	9.847	4.700	0.475	1.828	100.020
71	0.069	17.695	17.434	40.672	0.447	8.380	6.999	0.495	7.756	99.947
72	0.066	20.097	22.074	42.101	0.365	9.295	4.302	0.329	1.961	100.592
73	0.081	19.839	22.448	41.789	0.359	9.162	4.367	0.317	1.668	100.030
74	0.040	15.296	23.599	41.160	0.281	10.315	9.267	0.122	0.073	100.153
75	0.040	20.220	19.790	41.404	0.369	7.200	4.906	0.230	5.457	99.617
76	0.105	20.131	22.269	41.725	0.382	9.584	3.632	0.367	1.250	99.445
77	0.050	18.625	22.548	41.693	0.402	10.981	4.498	0.279	1.052	100.128
78	0.038	19.950	21.058	41.868	0.342	7.702	4.854	0.275	3.587	99.673
79	0.050	19.718	20.633	41.476	0.369	8.152	4.903	0.279	3.888	99.467
80	0.066	19.436	19.499	41.051	0.362	7.902	5.153	0.270	5.734	99.471
81	0.043	19.776	19.448	41.312	0.394	7.360	5.363	0.130	6.377	100.203
82	0.051	19.192	21.759	41.690	0.413	10.229	4.700	0.462	1.529	100.025
83	0.042	20.427	22.635	42.244	0.349	8.031	4.333	0.214	1.836	100.112
84	0.073	19.517	21.934	41.793	0.458	10.231	4.263	0.387	1.486	100.144
85	0.042	20.013	19.089	41.387	0.332	7.116	5.233	0.312	6.087	99.610
86	0.038	20.325	20.723	41.723	0.371	7.324	4.879	0.214	4.253	99.848

SAMPLE	Na2O	SiO2	Al2O3	MgO	Cr2O3	MnO	FeO	NiO	K2O	CaO	TiO2	Total
a3	1.414	55.523	0.261	16.236	2.115	0.045	2.116	0.038	0.007	22.734	0.112	100.601
a4	1.572	55.69	1.232	16.299	1.122	0.077	3.251	0	0.01	21.198	0.217	100.668
a5	1.433	56.111	0.727	16.332	1.352	0.076	3.018	0.01	0.017	22.022	0.195	101.294
b6	2.306	55.996	2.719	16.418	1.418	0.115	3.39	0.041	0.017	18.241	0.232	100.892
b5	1.535	55.82	0.765	16.296	1.481	0.089	3.113	0.053	0.008	21.892	0.205	101.257
b4	4.002	56.21	5.273	15.148	0.802	0.125	4.725	0.023	0.013	14.093	0.21	100.625
b3	2.473	55.692	2.845	15.911	1.45	0.116	3.266	0.051	0.022	18.289	0.252	100.368
c1	1.609	55.632	1.285	16.272	0.949	0.103	3.374	0.003	0.022	21.178	0.24	100.667
c2	1.777	55.07	2.398	15.823	1.681	0.085	1.862	0.042	0	22.19	0.105	101.031
c3	3.226	55.947	3.943	15.767	0.81	0.114	4.566	0.024	0.019	16.011	0.244	100.669
c5	1.353	55.465	2.592	16.418	0.241	0.013	1.504	0.025	0	23.099	0.053	100.765
c7	1.769	55.502	1.343	15.904	1.355	0.074	2.689	0.065	0.011	21.027	0.224	99.961
c8	1.426	55.705	0.285	16.425	2.01	0.063	1.744	0.025	0.008	22.634	0.167	100.494
d8	1.723	55.461	1.366	16.181	0.997	0.089	2.784	0.029	0.022	20.989	0.235	99.876
d6	1.55	55.726	1.085	16.116	1.105	0.075	2.924	0.019	0.014	21.423	0.22	100.259
d5	1.705	55.664	0.744	16.095	1.723	0.088	2.538	0.038	0.008	21.757	0.175	100.537
d4	1.584	55.596	0.265	16.088	2.284	0.05	1.676	0.01	0	22.336	0.14	100.031
d3	1.738	55.463	0.554	15.999	2.444	0.044	1.693	0	0	22.009	0.123	100.066
d2	2.166	55.395	2.041	16.09	1.291	0.09	2.785	0.033	0.025	19.755	0.237	99.907
d1	3.892	55.992	5.02	14.863	0.681	0.118	4.082	0.056	0.008	14.536	0.227	99.474
e2	2.731	56.24	3.342	16.039	0.802	0.116	3.556	0.043	0.016	16.664	0.232	99.781
e3	2.301	55.532	1.94	15.934	2.553	0.058	1.804	0.038	0.016	19.451	0.168	99.795
e4	1.423	55.463	0.51	16.35	1.428	0.061	2.199	0.011	0.002	22.499	0.168	100.115
e5	1.45	55.671	0.365	16.461	1.855	0.031	1.733	0.037	0.013	22.661	0.143	100.42
e6	1.322	55.895	1.623	17.564	0.403	0.11	3.385	0.055	0.047	19.856	0.177	100.437
e7	2.748	55.895	2.252	15.176	1.903	0.061	3.084	0.047	0.006	18.617	0.32	100.111
e8	1.623	55.79	0.607	15.982	1.766	0.049	2.251	0.041	0.004	22.064	0.175	100.351
f8	2.398	55.88	2.779	15.989	1.33	0.097	2.898	0.038	0.022	18.528	0.285	100.244
f7	2.463	55.814	2.619	16.196	1.497	0.083	2.856	0.025	0.03	18.15	0.265	99.998
f5	2.953	56.173	3.461	15.956	0.738	0.102	3.727	0.018	0.012	16.661	0.225	100.028

Appendix B **Mineral Analysis Results** **Clinopyroxenes from "V" concentrate**

SAMPLE	Na2O	SiO2	Al2O3	MgO	Cr2O3	MnO	FeO	NiO	K2O	CaO	TiO2	Total
f4	1.686	55.532	0.833	15.752	1.54	0.072	2.79	0.017	0.012	21.351	0.158	99.745
f3	3.409	56.128	4.083	15.949	0.802	0.121	4.015	0.028	0.02	15.045	0.239	99.84
f1	3.447	56.107	4.212	15.748	1.115	0.105	3.61	0.018	0.02	14.9	0.188	99.47
g1	1.618	55.553	0.877	16.029	0.612	0.041	2.012	0	0.011	21.642	0.2	98.595
g3	1.516	55.801	0.863	16.3	1.226	0.072	2.651	0.001	0.016	21.621	0.217	100.287
g5	1.399	55.827	1.786	17.41	0.415	0.103	3.551	0.034	0.037	19.253	0.19	100.005
g6	1.411	55.827	1.699	17.455	0.453	0.097	3.287	0.008	0.043	19.807	0.207	100.292
g7	1.363	55.617	0.174	16.271	1.317	0.053	2.172	0.081	0	23.063	0.128	100.239
g8	3.09	56.069	3.887	16.261	0.877	0.13	3.931	0.046	0.011	15.145	0.257	99.702
h8	2.011	55.748	1.683	15.881	1.44	0.067	2.821	0.08	0.018	20.243	0.319	100.312
h7	1.597	55.527	1.068	16.043	1.16	0.08	2.819	0.062	0.018	21.452	0.235	100.063
h6	1.547	55.566	0.444	16.299	2.146	0.053	1.72	0	0	22.507	0.142	100.425
h5	1.818	55.658	0.933	16.029	1.603	0.096	2.837	0.031	0.001	21.262	0.202	100.469
h3	3.685	56.623	4.639	15.899	0.681	0.111	4.109	0	0.012	14.133	0.237	100.129
h2	3.22	56.366	3.79	16.047	0.953	0.088	3.865	0.001	0.023	15.313	0.224	99.889
h1	1.58	55.746	0.854	16.256	1.473	0.066	2.456	0.029	0.023	21.806	0.178	100.467
i2	1.609	55.557	1.098	16.097	1.201	0.062	2.937	0.056	0.016	21.539	0.249	100.421
i3	1.708	55.367	0.937	15.868	1.326	0.075	2.952	0.062	0.016	21.293	0.188	99.791
i4	1.595	55.497	1.06	16.206	1.101	0.061	2.779	0	0.004	21.599	0.207	100.107
i5	3.06	55.737	3.847	15.765	0.794	0.119	3.881	0.009	0.012	16.221	0.259	99.702
i6	2.507	55.746	2.762	15.99	1.445	0.092	2.869	0.004	0.016	18.79	0.282	100.503
i7	2.862	55.87	3.393	16.287	0.795	0.105	3.888	0.001	0.017	16.342	0.219	99.779
i8	2.018	54.483	1.816	17.295	1.554	0.076	2.682	0.005	0.027	18.391	0.292	98.638
j7	2.447	55.88	2.764	16.032	1.377	0.088	2.806	0.041	0.022	18.403	0.264	100.123
j6	1.591	55.636	0.754	16.082	1.559	0.052	2.422	0.045	0.001	21.75	0.177	100.069
j4	2.003	55.743	2.318	17.096	1.061	0.083	3.088	0.069	0.017	18.297	0.175	99.951
j3	1.967	55.559	1.665	15.997	1.447	0.087	2.873	0	0.028	20.257	0.27	100.15
j2	3.618	56.235	4.582	14.873	0.623	0.116	3.997	0.06	0.024	15.804	0.27	100.202
j1	4.092	56.618	5.349	14.674	0.628	0.088	3.98	0.032	0.013	14.467	0.205	100.148

Appendix B **Mineral Analysis Results** **Orthopyroxene from "V" Concentrate**

POINT	Na2O	SiO2	Al2O3	MgO	Cr2O3	MnO	FeO	NiO	K2O	CaO	TiO2	Total
1	0.147	59.213	0.597	35.491	0.307	0.115	4.564	0.116	0.000	0.467	0.072	101.088
2	0.139	59.318	0.574	35.438	0.379	0.107	4.209	0.101	0.006	0.437	0.078	100.786
3	0.232	58.687	0.712	33.997	0.231	0.112	5.188	0.134	0.000	0.618	0.067	99.979
4	0.106	59.312	0.588	35.753	0.370	0.123	3.895	0.064	0.000	0.368	0.045	100.625
5	0.129	59.290	0.582	35.557	0.343	0.077	4.090	0.041	0.000	0.360	0.055	100.525
6	0.228	59.012	0.618	34.065	0.224	0.111	5.349	0.075	0.005	0.691	0.085	100.463
7	0.131	59.686	0.278	35.653	0.298	0.130	4.059	0.092	0.002	0.369	0.048	100.749
8	0.212	58.471	0.659	34.052	0.199	0.115	5.079	0.045	0.000	0.623	0.097	99.550
9	0.201	58.952	0.665	34.184	0.216	0.115	5.142	0.052	0.000	0.624	0.107	100.258
10	0.143	59.626	0.605	35.630	0.409	0.116	3.919	0.107	0.000	0.374	0.038	100.967

Appendix B Mineral Analysis Results Chromites from "V" Concentrate

POINT	SiO2	Al2O3	MgO	MnO	FeO	NiO	TiO2	Cr2O3	CaO	ZnO	Total
1	0.004	1.243	8.184	0.461	31.645	0.160	3.081	53.513	0.024	0.128	98.443
2	0.000	1.185	8.085	0.461	32.081	0.150	3.129	53.468	0.000	0.124	98.683
3	0.021	6.815	9.109	0.399	28.193	0.132	0.812	53.187	0.014	0.111	98.794
4	0.053	6.350	8.595	0.343	28.376	0.140	0.841	52.936	0.008	0.147	97.789
5	0.000	1.304	7.634	0.436	37.123	0.183	3.863	47.382	0.000	0.101	98.026
6	0.000	7.191	9.144	0.387	26.400	0.104	0.160	55.157	0.001	0.177	98.723
7	0.002	6.825	9.993	0.362	25.631	0.094	0.172	54.830	0.013	0.133	98.054
8	0.002	7.635	9.995	0.443	25.130	0.107	0.093	55.067	0.000	0.161	98.633
9	0.004	6.426	8.957	0.359	24.927	0.093	0.145	56.533	0.000	0.154	97.598
10	0.017	0.499	5.750	0.533	46.872	0.154	3.618	39.542	0.000	0.133	97.119
11	0.000	0.465	5.493	0.449	51.015	0.210	4.497	33.833	0.007	0.122	96.092
12	0.000	6.895	9.356	0.394	27.938	0.104	0.325	54.143	0.001	0.136	99.293
13	0.028	2.447	8.816	0.381	30.388	0.123	3.551	52.279	0.007	0.127	98.148
14	0.028	9.483	11.189	0.262	19.033	0.094	0.484	58.466	0.000	0.167	99.206
15	0.034	9.389	10.890	0.266	18.868	0.056	0.492	58.959	0.010	0.136	99.100
16	0.060	5.485	8.115	0.391	28.233	0.061	0.187	55.758	0.000	0.174	98.464
17	0.000	1.058	5.145	0.349	30.068	0.163	2.816	55.517	0.035	0.126	95.276
18	0.034	3.618	11.625	0.296	19.551	0.112	0.946	62.914	0.000	0.072	99.166
19	0.051	3.546	9.648	0.271	19.028	0.106	0.966	63.761	0.000	0.085	97.463
20	0.058	1.268	7.468	0.467	37.015	0.182	3.671	47.531	0.000	0.105	97.763
21	0.000	1.171	6.775	0.414	37.956	0.187	3.790	47.263	0.027	0.095	97.679
22	0.006	0.521	7.685	0.544	33.357	0.123	2.994	52.763	0.000	0.101	98.096
23	0.019	0.588	7.010	0.411	32.145	0.171	3.108	52.418	0.003	0.122	95.994
24	0.066	6.732	11.147	0.301	23.651	0.150	2.132	54.530	0.000	0.050	98.759
25	0.043	6.469	10.472	0.291	23.846	0.174	2.280	54.285	0.011	0.076	97.948
26	0.000	0.920	7.145	0.455	38.091	0.150	3.213	47.575	0.003	0.162	97.712
27	0.009	0.952	7.407	0.420	40.413	0.188	4.032	43.960	0.000	0.111	97.491
28	0.004	12.705	11.074	0.280	23.874	0.123	0.170	50.504	0.001	0.190	98.926

Appendix B   Mineral Analysis Results   Chromites from "V" Concentrate

POINT	SiO2	Al2O3	MgO	MnO	FeO	NiO	TiO2	Cr2O3	CaO	ZnO	Total
29	0.036	10.063	10.965	0.323	22.825	0.071	0.133	54.875	0.000	0.159	99.451
30	0.009	4.329	9.227	0.389	27.700	0.139	0.871	55.499	0.000	0.149	98.311
31	0.017	3.739	7.824	0.365	26.534	0.136	0.837	58.035	0.011	0.134	97.634
32	0.017	5.205	8.332	0.420	34.020	0.153	1.686	47.909	0.000	0.116	97.858
33	0.000	5.207	8.518	0.414	33.831	0.153	1.661	47.895	0.022	0.147	97.848
34	0.000	11.707	11.149	0.311	22.081	0.111	0.599	52.586	0.000	0.179	98.723
35	0.000	10.626	10.207	0.303	22.138	0.116	0.615	53.064	0.000	0.167	97.237
36	0.017	3.964	7.355	0.334	25.749	0.060	1.289	56.877	0.000	0.146	95.792
37	0.011	2.931	9.090	0.394	29.819	0.140	1.740	54.923	0.017	0.102	99.167
38	0.011	2.891	8.164	0.391	28.799	0.121	1.625	54.779	0.008	0.098	96.887
39	0.011	8.389	9.022	0.484	28.108	0.088	0.560	51.838	0.000	0.228	98.728
40	0.000	7.675	8.619	0.427	28.018	0.089	0.499	52.727	0.000	0.179	98.232
41	0.009	6.613	10.517	0.362	23.920	0.079	0.587	57.279	0.003	0.106	99.474
42	0.002	5.523	9.365	0.395	23.630	0.108	0.587	58.859	0.000	0.101	98.571
43	0.000	0.983	7.441	0.426	35.753	0.162	3.209	50.365	0.006	0.147	98.492
44	0.032	1.115	8.816	0.350	35.803	0.202	3.623	47.072	0.000	0.105	97.117
45	0.011	2.556	9.134	0.387	30.208	0.169	2.866	53.156	0.000	0.147	98.634
46	0.011	2.623	9.549	0.386	29.891	0.192	2.819	52.383	0.000	0.101	97.955
47	0.004	10.560	11.179	0.271	21.009	0.087	0.040	55.863	0.014	0.144	99.172
48	0.000	10.832	10.194	0.229	20.517	0.067	0.042	55.419	0.006	0.111	97.416
49	0.032	9.878	10.585	0.350	22.466	0.075	0.042	55.052	0.010	0.153	98.643
50	0.024	9.392	9.741	0.305	22.556	0.089	0.040	55.675	0.001	0.173	97.995
51	0.015	11.034	11.379	0.254	21.307	0.092	0.105	55.357	0.000	0.128	99.672
52	0.000	12.191	12.275	0.265	20.759	0.073	0.108	53.380	0.003	0.152	99.205
53	0.000	2.999	8.765	0.381	30.374	0.153	1.716	53.595	0.000	0.091	98.073
54	0.019	2.726	8.315	0.390	30.316	0.148	1.715	54.733	0.000	0.111	98.472
55	0.034	2.628	9.214	0.393	29.300	0.172	2.759	53.732	0.000	0.124	98.356
56	0.034	2.500	8.657	0.402	29.539	0.168	2.804	54.250	0.000	0.129	98.482
57	0.011	8.164	8.166	0.501	32.899	0.070	0.240	47.896	0.000	0.162	98.110
58	0.000	1.978	7.266	0.518	38.180	0.150	1.256	46.987	0.013	0.092	96.440
59	0.075	7.414	12.029	0.284	19.768	0.143	0.704	58.554	0.000	0.107	99.078

Appendix B **Mineral Analysis Results** **Chromites from "V" Concentrate**

POINT	SiO2	Al2O3	MgO	MnO	FeO	NiO	TiO2	Cr2O3	CaO	ZnO	Total
60	0.039	6.957	11.230	0.262	19.983	0.146	0.721	58.801	0.000	0.061	98.199
61	0.000	2.577	9.264	0.332	30.806	0.199	3.106	52.607	0.000	0.128	99.018
62	0.043	2.498	8.796	0.380	30.011	0.201	2.951	52.861	0.003	0.087	97.830
63	0.036	8.504	9.058	0.452	28.086	0.103	0.185	52.057	0.018	0.188	98.689
64	0.019	9.239	9.527	0.442	28.268	0.060	0.240	50.134	0.001	0.192	98.122
65	0.000	6.626	9.595	0.383	26.782	0.098	0.102	55.493	0.003	0.169	99.252
66	0.024	6.042	10.069	0.405	25.615	0.102	0.095	56.050	0.015	0.137	98.555
67	0.053	5.360	10.973	0.263	26.772	0.140	3.389	52.336	0.000	0.108	99.396
68	0.062	5.349	8.791	0.267	25.656	0.196	3.505	52.725	0.001	0.091	96.644
69	0.000	2.749	5.409	0.287	49.446	0.332	2.442	35.875	0.000	0.134	96.673
70	0.000	2.698	5.326	0.297	49.881	0.361	2.492	36.024	0.000	0.122	97.201
71	0.011	1.154	8.602	0.311	31.291	0.162	4.852	51.294	0.015	0.083	97.777
72	0.071	6.611	11.674	0.291	21.722	0.139	2.013	56.660	0.000	0.083	99.264
73	0.068	7.027	11.419	0.253	21.300	0.136	1.963	56.110	0.000	0.086	98.363
74	0.030	10.770	10.270	0.395	23.209	0.107	0.884	52.753	0.000	0.176	98.594
75	0.009	8.790	9.527	0.338	23.092	0.073	0.814	55.336	0.020	0.168	98.165
76	0.013	0.835	7.269	0.487	36.654	0.214	3.489	48.756	0.000	0.112	97.829
77	0.000	0.979	8.867	0.333	36.353	0.207	3.770	46.840	0.000	0.107	97.456

Element	CaO	Sc	TiO2	V	Ni	Ga	Sr	Y	Zr	Nb	La	Ce	Pr
Isotope	42	45	47	51	60	69	88	89	90	93	139	140	141
Unit	wt%	ppm	wt%	ppm	ppm	ppm	ppm	ppm	ppm	ppm	ppm	ppm	ppm
9K18A04 1	5.20	215.09	-0.39	241.69	9.09	5.79	0.17	25.71	70.04	0.03	0.00	0.47	0.14
9K18A05 1	6.50	407.72	-0.91	393.01	56.98	11.35	8.60	32.81	39.96	1.65	1.92	2.87	0.37
9K18A06 1	5.40	234.86	-0.35	287.24	16.56	6.92	0.09	26.44	41.52	-0.02	0.01	0.36	0.04
9K18A07 1	4.70	226.77	-1.00	401.18	2.01	8.28	0.25	13.08	26.75	0.21	-0.03	0.13	-0.03
9K18A08 1	5.60	205.79	-0.34	314.75	49.18	2.87	0.72	4.26	29.50	-0.03	0.02	0.21	0.10
9K18A09 1	4.40	245.07	-1.05	289.17	58.72	8.09	0.38	15.64	24.92	0.21	0.01	0.17	0.03
9K18A10 1	5.90	215.01	-1.08	332.57	32.16	5.26	0.56	10.41	32.43	0.31	0.02	1.06	0.23
9K18A11 1	5.70	333.73	-1.53	546.77	44.77	6.32	0.41	9.80	36.91	0.41	0.02	0.32	0.11
9K18A12 1	4.60	126.73	-1.63	206.53	15.24	7.80	2.44	27.01	32.92	0.07	0.11	0.47	0.02
9K18A13 1	4.60	137.52	-4.24	219.12	31.12	6.54	0.09	17.31	21.06	0.05	0.01	0.20	-0.01
9K18A14 1	5.70	178.11	-0.60	137.41	6.75	0.00	0.08	8.30	1.62	-0.13	0.05	0.35	0.09
9K18A15 1	4.40	118.99	4.28	211.47	32.53	8.76	0.23	19.79	26.49	0.01	-0.01	0.07	0.02
9K18A16 1	4.90	130.13	1.68	285.61	38.41	5.98	-0.01	9.33	21.96	-0.03	-0.01	0.08	0.03
9K18A17 1	3.60	174.74	1.45	168.94	18.79	3.12	0.20	19.20	19.75	-0.04	0.02	0.01	-0.02

Nd	Sm	Eu	Gd	Tb	Dy	Ho	Er	Tm	Yb	Lu	Hf	Th	U
146	147	151	157	159	163	165	167	169	172	175	178	232	238
ppm	ppm	ppm	ppm	ppm	ppm	ppm	ppm	ppm	ppm	ppm	ppm	ppm	ppm
2.26	1.98	0.99	4.43	0.94	6.06	1.32	4.00	0.55	3.70	0.59	1.91	0.02	0.06
2.05	0.37	0.51	1.83	0.59	5.78	1.68	6.28	1.11	7.42	1.42	1.57	0.36	0.06
1.40	1.58	0.79	2.07	0.62	5.10	1.29	4.29	0.65	4.24	0.70	0.98	0.03	0.01
0.46	0.26	0.28	1.15	0.25	2.27	0.55	2.11	0.27	2.55	0.38	0.73	0.02	0.01
0.80	0.73	0.39	1.17	0.18	1.00	0.14	0.26	0.12	0.88	0.17	0.79	0.05	0.03
0.62	0.41	0.24	1.12	0.29	2.79	0.72	2.54	0.41	2.83	0.47	0.97	0.03	0.01
2.17	1.25	0.30	1.75	0.35	2.25	0.46	1.19	0.24	1.28	0.26	0.86	0.07	0.11
1.35	0.85	0.38	1.50	0.27	1.95	0.42	1.16	0.21	1.47	0.25	1.11	0.00	0.03
0.55	0.77	0.29	1.98	0.53	4.32	1.13	2.92	0.52	3.22	0.61	0.54	0.07	0.04
0.51	0.45	0.26	1.17	0.31	2.60	0.71	2.36	0.33	2.56	0.40	0.48	0.06	0.05
0.30	-0.02	0.05	0.25	0.12	1.11	0.25	1.25	0.20	1.86	0.34	-0.01	0.00	0.07
0.26	0.35	0.24	1.44	0.35	2.79	0.72	2.29	0.36	2.63	0.40	0.79	0.00	0.00
0.43	0.34	0.18	0.96	0.20	1.46	0.29	1.02	0.16	1.21	0.21	0.63	0.02	0.01
0.20	0.03	0.13	0.60	0.22	2.28	0.68	2.65	0.48	3.67	0.63	0.51	0.00	0.01